STRATAL GEOMETRIES OF TUSCAN DEPOSITS IN BIG CHICO CREEK CANYON OUTCROPS AND IN THE SUBSURFACE UNDERLYING CHICO, CALIFORNIA

_____

A Thesis

Presented

to the Faculty of

California State University, Chico

_____

In Partial Fulfillment

of the Requirements for the Degree

Master of Science

in

Geosciences

_____

by

Marisol Gonzalez

Fall 2014

STRATAL GEOMETRIES OF TUSCAN DEPOSITS IN BIG CHICO CREEK CANYON OUTCROPS AND IN THE SUBSURFACE UNDERLYING CHICO, CALIFORNIA

A Thesis

by

Marisol Gonzalez

Fall 2014

APPROVED BY THE DEAN OF GRADUATE STUDIES
AND VICE PROVOST FOR RESEARCH:

_____
Eun K. Park, Ph.D.

APPROVED BY THE GRADUATE ADVISORY COMMITTEE:

_____
Todd Greene, Ph.D., Chair

_____
Russell Shapiro, Ph.D.

_____
Glen Pearson, PG

ACKNOWLEDGMENTS

This project would not have been possible without the emotional and financial help of my family and fiancé Patrick DeCarvalho. Thank you to my mom, Cheryl Marden, for being my number one cheerleader, and working so hard to provide me with a college education. Patrick, I am grateful for your patience and understanding through this process, and for allowing me the financial means to quit my job and focus on school. Your wicked sense of humor kept me laughing, even on the most stressful days. Patrick, you truly are my best friend.

I would like to express gratitude to my field assistant, Katie Reich, for going in the field with me during one of the hottest summers of the year. Thank you to Kathi McCarthy and Amy Gentry, for helping me with field work, editing, being a shoulder to cry on, and most of all, for being great friends.

To Dr. Todd J. Greene, Dr. Russell Shapiro and Glen Pearson, thank you for your valued suggestions, and for being on my thesis committee. I owe my interest in sedimentology and stratigraphy to Dr. Shapiro and him for his introduction class on the subject. Glen, your real world knowledge is invaluable and I learn something new on the Tuscan every time we chat. Finally, thank you Dr. Greene for being my advisor and providing me with the framework and background to complete this study. Dr. Greene always made time to personally help me both in the class room, with field work and edits. I am extremely privileged to have worked with you and will be forever indebted.

Finally, I would like to thank Big Chico Creek Ecological Reserve (BCCER) and Bidwell Park for special access to the Tuscan Rocks and the BCCER, and the Department of Geological and Environmental Sciences at California State University, Chico for providing funding for this project. I received a 2012 research grant from BCCER, which I used to take aerial geologic photomosaics. Also, in 2012 I received a research grant from Department of Geological and Environmental Sciences at California State University, Chico which I used to produce thin sections.

I will leave this program as a better geologist, and I will always be grateful for the help and support which I have received.

TABLE OF CONTENTS

PAGE

CHAPTER PAGE

PAGE

Appendices

LIST OF TABLES

LIST OF FIGURES

FIGURE PAGE

FIGURE PAGE

ABSTRACT

STRATAL GEOMETRIES OF TUSCAN DEPOSITS IN BIG CHICO CREEK CANYON OUTCROPS AND IN THE SUBSURFACE UNDERLYING CHICO, CALIFORNIA

by

Marisol Gonzalez

Master of Science in Geosciences

California State University, Chico

Fall 2014

The late Pliocene Tuscan Formation, in the northern Sacramento Valley is an established aquifer system. However, little is known about its hydrogeologic units in terms of dimensions, textures (facies), and heterogeneity. Due to a lack of well data, regionally extensive mappable surfaces, and age control, it is difficult to divide the Tuscan into units that can be correlated. In addition, the Tuscan outcrop has been historically divided by gross lithologic differences without attention to depositional processes or time-correlative surfaces. The existing stratigraphic scheme is therefore inadequate to characterize Tuscan stratigraphy in more local areas of investigations.

For this study, the complexity of Tuscan deposits warrants field work and subsurface investigation. Fieldwork methodology involved mapping eight stratigraphic sections, (plus five previously mapped southern sections) on Musty Buck Ridge (MBR)

in Big Chico Creek Canyon. Mapping of individual flow units on MBR allowed for recognition of major lithofacies in the Tuscan: breccia (matrix and clast-supported), conglomerate (matrix and clast-supported), massive sandstone (cross-bedded and planar laminated), mudstone and re-worked tuff. Environmental interpretations of Tuscan lithofacies were then grouped together and correlated to define facies associations: volcanic debris flow, hyperconcentrated flow, normal stream deposits, distal debris flow, flood deposits, and re-worked tuff. Major changes of facies associations were used to create timelines (MBR 1-11 from oldest to youngest) binding correlative packages on Musty Buck Ridge.

The subsurface component of the study focuses on composition, texture and geometry of the Tuscan Formation by using petrographic analysis from three wells to establish a Red Bluff Formation–top Tuscan Formation boundary. A point count method of individual (metamorphic vs. volcanic) sand grains was conducted to delineate the boundary, combined with data such as driller completion reports and resistivity pattern recognition to complete a 3D surface map and three cross-sections. The mapped surface depicts the topography of the paleo-valley prior to the deposition of the Red Bluff Formation. Establishing the Red Bluff Formation–top Tuscan Formation boundary is important because the city of Chico receives its water both above and below this boundary.

Results from this study indicate that Tuscan deposits depict cycles of volcanic activity interpreted to trigger large debris flows, followed by restoration to normal stream flow conditions. Along Musty Buck Ridge, older deposits near the base of sections

(MBR1-2) reflect a distal volcanic fan environment interbedded with normal stream flow deposits, that progressively become more proximal in younger northeastern units. MBR2-5 is dominated by normal stream deposits, interpreted to be one large debris flow (MBR3-4). Younger deposits are dominated by massive debris flows interbedded with normal stream flow deposits (MBR5-11).

The outcrop and subsurface results in this study provide a depositional history, stratigraphy, and aid existing models of the hydrogeology of the Tuscan Formation. Development of the spatial geometry of additional Tuscan outcrop cliffs will expand the understanding of the Tuscan Formation. Additional well data will further the identification of other key surfaces in the Tuscan Formation, adding to a growing database that could eventually be used to create an accurate subsurface model of the Tuscan aquifer system.

CHAPTER I

INTRODUCTION

The late Pliocene Tuscan Formation, in the northern Sacramento Valley is an established aquifer system. In the Sacramento Valley, groundwater from the aquifer provides thirty-one percent of the water supplies for agriculture and urban uses in the region (DWR Bulletin 118, 2003). Historically, surface water in the Sacramento Valley has been abundant; groundwater development was used primarily as a supplement to the surface water supply. Groundwater provides approximately 2.5 million acre feet (maf) of the 8 maf needed for municipal, agricultural and industrial water supplies (DWR Bulletin 118, 2003). Currently, interest and reliance on groundwater continues to increase due to new environmental laws, regulations, droughts, higher human populations, anadromous fisheries, riparian habitats, and more competition for surface water. Fulton et al. (2012) estimated 6,519 domestic wells and 2,590 irrigation wells located in the Sacramento Valley prior to 1970. Today, Fulton et al. (2012) estimates that there are 31,006 domestic wells and 6,040 irrigation wells in the Sacramento Valley. With this increase, the need to further our knowledge of the Tuscan Aquifer, which contains this important natural resource, has increased as well.

The Tuscan Formation deposits are composed of 3.2 to 1.8 million year old breccia, conglomerate, sandstone and mudstone deposits, all dominated by volcanic clasts derived from the ancient Mt. Yana volcanic complex near Lake Almanor (Evernden et

al., 1964; Lindberg et al., 2006; Lydon, 1968). Tuscan Formation rocks outcrop near north Red Bluff and continue south towards Oroville, California, covering an area of 5,180 km^2 (Lydon, 1968). The Tuscan Formation dips southwest in the subsurface and interfingers with the Tehama Formation in the center of the basin.

Musty Buck Ridge located in Chico's Upper Bidwell Park and Big Chico Creek Ecological Reserve (BCCER) contains the one of the best exposure accessibility to Tuscan Formation outcrops (Figure 1). Along with 50 monitoring wells under the City of Chico providing subsurface geophysical data, the Chico area is an excellent location to study Tuscan deposits.

The objective of this study is to collect data and interpret the depositional history and stratal geometries of the Tuscan deposits on Musty Buck Ridge so that subsequent studies may use these results in modeling the Tuscan Aquifer system. This study involves both field work and subsurface investigation. For the field based component, it is hypothesized that the previous lithostratigraphic nomenclature for the Tuscan defined by Harwood and Helley (1987) does not sufficiently represent the depositional complexity and that a new depositional process and facies-based approach is needed. This new depositional process and facies-based approach includes multiple elements involving field work, characterization of lithofacies, facies associations, interpretation of the environment of deposition, as well as establishing and mapping time correlative boundaries for Tuscan deposits in Big Chico Creek Canyon. For the subsurface component of the investigation, major surfaces from outcrop as well as well logs and petrographic sand compositional data were used to locate the boundary between

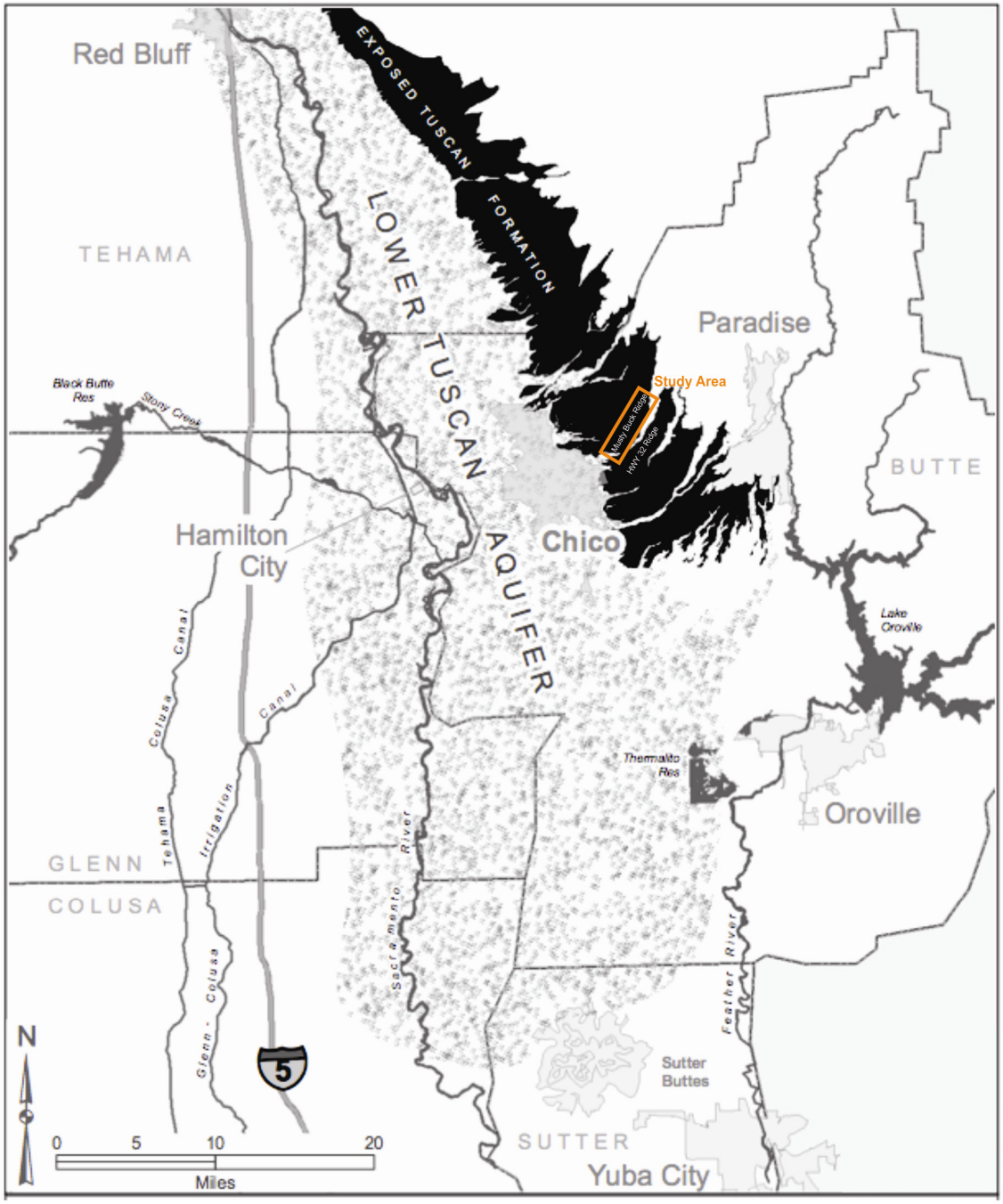

Figure 1. Map of surface exposure of Tuscan Formation and estimated subsurface extent of lower Tuscan Aquifer.

Map shows the location of the Tuscan Formation in both in outcrop and subsurface. Outcrop study area of this thesis is located on Musty Buck Ridge, highlighted by the orange box. Modified from Watersheds.us data: USGS 1981, DWR2006, CaSIL2000, GCID2006, CalFish2003.

the Tuscan Formation and the overlying Red Bluff Formation. Subsurface and outcrop results of this study provide the preliminary data to build geologic framework and model of individual Tuscan flows.

In order to meet these objectives, this thesis is organized as follows: Chapter II provides a geologic background of the Tuscan from previously published literature and modern analogs of volcaniclastic deposits providing insight and a general understanding of the Tuscan and the local geology; Chapter III describes the methodology and procedure of the study to facilitate replicability in future studies of the Tuscan; Chapter IV summarizes data and results from stratigraphic field work, outcrop characterization and petrographic analysis; Chapter V discusses the newly established stratigraphic framework on Musty Buck Ridge based on results outlined in Chapter IV. Chapter V concludes by addressing the implications and applicability of the results and how this study can add to the growing database that will further the groundwater modeling efforts of the Tuscan Aquifer system.

CHAPTER II

BACKGROUND

Geologic Setting

Northern California's complex geologic history contains remnants of ancient convergent boundaries that were later disrupted by a modern transform boundary. The northern Sacramento Valley is located between the Sierra Nevada to the east, and the California Coast Ranges to the west. The deeper rocks in the valley are predominantly marine sedimentary rocks, ranging in age from Late Jurassic to early Miocene, unconformably capped by alluvial deposits and volcanic rocks from the early Miocene to Holocene (Harwood and Helley, 1987). The Sacramento Valley first formed as a late Mesozoic forearc basin between the accretionary trench represented by the Franciscan Group of the Coast Ranges and the eastern magmatic arc complex whose roots have been exposed in the Sierra Nevada (Harwood and Helley, 1987).

By the end of the Nevadan Orogeny (Late Jurassic), the Sierra Nevada consisted of deformed Paleozoic and allochthonous Mesozoic terranes creating three major tectonic belts (Schweickert et al., 1984): Western Belt (also known as the Smartville Complex), the Central Belt, and the Eastern Belt. Each belt has a different stratigraphic and deformational history (Day et al., 1985). Within the belts of the northern Sierra are northwest trending folds and steeply dipping faults that developed during the Late Jurassic Nevadan Orogeny collectively called the Foothill Fault System (Day et al.,

1985). In the Central Belt, plutons with compositions ranging from gabbro to granodiorite intruded and deformed the pre-existing igneous and sedimentary rocks (Schweickert et al., 1984). A large flux of granitic intrusions began 120 Ma. during the Cretaceous in the western portion of the Sierra Nevada. These plutons intruded on older Jurassic plutons and migrated steadily eastward for 40 m.y. (Cecil et al., 2012; Chen et al., 1982; Everndeen and Kistler, 1970). The highest tectonic unit is the Smartville ophiolitic complex which overlies rocks of the Central Belt along a steeply west dipping fault contact (Moores and Day, 1984). There are currently two models for the Nevadan Orogeny: a collision of an oceanic arc with an Andean-style subduction zone, or in situ development of a rifted arc along the North American margin followed by transpression (Moores and Day, 1984). Moores and Day (1984) argue for the collisional model due to the evidence of a major folded overthrust sheet of ophiolitic rocks that first thrust eastward and then are altered by vertical to west-directed folds and reverse faults.

During the Late Cretaceous, the basin uplifted and tilted to the southwest (Harwood and Helley, 1987). On the northeastern margin of the Sacramento Basin nonmarine and shallow marine deposition occurred (Nilsen and Imperato, 1990). Harwood and Helley (1987) believe periods of uplift and subsidence caused by Paleogene subduction and lateral faulting continued to affect the depositional basin throughout the early Cenozoic. During these cycles of uplift, four distinctive submarine canyons developed, filled with transgressive marine sequences.

According to Griscom and Jachens (1989), three lithospheric plates meet at the Mendocino Triple Junction (MTJ) along the northern tip of the San Andreas Fault: the

Juan de Fuca (sometimes called the Gorda plate), Pacific Plate, and North American Plate. Currently, the Juan de Fuca plate subducts eastward beneath the North American Plate north of the MTJ. However, during the past 29 m.y., the MTJ first formed near Los Angeles and then continued to migrate northwest creating volcanism and effectively lengthening the San Andreas Fault.

As the MTJ migrated northward in the late Oligocene to early Miocene, marine sedimentation was replaced by fluvial deposition and volcanic activity to the east within the Sierra Nevada. Eruptions of volcanic rhyolitic tuffs began during the Oligocene continuing through the early-mid Miocene, followed by large andesitic eruptions along the crest of present day Sierra Nevada. After the rhyolitic and andesitic eruptions, andesitic mudflows followed ancient drainages down the western slopes of the Sierra during the middle Miocene through the early Pliocene (Wagner and Saucedo, 1990). Harwood and Helley (1987) hypothesize the Pliocene-aged Tuscan Formation contains many of these mudflow units.

Stratigraphic Units: The Sierran Basement

The Sierran Basement rocks consist of late Jurassic though Cretaceous aged metamorphic rocks. In Chico, deposits from the Sierran Basement rocks are complex and likely a result of a strong Nevadan overprint deformation on the Western Belt/Central Belt contact (Figure 2) (J. Kato, personal communication, August 8, 2013). The Western Belt, also known as the Smartville complex is the westernmost major tectonic unit in the Northern Sierra Nevada (Day et al., 1985). The Western Belt is a rifted volcanic arc

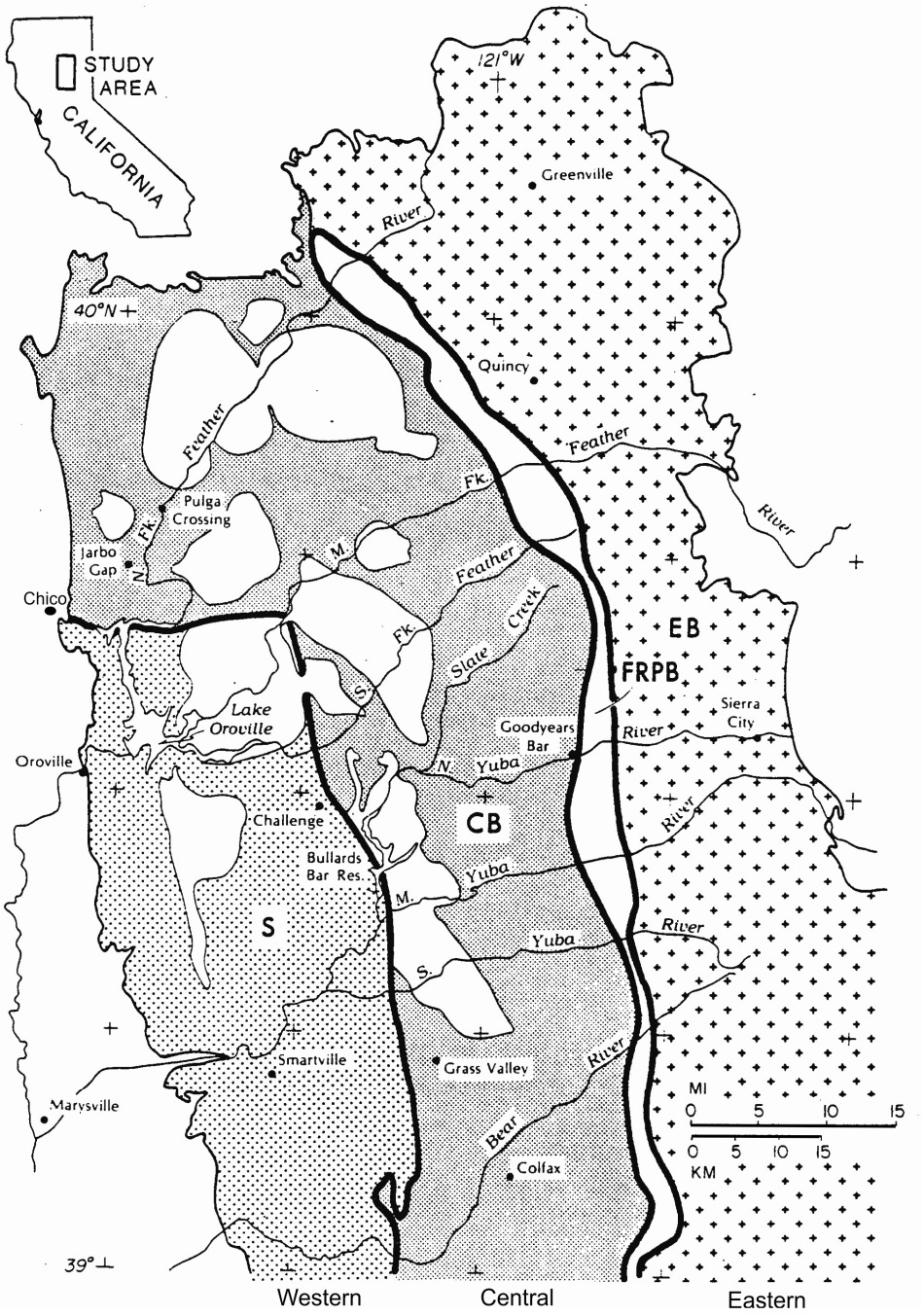

Figure 2. Tectonic map of the northern Sierra Nevada foothills region.

Map depicts from east to west and in structurally descending order: Western belt, Central belt and Eastern belt. Chico, CA is on trend with the Central Belt-Western belt contact. Modified from Day, H.W., Moores, and E.M., Tuminas, A.C., 1985, Structure and Tectonics of the Northern Sierra Nevada: Geol. Soc. Am. Bull., 96, p. 436-450 (fig 1).

complex that consists of serpentinized ultramafic rock (commonly occur fault-bounded blocks), pillow basalt, gabbro plutons, diorite plutons, slate, greenschist, and sub-green schist (Day et al., 1985). Unmetamorphosed Upper Cretaceous and lower Tertiary sedimentary rocks in the Great Valley overlay the Western Belt. A steeply dipping zone of penetrative faulting and foliation occur on the northern and eastern margins of the belt. The most northerly outcrop evidence of the Western Belt is at Glover Ridge, near Lake Oroville.

The Central Belt is composed of ultramafic, plutonic, and sedimentary rocks, variably metamorphosed from low to medium grade caused by one or more periods of faulting, isoclinal folding, and intruded granitic plutons of the Sierran batholith (Late Jurassic to Early Cretaceous age) (Day et al., 1985).

The Central Belt contains two different bedrock complexes: in the north, the Devonian to Permian aged Shoo Fly Complex occupies most of the belt which is overlain by a pyroclastic sequence. Metamorphic grade does not rise above chlorite grade. The southern portion of the Central Belt, just south of Placerville, California, is dominated by the Calaveras Complex composed medium to high-grade metamorphic rocks flanked to the east by a narrow strip of the Shoo Fly Complex (Schweickert et al., 1984). Sedimentary sequences rich in chert and argillite underlies the Central Belt (Day et al., 1985). Weakly metamorphosed Central Belt rocks are composed of intercalated slate, argillaceous sandstone, bedded to massive chert, pebbly-mudstone and conglomerate, and isolated blocks of fossiliferous limestone (Day et al., 1985). Creely (1965) mapped the

rock units near the northwest end of Lake Oroville as the Calaveras Formation and described the rocks as a shale matrix mélange.

Chico Formation

The Upper Cretaceous (Coniacian-Lower Campanian) aged Chico Formation can be found along the western, northern and eastern margins of California's Great Valley (Haggart and Ward, 1984). The Chico Formation dips gently southwest, almost continuously along the Big Chico Creek, Little Chico Creek, and Little Butte Creek. The Chico Formation has an estimated thickness of 615 m to 915 m (Nilsen et al., 1990) and can be split up into defining members: cobble conglomerate of the basal Ponderosa Way Member; coarse grained conglomerate sandstone of the overlying Musty Buck Way Member; fine grained silty sandstone of the uppermost Ten Mile Member; and the mudstone Kingsley Cave Member (Haggart and Ward, 1984).

Haggart and Ward (1984) state that the Chico Formation represents a transgressive sequence, from coarse-grained fluvial conglomerates at the base of the unit, to finer grained mudstone at the top of the unit.

Lovejoy Basalt

The Lovejoy Basalt erupted in the middle Miocene during a period of widespread and voluminous mafic magmatism (Christiansen et al., 2002). Redwine (1972) theorized that the Lovejoy Basalt erupted from a fissure at Thompson Peak just south of Susanville, California, flowed a maximum of 240 kilometers across the northern

end of the Sierra Nevada and funneled through one or more paleo-canyons into the modern day Sacramento Valley.

Studies by Garrison et al. (2008) measure the Lovejoy Basalt maximum exposed thickness of ~ 245 meters. It is a dense, low-MgO aphyric-dominated flood basalt occurring in isolated exposures in a northeast-southwest trending band extending from the Honey Lake Fault scarp across the northern end of the Sierra Nevada to the Sacramento Valley. The basalt has an "ink black" appearance due to the high glass content (30%-40%) and a fine-grained groundmass consisting of a microcrystalline plagioclase and olivine. It is highly jointed and fractured, and it can exhibit columnar jointing forming cliffs and talus slopes.

The age of the Lovejoy Basalt has been widely debated due to the loss of argon from weathering and alteration of clay minerals. Through the use of $^{40}Ar/^{39}Ar$ step-heating spectra, a 15.4 Ma age was obtained from five samples in a study by Garrison et al. (2008). Garrison et al. (2008) hypothesized that the Lovejoy Basalt is material from the migration of the Yellowstone mantle plume and the Columbia Flood basalts due to their similar geochemistry. The Lovejoy Basalt does not appear subduction related due to its geochemical differences from the Cascade arc lava.

Tuscan Formation

Harwood et al. (1981) model divides the Pliocene-aged Tuscan Formation into four separate members from oldest to youngest: Unit A, Unit B, Unit C and Unit D. The upper Tuscan Formation is defined by Units C and D, and Units A and B define the lower

Tuscan Formation (Harwood and Helley, 1985). Unit A is about 65 meters thick and consists of interbedded lahar deposits, volcanic conglomerate deposits, volcanic sandstone, and siltstone. The volcanic sandstone contains fragments of metamorphic rock, white to dark gray in color with clasts reaching 20 cm in diameter. Some metamorphic fragments can contain white vein quartz, chert, greenstone, and serpentinite. Similar to Unit A, Unit B and Unit C of the Tuscan Formation have interbedded lahar deposits, volcanic sandstone and siltstone, but coarse boulder breccia is more abundant in Unit B than in Unit A. Unit B is about 130 meters thick. Unit C is predominantly breccia deposits with fragments of angular to sub-rounded volcanic fragments in a matrix of gray-tan mudstone. Unit C contains breccia deposits with reverse grading. The thickness of Unit C breccia deposits can range from 0.5-10 meters thick. The total thickness of Unit C is approximately 50-80 meters. According to Harwood and Helley (1985), Units B and C do not contain metamorphic clasts. Unit D is a fragmental deposit, characterized by large monolithologic masses of andesite, pumice, and a fragmented obsidian mudstone matrix. Unit D is approximately 10-50 meters.

Red Bluff Formation

The Pleistocene-aged Red Bluff Formation rocks contain metamorphic and volcanic rocks, coarse red gravel with some interstratified sand and silt reworked from the older deposits discussed above. Currently, little study has been done on the origins of the Red Bluff Formation deposits. Multiple theories of the Red Bluff deposition exist. One theory is that the Red Bluff Formation is made of local sediments from surrounding

foothills (metamorphic and volcanic rocks being derived from the Klamath Mountains and Cascades), forming alluvial fans that deposited upon a pediment (Buer, 2007; Harwood et al., 1981; Helley and Jaworowski, 1985). Another theory proposed by Duncan (2005) is that the Red Bluff Formation is the result of glacial outwash, primarily on the Klamath Mountains and Cascades during glacial times due to the high silt and gravel content in the deposits. The glacial outwash formed open fans and was followed by a period of stream incision during interglacial times. Smaller subsequent glaciations were not capable of refilling channels and were preserved as inset terraces of the Modesto Formation. The Red Bluff Formation became highly weathered due to pedogenic processes, leading to the deep red color of the formation. After deposition, the Red Bluff Formation was subjected to Quaternary structural deformation, primarily indicated by surface deformations such as the Corning Dome, Battle Creek Fault, and Inks Creek fold system.

Modesto Formation

Pleistocene-aged Modesto Formation is divided into two members: the upper and lower member. The upper member of the Modesto Formation consists of gravel, sand, silt, and clay from the Sierran/Cascadian foothills, the Klamath Mountains and the Coast Ranges. The Modesto Formation is lithologically similar to the Red Bluff Formation, but finer grained, less gravel, less indurated and less oxidized giving it a lighter color than the red-colored Red Bluff (Harwood et al., 1981).

Review of Tuscan-related Literature

The distribution of Tuscan rocks was regionally characterized by Lydon (1969) and Harwood and Helley (1987) of the U.S. Geological Survey and locally mapped in Big Chico Creek Canyon as a Master's thesis by Doukas (1983) providing the best-to-date map of the Tuscan units along Big Chico Creek. Although these studies provided detailed descriptions of the structural geology of the Tuscan and general unit descriptions, little work has focused on the detailed sedimentology of the Tuscan and its internal structure. Numerous CSU student projects provide an excellent basis to continue work on the Tuscan (Moody and Teasdale 2006; Smith et al., 2008, Skartvedt-Forte, 2006). This study will build upon their work by providing a higher resolution understanding of the depositional history, stratigraphy, and ultimately hydrogeology of the Tuscan Formation.

One of the most extensive studies on the Tuscan Formation is by Phillip A. Lydon (1969). Lydon (1969) determined that the Tuscan Formation is exclusively volcanic in origin and he uses the term "lahar" to describe the Tuscan due to the volcanic breccia. Lydon (1969) observed olivine basalt and pyroxene andesite as the most common rock type clasts in the formation. The lahars formed "lobe like or sheet like shapes" and covered up to 2000 square miles with a maximum exposed thickness of 1700 feet. Lydon (1969) believed that the water needed to create the mobility of the flows came from magmatic or meteoric sources and not necessarily from melted snow or ice. Heavy rainfall could have also been a catalyst needed to create a flow from dry brecciated debris.

Harwood and Helley (1987) produced the first geologic map that included their nomenclature of the Tuscan Formation. They divided the Tuscan on a regional scale into four units: A, B, C, D (see Stratigraphic Units section for more details). Structurally, they observed that uplift from the northern Sierra Nevada created monoclinal flexure and a fault rupture beneath the surface forming the Chico Monocline (Figure 3). The Chico Monocline has northwest trending, southwest facing flexure which bounds the northeast side of the Sacramento Valley between Chico and Red Bluff. East of the Chico Monocline, the average Tuscan Formation dip is 5° southwest. Along the monoclonal flexure, Tuscan Formation bedding steepens, reaching a dip of 20°-25°. Average bedding dips becomes gentler (2°-5°) south of Chico as the monocline disappears north of Oroville. Due to tectonic uplift of the late Cenozoic, stream gradients steepened and erosion increased. The steepened stream gradients allowed the volcanic material from the Tuscan Formation along with coarse, bouldery alluvial material to be deposited as the Red Bluff Formation (Harwood & Helley, 1987; Larsen et al., 2002).

One of the most detailed geologic maps of the Tuscan Formation in the Big Chico Creek area was part of a Master's thesis from San Jose State University (Doukas, 1983). Doukas' map of the Big Chico Creek area was incorporated into the map of Harwood and Helley (1987), focusing on structure, and using the simplified ABCD model to map the Tuscan units.

Holly Brunkal's (2003) Master's thesis describes Tuscan facies from three depositional systems: debris flow/ hyperconcentrated flood-flow facies; fluvial channel facies; and flood plain/overbank facies. The Tuscan Formation is divided into proximal,

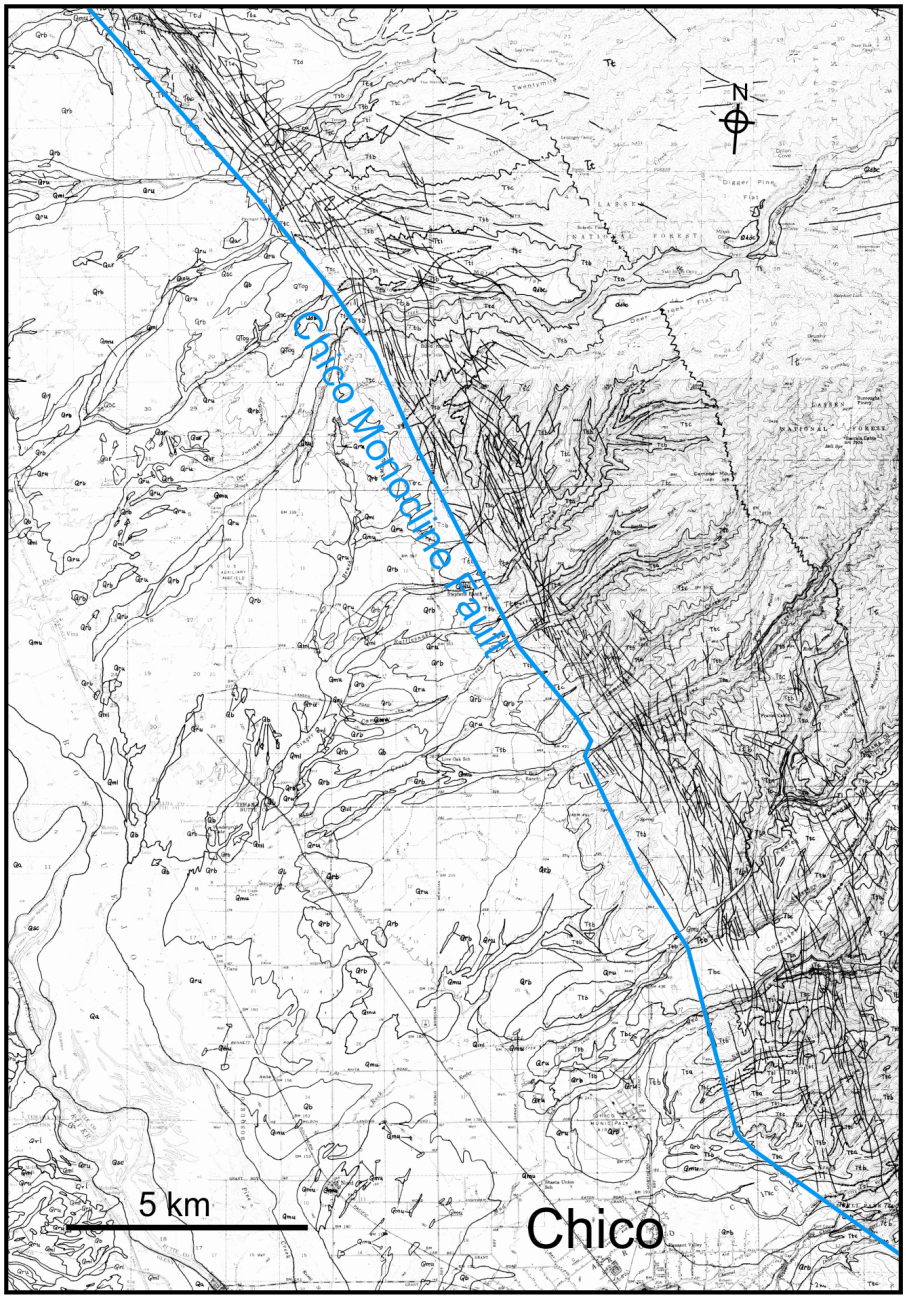

Figure 3. Map of Chico Monocline.

Map of the Chico Monocline and fracture zone. Strata are faulted and fractured by a major east-dipping reverse fault below the surface. Modified from Helley, E., Harwood, D. (1985), Geologic map of the late Cenozoic deposits of the Sacramento Valley and northern Sierran foothills, California. U.S. Geological Survey Miscellaneous Field Studies Map MF-1790: 24 pp., 5 sheets, scale 1:62,500.

medial and distal setting environments. Brunkal concluded that in the medial to distal setting, environments of the Tuscan Formation are fluvially dominated while the upper Tuscan is debris flow dominated. Brunkal's stratigraphic sections were measured at the Neal Road Landfill southeast of Chico, Tuscan Springs and at Upper Bidwell Park, east of Chico. While Brunkal's study provided a large scale study of the Tuscan Formation, only three stratigraphic sections were measured and do not provide enough detail to fully characterize the Tuscan Formation and its individual flow units.

Margaret Skartvedt-Forte's (2006) Master's thesis from Chico State University developed "three-dimensional stochastic realization derived from a geostatistical analysis" using Groundwater Modeling System (GMS) software. By adapting a volcanic fan apron model to the Tuscan Formation in her geostatistical analyses, Skartvedt-Forte (2006) was able to identify flow paths, connectivity of the water-bearing units, and confinement of the aquifer system. Skartvedt-Forte's (2006) study provided excellent numerical data and statistical probabilities; however, the study did not focus on incorporating geologic data into the model. Further detailed geologic information from mapping the Tuscan Formation would help make the model more applicable to groundwater modelers.

There have been many smaller, yet disjointed projects and abstracts by Chico State students and faculty on the Tuscan Formation which serve as good site specific studies (e.g., measured stratigraphic columns (Alward and Springhorn, 1996), paleocurrent analysis (Moody and Teasdale, 2006), and geochemical provenance studies (Hall, 2011)).

For example, Jennifer Hall (2011) studied the Tuscan Formation-Red Bluff Formation boundary. Hall looked at 13 samples from three wells located at Hegan Lane, Chico, drilled by the company Mactec, and funded by the company ABB. Cuttings from the wells were used to tabulate relative percentages of quartz grains, feldspar types, rock fragment types (metamorphic, volcanic, sedimentary) along with other diagnostic minerals. Hall was able to determine a boundary between the two formations; the Tuscan samples contained almost 100% volcaniclastic grains, and the Red Bluff samples consisting of a mixture of volcaniclastic, metamorphic, and sedimentary rock fragments. Hall concluded that the changes reflect a dominant volcanic source for the Tuscan grains that then switched to mixed sources for Red Bluff grains, which may have occurred during a 1 m.y. long uniformity between the two formations. This study will build on Hall's methodology by providing more data from additional wells.

Volcaniclastic debris flow processes from sedimentary textures in the southern Tuscan Formation were studied by Carlton et al. (2008). They studied two debris flow deposits (a top flow and bottom flow were identified; both flows are ~10 m thick) and measured clast size distribution as well as matrix grain size distribution from digital analysis of Back Scatter Electron (BSE) images. Carlton et al. (2008) also used XRD analyses to identify mineral phases in the matrix. They concluded that the top flow and bottom flow were both cohesive debris flows from a lahar deposit which was clay-rich and resisted inverse grading. Both flows contained cristobalite, opal, and montmorillonite, indicating that there must have been hydrothermal alteration of the volcanic rock due to the high concentrations of these minerals. The bottom flow was

interpreted as a transitional facies between a cohesive debris flow and a hyperconcentrated stream flow. However, Carlton et al. (2008) only described two flows of the Tuscan Formation making it difficult to apply their data to the entire unit.

Linberg et al. (2006) characterized the lithology of the Tuscan Formation debris flows in Big Chico Creek. Major element XRF analyses of clasts from the debris flow units are dominated by calc-alkaline, medium-K series basaltic andesites, but range from basalt to andesite. Mafic lithics and olivine crystals were found in the sandy matrix. Lindberg et al. (2006) believe that the source of the Tuscan Formation flows came from an ancient cinder cone or series of mafic cinder cones similar to the modern Cascades called the Yana Volcanic Center, which include the ancient volcanos Mount Yana and Mount Maidu. Based on radiometric K-Ar and Ar-Ar dating of samples from the Yana Volcanic Center, volcanic activity occurred between 2,695 +/- 79 and 3,030 +/- 38 Ka. These dates coincide with the age constraints of the Tuscan, the Nomlaki Tuff (3.27Ma) and Ishi Tuff (1.8 Ma) providing further evidence the Tuscan is a remnant from the Yana Volcanic Center.

Difficulties Defining Tuscan Stratigraphy

Age Dating

Age constraints on the Tuscan Formation are from the Ishi Tuff (1.8 Ma) and the Nomlaki Tuff (3.27 Ma).This assumes that the Nomlaki Tuff is the basal unit of both the Tuscan Formation and the Tehama Formation (Lydon, 1969). The late Pliocene age is based on Blancan fauna found in the Tehama Formation 10 feet above the Nomlaki Tuff,

6 miles northwest of Flournoy (Russell and VanderHoof, 1931). Potassium-argon dates by Evernden(1964) support the age of 3.3 million years to 1.5 million years. Extrapolating downward from the top of Chron C2An.2r, Henry and Perkins (2001) estimate the age of the Nomlaki ash bed at 3.27 ± 0.04 Ma using the Cande and Kent (1995) magnetic polarity timescale.

Due to the reworked nature of the Nomlaki Tuff, identification in the field is difficult and it can often be mistaken for other units. Currently, there is no chemical identification of Nomlaki Tuff in Upper Bidwell Park. In addition to potential misidentification of the Nomlaki Tuff, age dated samples are 25 miles from Upper Bidwell Park providing further age uncertainty in the study area.

Terminology

The Tuscan Formation has been defined as a lahar by Lydon et al. (1968). However, the definition of "lahar" has been used in many different ways by different researchers. It is therefore difficult to simply lump the Tuscan in an arbitrary category such as a lahar because it is a much more complex formation containing deposits from debris flow facies, fluvial facies and transitional flow units. Smith and Lowe (1991) explain that traditionally, lahars have been described as volcanic debris flows and their deposits. Lahars have also been described as a more complex phenomenon consisting of rapid flowing sediment, mixture of rock, debris and water from a volcanic event or events, as well as multiple flow types and transformations. The term "lahar" has also commonly been used to describe any poorly sorted volcaniclastic sedimentary deposits,

even if the unit is lacking evidence for debris flow deposition. Due to the ambiguous definition of "lahar", it has been suggested by Smith (1986) that the term be abandoned.

Another term often used when describing the Tuscan is diamictite: any poorly sorted sedimentary rock with great variation in clast sizes, potentially encompassing breccia and conglomerate (Schoenborn and Fedo, 2012). The term diamictite describes sedimentary features of the Tuscan Formation but it does not fully encompass the complex variety of depositional processes of the formation. More descriptive terms such as debris flows, hyperconcentrated flows, debris avalanches and normal stream flows may be more appropriate when describing the Tuscan Formation.

Finally, the Tuscan has historically been referred to as a "tuff breccia." A tuff is defined as deposits that are composed of mostly reworked ash, directly ejected from a volcanic source. While the Tuscan contains tuff deposits (e.g., Ishi Tuff, Nomlaki Tuff and thin beds of tuff), it is not a true tuff. Rather, it contains a complex structure consisting of interbedded debris flow breccias, intermediate hyperconcentrated flow deposits, conglomerates and sandstones from normal stream flows.

Smith (1986), Smith and Lowe (1991), and Walton and Palmer (1988) give full descriptions of lahars, volcanic debris flows and their lithofacies. Although these studies were conducted in the Marysvale Volcanic Field, Utah, and Mount St. Helens, their facies and depositional environments are similar to that of the Tuscan Formation. Smith and Lowe's (1991) study defines flow types within lahar deposits as normal stream flows, hyperconcentrated flows, debris flows and debris avalanches. Normal stream flows are turbulent leading to abundant traction-related structures. Deposits may contain well

sorted cross-bedded sands with scour-and-fill structures though poorly sorted deposits with angular grains can occur. Hyperconcentrated flow is only partially turbulent, may be normal graded, coarse grained, and can often resemble high-density turbidites. Debris flows have poor sorting, reverse to normal grading and were deposited en masse. Debris flows are commonly laminar though exceptions occur on steep slopes where it is possible to have turbulent flow. During extreme conditions, large voluminous landslides can produce debris avalanches. Due to transportation of large block source material "hummocky upper surfaces" often called "lahar mounds" may be created in debris avalanches.

This thesis will utilize the terminology normal stream flow, hyperconcentrated flow, debris flow and debris avalanche when describing the Tuscan deposits as an alternative to lahar and diamictite.

Modern Analogs

In order to interpret ancient volcanic sequences and the sedimentology of volcaniclastic deposits, understanding the processes, facies, textures, sedimentary structures, and composition of modern volcanic sediments is vital (Vessell and Davies, 1981; Skartvedt-Forte, 2006). Three examples that have particular relevance to Tuscan deposition include: 1) Mt. Fuego, Guatemala, 2) Mt. St. Helens, Washington, and 3) Casita and San Cristóbal, Nicaragua.

Mount Fuego, Guatemala

Observations by Vessell and Davies (1981) on the modern volcanic regions, more specifically, the modern forearc basin of Guatemala, can be used to correctly interpret and model ancient volcanic sequences such as the Tuscan Formation. Due to volcanic activity, the modern forearc basin of Guatemala, an area between the volcano Mount Fuego and the Pacific coast receives non-marine sediments from the deposition of airfall ash, debris avalanches, debris flows, and fluvial sedimentation (Vessell and Davies, 1981 and Skartvedt-Forte, 2006). According to Vessell and Davies (1981) (Figure 4), volcanic sediments progressively change in characteristics with increasing distance from the magmatic arc: 1) volcanic core facies, 2) proximal volcaniclastic facies, 3) medial volcaniclastic facies and 4) distal volcaniclastic facies. Distinctions between these four facies are based upon lithology, grain size, sedimentary structures and genesis. In order to place Tuscan deposition in proper context, all four facies will be discussed below; however, based on field observations in Big Chico Creek Canyon, the distal volcaniclastic facies appear to be the most appropriate analog.

Sediments in the proximal volcaniclastics facies consist of matrix-supported breccia interbedded with volcanic ash. Grain sizes are extreme, ranging in clay size to boulders +/- 6 meters in diameter. Thickness of breccia beds range from 0.5 to 15 meters and form the dominant rock type in this facies, and are a product of debris avalanches. Interbeds of airfall ash are deposited during episodes of debris avalanche inactivity, and are often preserved due to the non-erosive bases of debris avalanches. Fluctuations of eruption intensity can be measured by size grading of individual ash beds: 1) ash beds are

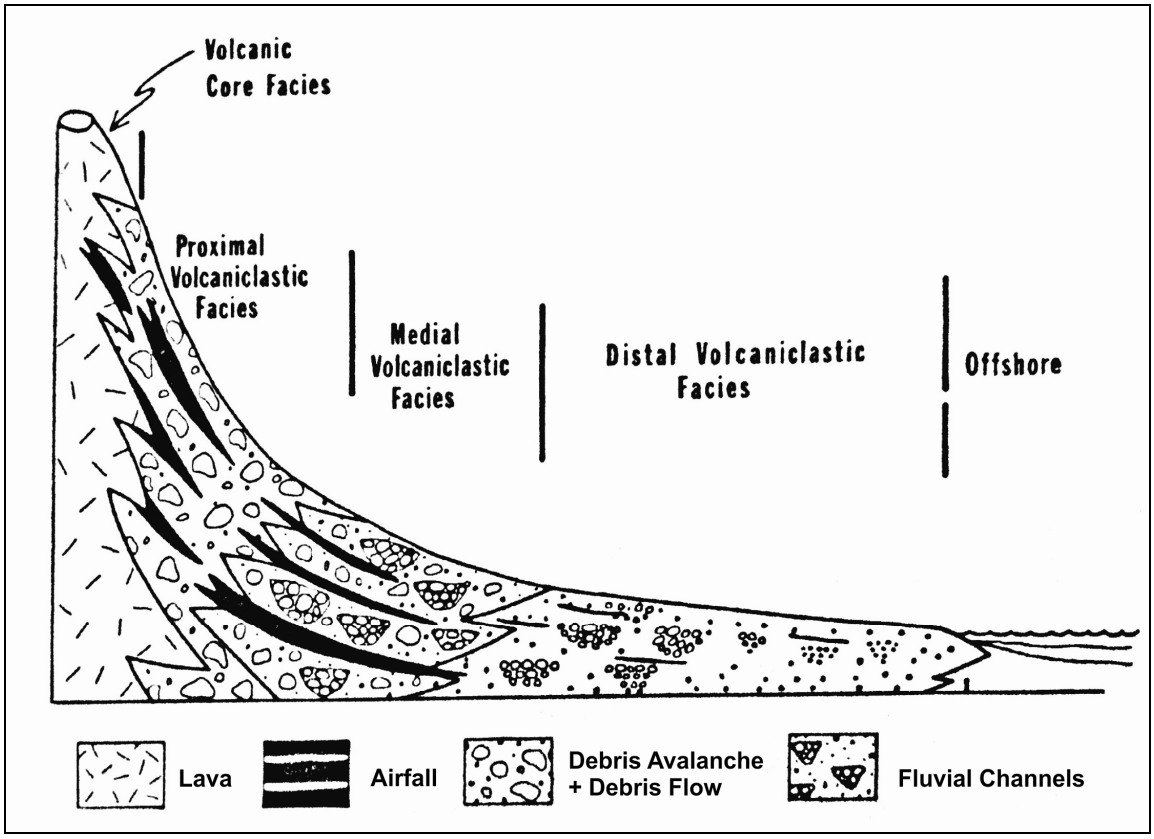

Figure 4. Volcanic Apron Model.

Four distinctive facies may be recognized in the lateral and vertical distribution of deposits: volcanic core facies, proximal volcaniclastic facies, medial volcaniclastic facies and distal volcaniclastic facies. Modified from Vessel, R.K., and Davies, D.K., 1981, Nonmarine sedimentation in an active fore arc basin: Soc. Econ. Paleont. Mineral. Publ. 31, p. 31-45 (Fig. 4).

reverse graded during an increase of eruption intensity 2) normal graded (upwards fining) beds are a result of decrease eruption intensity. Grading is a result of eruption intensity rather than transport distance.

Medial volcaniclastic facies consist of interbedded matrix-supported breccia and conglomerate, often with coarse sand and thin layers of ashfall. Observations of freshly deposited units in Guatemala display parallel bedding that alters after three to five

years exposure due to extreme weathering and diagenesis. Breccia in the medial facies are produced by debris flows due to the saturation of loose, unconsolidated debris avalanche deposits during times of intense tropical rains. Volcano Fuego debris flows contain less than one percent clay, are non-turbulent, with high yield strength capable of moving large boulders +/- 6 meters in diameter. Similar to the debris avalanches, debris flows do not have erosive bases, preserving airfall ash blankets in the mid-fan and fan-based areas of alluvial fans. Conglomerates and coarse sands are produced from fluvial activity in channels during floods and almost always erode airfall ash beds. Rapidly aggrading systems, coarse sands, and conglomerates dominate distal volcaniclastic facies. Braided or meandering fluvial systems dominate sedimentation, but most sedimentation occurs during floods.

Based on observations in Guatemala, fluvial deposits pose a special problem of recognition because of their high degree of variability. Vessell and Davies (1981) generalize coarse grained fluvial deposits occur near the cone, in areas of high slope, associated with alluvial fans, often being difficult to distinguish from debris flows. However, fine grained fluvial sediments are deposited in flood and low stage flow, occurring in low-sloped areas and coastal plains. In ancient volcaniclastic deposits recognition is difficult because of their susceptibility to rapid digenesis.

Studies on the active volcano Mount Fuego have shown that sedimentation occurs during repeated cycles, each cycle consisting of four phases. Phase 1 is the Inter-Eruption Phase, characterized by lows rates of sedimentation, incision and meandering streams, and delta re-working lasting 80-125 years. Phase 2 is the eruptive phase and is

dominated by ejection of airfall ash and debris avalanches lasting up to one year. Phase 3 is the fan building phase dominated by debris flows and deposition of coarse grained fluvial sediments and can last up to two years after the eruption. Phase 4 is the braiding phase lasting up to 20-30 years after the eruption and it is characterized by large volumes of sediment in the stream system, transformation of the incised meandering channels to braided channels, and rapid deltaic progradation. Change from meandering to braided channels is a response to the amount of sediment introduced into the fluvial system, rather than change of slope or rainfall. Sedimentation in the Tuscan Formation has apparent cyclicity similar to Mount Fuego with all four phases represented within the Tuscan deposits. Due to the lack of age dating within the Tuscan, modern volcano analogs such as Mount Fuego, may provide some insight into timing and the cyclical patterns that may have occurred during deposition of the Tuscan.

Mount St. Helens, Washington USA

Mount St. Helens, located in the Cascade Range of southwestern Washington has been one of the most thoroughly studied volcanoes following the May 18, 1980 eruption (Major et al., 2005). Many of these studies conducted on Mount St. Helens include research on both prehistoric and modern debris flow events. Modern day debris flows from Mount St. Helens may be very similar to that of the Pliocene-aged Tuscan Formation based on depositional texture as well as the transport distance from Mount Yana to Big Chico Creek Canyon (Figure 5). Studying these modern debris flows provides evidence for what may have been the catalyst of the Tuscan Formation's large debris flows.

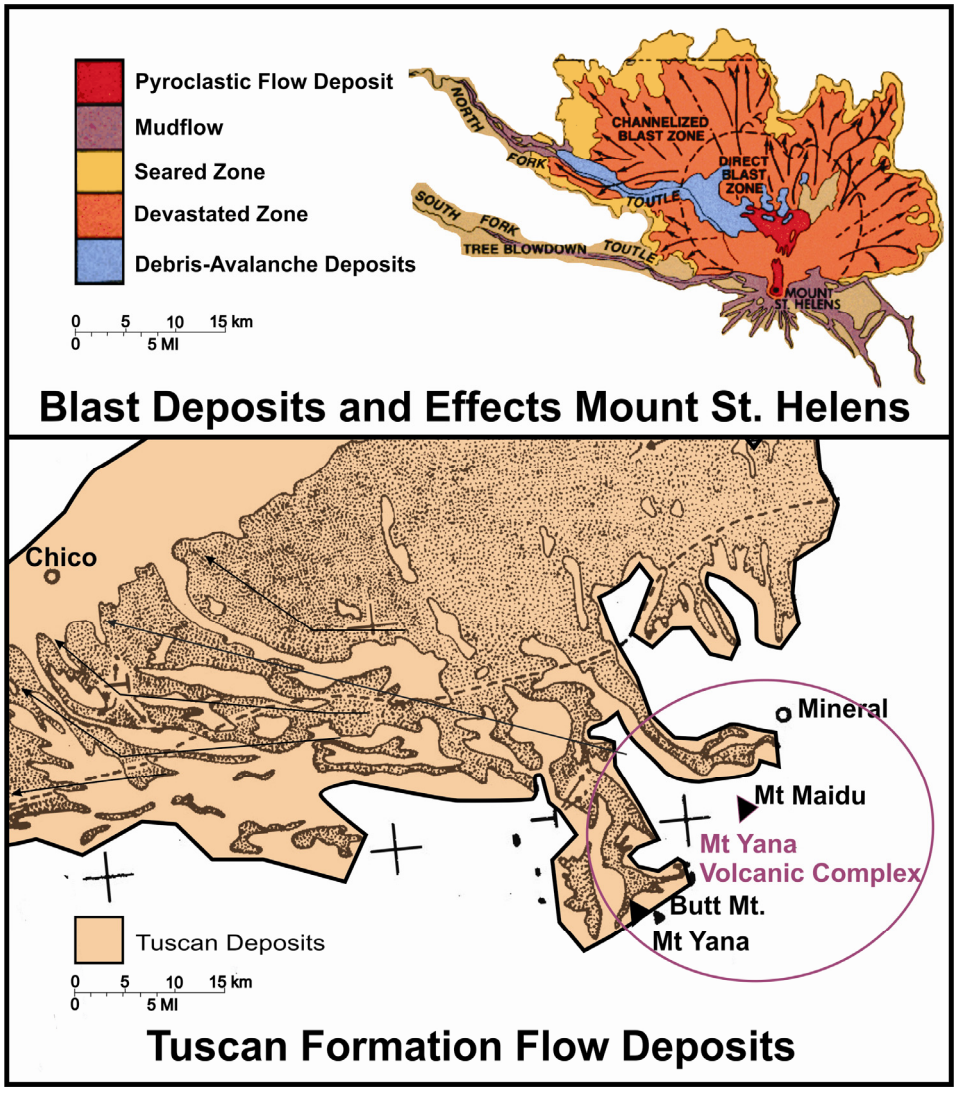

Figure 5. Flow comparison of the Tuscan Fm. vs. flows of Mount St. Helens 1980 eruption.

Map depicts a flow comparison of the Tuscan and flows from Mount St. Helens 1980 eruption. Both maps are the same scale. Although the Tuscan encompasses a much larger area, deposits from the Tuscan and Mount St. Helens flows follow channelized pathways. Black arrows represent flow direction. The lower figure is modified from Lydon, P.A., 1968, Geology and Lahars of the Tuscan Formation, Northern California. Geological Society of America Memoir, p. 441-475 (Fig. 3); the upper figure is modified from Keiffer, S.W., 1981, Fluid dynamics of May 18 blast at Mount St. Helens, The 1980 eruption of Mount St. Helens, Washington: U.S. Geological Survey Professional Paper 1250, p. 379-400..

Mount St. Helens has erupted and discharged debris flows episodically for more than 50,000 and possibly up to 300,000 years (Crandell, 1987). Mullineaux and Crandell (1962) state that eruptions from Mount St. Helens have produced numerous debris flows, some extending more than 40 miles down western valleys of the volcano. Debris flows tend to be composed mainly of nonvesicluar rock fragments, attributing their great distance of mobility to water rather than gas emitted from particles in the matrix.

Within a few minutes of the May 18, 1980 eruption, numerous debris flows were generated on Mount St. Helens, two of the largest debris flows originated on the eastern side of the volcano (Pierson, 1985) travelling up to tens of kilometers (Major et al., 2005).

According to Pierson (1985), two larger debris flows ran down two parallel channels (Pine Creek and Muddy River) into the Swift Reservoir. Peak debris flow discharge probably exceeded 250,000 m^3/s initially, but decreased exponentially as it flowed in the downstream direction. Erosion and deposition in the flow path exceeded 1.4 x $10^7 m^3$ of water and rock debris. Two large debris flows evolved from a single surge that was gas mobilized and turbulent, incorporating water most likely from melted snow and groundwater expelled during the initial explosion. Deposits in the debris flows contained angular to sub-angular cobbles of blue-gray dacite with a sandy matrix (Janda et al., 1981).

Modern debris flows from Mount St. Helens demonstrate how complex and variable debris flows from snow-clad volcanoes can be. Debris flow events can be

triggered by a variety of mechanisms consisting of the melting of snow pack that is then mixed with volcanic debris during eruptions, landslides, flood surges, glacier outburst floods, and rainfall (Major et al., 2005). Multiple mechanisms triggering debris flows can occur during a single eruption event. Similar triggers are likely to have caused debris flows in the Tuscan Formation.

Debris flows generated by melting of snow pack are common during eruptions of Mount St. Helens. Melting of snow pack flows tend to have short-lived hydrographs (discharge vs. time) and flow away from the volcano immediately (Major et al., 2005). Gigantic landslides can form during eruptions and rainfall, creating debris avalanches that can directly or indirectly generate destructive and very large debris flows. Major et al. (2005) construe that transformation from a debris avalanche to a debris flow may occur from a variety of ways: 1) direct transformation due to rainfall, 2) dewatering and local liquefaction, and 3) breaching of impounding lakes, forming flood waters that entrain sediment and evolve into debris flows. One of Mount St. Helens' larger known debris flows was caused by such an event when a landslide created dewatering and liquefaction to form a (108 m^3) debris flow that moved through the North Fork Toutle River (Janda et al., 1981).

Major et al. (2005) study of debris flows at Mount St. Helens suggest that debris flows undergo distal transitions of flow character from debris flows to hyperconcentrated flows and eventually to sediment-laden floods. Debris flows containing more than 3-5% clay sized sediment are more likely to maintain textual integrity over tens of kilometers travel distance, whereas debris flows containing less clay

tend to transform distally into hyperconcentrated flows over similar distances. Debris flows lacking clay are non-cohesive, eventually mixing with river flow, diluting, and dropping their gravel load, transforming into sandy flows that progressively develop into sediment-laden stream flows. Debris flows at Mount St. Helens typically have a lower clay percentage.

Similar to deposits in the Tuscan Formation, thickness of deposits vary greatly at Mount St. Helens and are highly influenced by topography and flow genesis. Major et al. (2005) ascertain that debris flows from ancient lake breakouts produced the thickest and most extensive deposits along the Toutle River Valley, forming a widespread terrace underlain by twelve meter thick cobble-rich sediment. Flows produced by snowmelt, liquefaction and dewatering, heavy rainfall, and glacier outburst floods produced thinner and less extensive deposits. Although topography exerts greater control on deposit thickness than genesis, inferring relationships between deposit thickness, flow depth, and the depositional process is difficult. Flows can deposit sediment progressively from head to tail, developing deposits that are thick relative to flow depth. In addition, multiple flows can stack without obvious stratigraphic distinction, producing deposits that appear to be from a single flow of *en masse* deposition. Stacked debris flows taking the form of a single flow may exist within the Tuscan Formation deposits.

Debris flows textures at Mount St. Helens vary widely, but they share common traits and generally can be separated into channel and floodplain facies (Major et al., 2005). Deposition of channel facies sediment occurs by flow within a confined channel, whereas deposition of floodplain facies sediment occurs by flow that spills over

channels. Channel and floodplain facies are composed of deposits that are typically poorly sorted, massive (unstratified), and consist of fragmental sediment ranging in size from microns to meters. Channel facies deposits are generally coarser than floodplain facies deposits, and are likely to have a framework that is clast-supported. Both channel and floodplain facies of debris flow deposits exhibit variations in grading, size, and dispersal. In both channel and floodplain facies, the coarsest gravel deposited can vary in size from only a few centimeters in diameter to several tens of centimeters in diameter; gravels may be randomly distributed within deposits, exhibit inverse grading or exhibit normal grading. Gravels are commonly inversely graded near the base of a deposit, ungraded in the medial section, and normally graded near the top of a deposit. Mount St. Helens debris flows contain high percentages of angular volcanic clasts that have not been reworked. However, stream alluvium entrained from channel beds and banks consisting of rounded clasts can also be incorporated.

Ancient and modern deposits at Mount St. Helens show that debris flow events are not random events but are clustered in time with volcanic eruptions. While floods are traditionally considered independent events with random distribution over time, Mount St. Helens has a history of large debris flows occurring during discrete eruption periods, separated by long dormant intervals ranging from a few centuries to many millennia (Major et al., 2005). Additionally, within these eruptive periods, debris flows commonly are clustered in time with a few years containing a series of flows followed by a dormant period (Scott, 1989).

Simple frequency analysis paints a poor picture due to the intermittent nature of eruptive periods. However, by focusing on periods when the volcano was active, a more accurate estimate of average recurrence intervals can be ascertained. The average recurrence interval of eruptions over the past 4,500 years is 130 years, using 15 overbank flows during the 1,930 years considered to be within eruptive periods (Scott, 1989). Based on the assumption that flow depths and deposit thicknesses from modern relationships apply to ancient flows, debris flows are capable of inundating floodplains throughout Toutle Valley to depths of at least two meters recurring at approximately 100 year intervals during periods of volcanic activity. Over the next few centuries, large debris flows from Mount St. Helens having discharges of several m^3/s should be anticipated (Major et al., 2005). Although precise date ranges do not exist for the Tuscan, it does appear to have an apparent cyclical pattern like Mount St. Helens. Studies of recurrent intervals of similar volcanic settings to the Tuscan may help to better understand the timing of Tuscan flows.

Casita and San Cristóbal, Nicaragua

Casita and San Cristóbal are part of a volcano complex in the Cordillera de Los Maribios, a 70 km segment of the Central American Volcanic Belt, and have been studied extensively by Scott et al. (2004), Vallance et al. (2004) and Kerle et al. (2003). Stratovolcano San Cristóbal is the highest, at 1745 m and currently the only active volcano in the complex. Stratovolcano Casita is 5 km east of San Cristóbal. It is the oldest of the volcanic complex Cordillera de Los Maribios and it is composed of a cratered ridge. The last eruption of Casita is estimated to be 8300 years ago. During late

October to early November 1998, torrential rains from Hurricane Mitch caused numerous volcanic slope failures. The largest and most devastating slope failure occurred at the Casita Volcano. Due to slope failure, a debris avalanche developed triggering a 3.5 million m^3 debris flow covering an area of approximately 12 km^2. Casita's debris avalanche transitioned from a debris avalanche to a hyperconcentrated flow and then to a debris flow as it moved down slope. The debris flow moved 10 km from its source downstream. The towns of le Porvenir and Rolando Rodriguez were destroyed in just 3 minutes by a 1-1.3 km wide debris flow with an average depth of 3-5 m. The 1998 Casita debris flow exposed at least three large debris deposit pathways providing further evidence that modern debris flows frequently flow along the same pathways over time (Vallance et al., 2004).

The source area of the debris avalanche on Casita contains volcaniclastic debris, fractured andesite and hydrothermally altered rock. Initiation, magnitude and behavior of the avalanche are most likely controlled by the highly porous, permeable material overlying the impermeable and hydrothermally altered rock. Water may have permeated the fractured and volcaniclastic parts of the failure area, while the more impermeable altered rock at depth would have forced pore water outward towards the slope, weakening resistance, and ultimately leading to slope failure. Fractures filled with water predating the 1998 debris flow event may have also lead to slope failure. The debris avalanche created from slope failure quickly released infiltrated water and transformed the flow into a hyperconcentrated flow. Aided by a slope angle of approximately 18 degrees, within 2.5 km from source, the hyperconcentrated flow

entrained enough sediment, to transform into a debris flow. Clast size ranged from boulder and cobble to pebbly clasts in a muddy matrix in the debris flow deposits. In the distal run out area, smooth, muddy deposits with few clasts were dominant.

Due to hydrothermal alteration, structural integrity of a stratovolcano is reduced. The reduction in integrity may persist long after magmatic activity has ceased leading to collapses creating debris avalanches which in turn can transform into debris flows. Active volcanoes such as San Cristóbal are less affected by intense rainfall, producing smaller flows in comparison to older, dissected and hydrothermally altered volcanoes like Casita. Casita demonstrates that large scale debris flows can exist on inactive volcanoes. The Tuscan Formation deposits are massive compared to modern volcanoes. A possible explanation is massive debris flows and hydrothermal alteration could have taken place on the Tuscan Formation long after magmatic activity ceased in the Mount Yana volcanic core complex.

CHAPTER III

METHODS

Data from the field component of this study consisted of eight stratigraphic sections on Musty Buck Ridge in Upper Bidwell Park and one section from Big Chico Creek Ecological Reserve (BCCER) (sections 6-13) (Figure 6). In addition, five southern sections (sections 1-5) in Upper Bidwell Park, mapped by Alward and Springhorn (2006) were included in the dataset. One stratigraphic section on the opposing southern ridge, Highway 32 ridge, created by Greene (2014, unpublished) was used to determine if flows are heterogeneous or homogenous between ridges.

Traditional stratigraphic mapping methods using a Jacob staff were used to measure unit thickness. Defining characteristics were defined and documented during field observations such as sedimentary structures, grain size, sorting, rounding of clasts and percentage of ash. Structural photogeologic mapping using acquired high-resolution cliff photographs taken by helicopter of Upper Bidwell Park and the BCCER helped document thickness, length, width, depositional trends, and internal textures of various flow units in the Tuscan Formation (Figure B-2). These photos complemented on-ground field work, providing a foundation for recognizing larger scale features and trends which would otherwise go unnoticed. After stratigraphic sections were mapped, they were combined with Alward and Springhorn (2006) stratigraphic sections and drafted on a panel. From the stratigraphic sections, lithofacies were created and then combined to

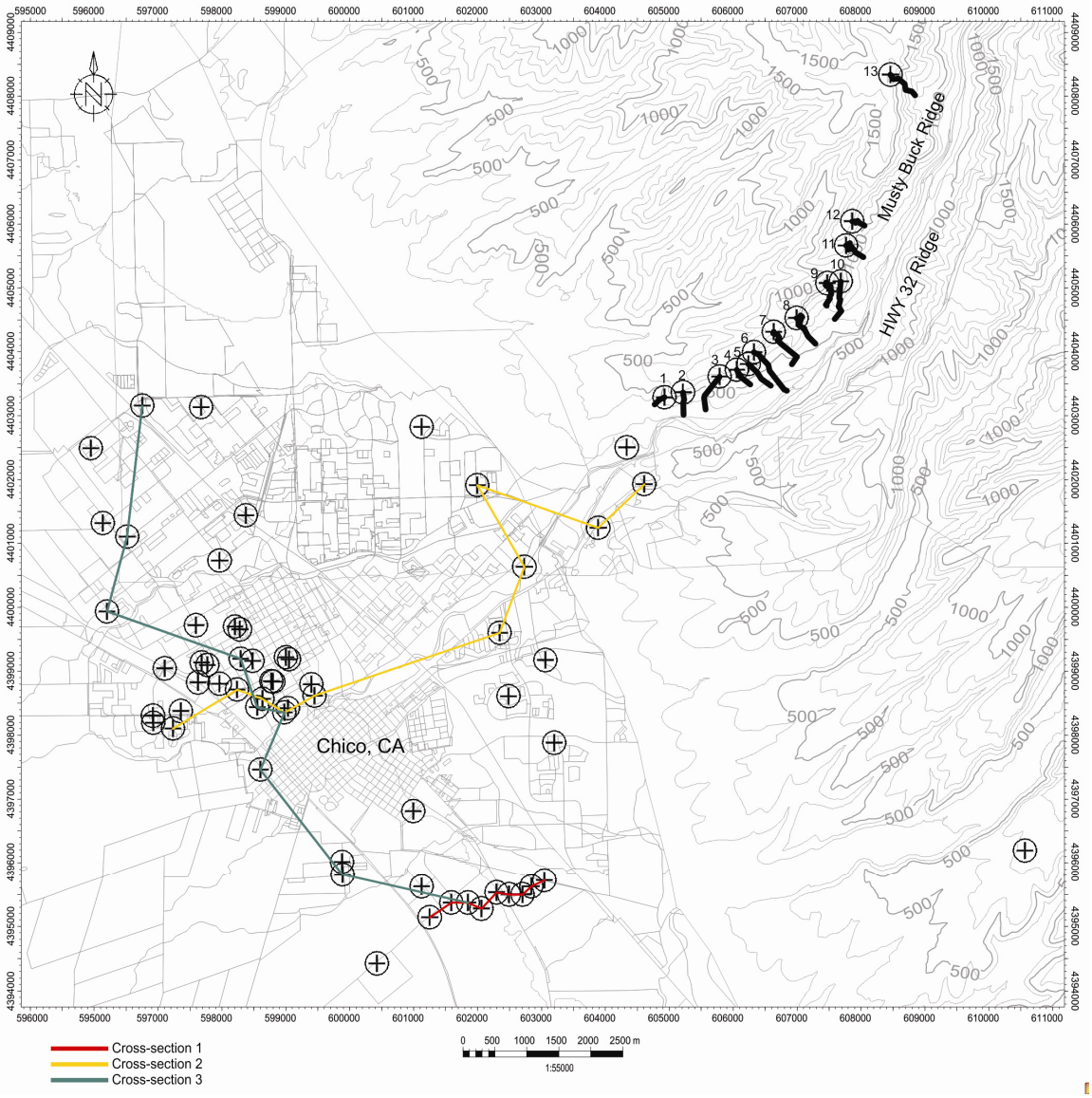

Figure 6. Map of sections 1-13, well locations, and cross-section location.

Map shows the location of 13 stratigraphic sections, 50 wells, and cross-sections 1-3. Five southern sections (sections 1-5) in Upper Bidwell Park were mapped by Alward and Springhorn, 2006.

create facies associations. Facies associations are used to define the Tuscan's sedimentary environments.

GPS locations of key surfaces were also acquired and then inputted into a 3-D modeling program (e.g., Petrel) to display the stratigraphic framework with the goal of correlating into the subsurface using nearby wireline logs of water wells. The laterally continuous surfaces were categorized from oldest to youngest as Musty Buck Ridge (MBR) 1 through 11.

The subsurface component of the study focuses on composition, texture and geometry of the Tuscan Formation in order to establish a Red Bluff Formation–top Tuscan Formation boundary. Petrographic analysis of sandstone well cuttings as well as geophysical analysis of well logs from Cal Water Service wells helped to determine a geologically-based stratigraphic boundary between the top of the Tuscan Formation (~1.8 million years old) and the overlying base of the Red Bluff Formation (500 thousand to 1 million years old).

Well cuttings samples derive from a monitoring study of the Skyway Plume in south Chico by the company ABB. The sonic drill cores produced continuous core, up to 250 feet deep, making it possible to precisely locate the sample depth. A total of 79 thin sections were produced from 3 wells, MW9, MW11, and MW13 (Figure 7). Well cuttings samples were sieved into 3 size fractions: mud, sand, pebbles. The sand-sized fraction was washed, cleaned, and sent to a lab to create thin-section grain mounts (false-rock stubs of epoxied sand grains glued to a glass slide and ground down to 30 microns thick). Using a petrographic microscope, grains were point counted to identify and record compositions of 300 sand sized grains per sample. Percentages of key diagnostic minerals were collected and recorded as relative percentages of: monolithic quartz (Qm),

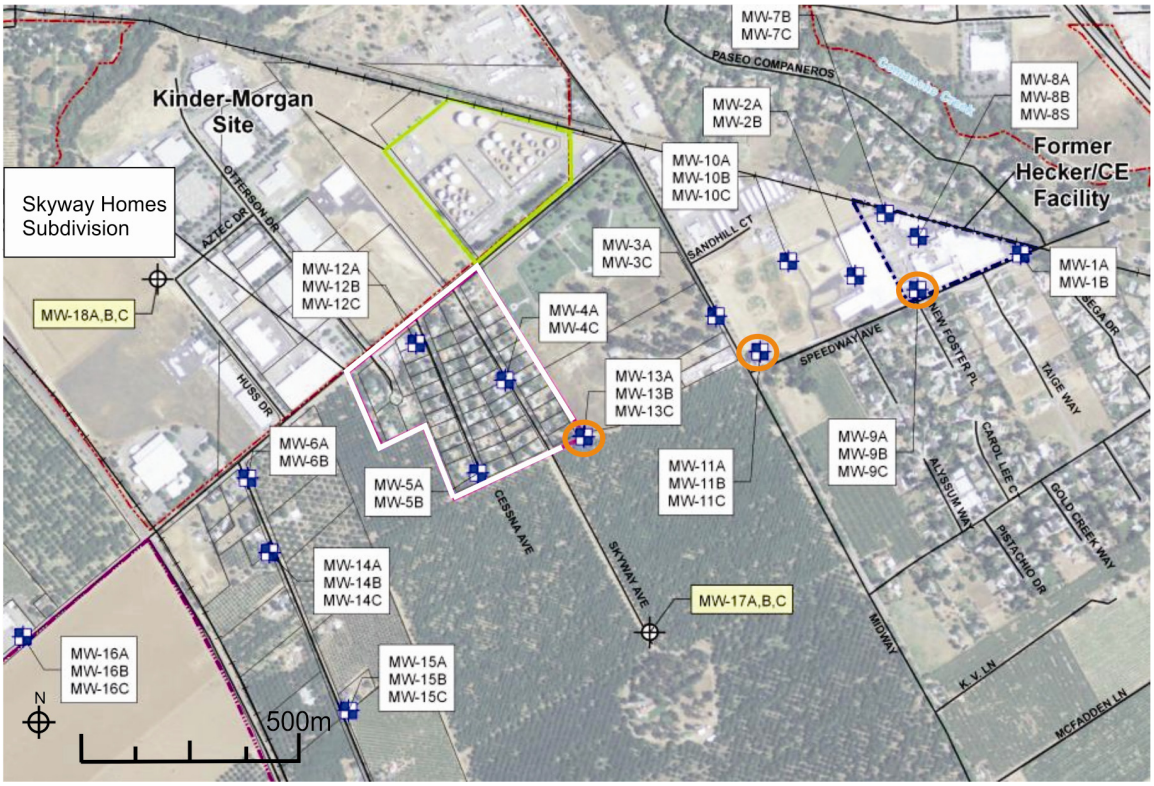

Figure 7. Map of Monitoring Wells (MW) in southern Chico. Seventy-nine thin sections were produced from 3 wells, MW9, MW11, and MW13 (circled is orange).

Modified from Mactec remedial investigation/feasibility study work plan, Skyway subdivision groundwater plume, Chico, California, 2008.

polycrystalline quartz (Qp), potassium feldspar (kspar), plagioclase (plag), lithic rock fragments (volcanic (Lv), metamorphic (Lm), sedimentary (Ls)), pyroxene and olivine (py/ol), micas, heavy minerals, and pumice. Grains of eroded, re-deposited sediment called intraclasts (Int) were tabulated as well.

Mineral percentages were used to determine a compositional change from the Red Bluff Formation to Tuscan Formation. Once a boundary had been determined, data was plotted along depth of the corresponding well log where it could be used as a baseline for correlation.

A map of the Red Bluff- top Tuscan boundary in the subsurface was created by correlating the petrographic analysis to nearby wireline logs. From these initial correlations, 50 wells in the Chico area with geophysical data were used to help define the Red Bluff-top Tuscan boundary in the subsurface. In addition to looking at resistivity, well completion reports (Appendix E) were used to identify compositional changes in the well that may indicate a boundary between the Tuscan Formation and the Red Bluff Formation. Three cross sections of the wells were produced to display the Red Bluff Formation-Tuscan Formation boundary (Figure 6). Cross-section 1 consists of the wells used for petrographic analysis, MW9, MW11, and MW13. Cross section 2 follows along dip of the Red Bluff Formation-Tuscan Formation boundary surface. Cross section 3 follows the surface along strike.

CHAPTER IV

RESULTS

Lithofacies Description

Lithofacies are subdivisions of sedimentary sequences based on lithology, grain size, physical, and organic sedimentary structures which predict a sedimentary environment from the defining characteristics (Siemers and Tillman, 1981).

For this study, eight lithofacies were identified in the Tuscan Formation. Each lithofacies is assigned a corresponding facies number. Facies associations were constructed by grouping characteristic lithofacies. Sedimentary environments were then interpreted from the facies associations: volcanic debris flows, channelized active creeks, and flood and distal deposits (Table 1).

L-1: Breccia, Matrix-Supported Lithofacies

L-1 (Figure 8) beds are commonly deposited as massive (structureless) thick deposits, ranging in thickness from 2 meters to 35 meters. *L-1* typically has a poorly sorted, fine- coarse sandy matrix. Clasts are angular to subangular, varying in average diameter from 1 centimeter to 3 meters boulders. Most *L-1* beds are structureless and non-graded, though reverse to normal grading does occur. Rip-up clasts, scoured surfaces and channel filling are also common. Typically, contacts between beds are sharp.

TABLE 1. LITHOFACIES

Facies No.	Lithofacies	Sedimentary Structures	Interpretation	Grain Size of matrix	Clast Size in diameter	Thickness Range
L-1	Breccia-matrix-supported	Poor sorting, reverse to normal grading when deposited en masse.	A large scale debris flow, formed when water rich, volcanic rock, and mud move down slope, commonly on active volcanoes.	Fine-Coarse sand	1cm-3m	2m-35m
L-2	Breccia-clast-supported		A large scale debris flow, formed when water rich, volcanic rock, and mud move down slope, commonly on active volcanoes		1cm-1m	0.5m-5m
L-3	Reworked tuff	Re-worked ash	Directly ejected from a volcanic source during an active airflow.	Very fine ash	.05cm-6cm	4cm-3m
L-4	Conglomerate-matrix-supported	Well-rounded clast , may be normally graded	Formed in active creeks, hyper-concentrated flows	Medium-Coarse sand	5mm-10 cm	2cm-3m
L-5	Conglomerate-clast-supported	Well-rounded clast. Clast are often imbricated	Formed in active creeks		1cm-0.5m	10cm -9m
L-6	Massive Sandstone	Massive, lacking sedimentary structures (e.g., cross bedding, planar laminations, or ripples). Often contains white lithics, which may be pumice fragments	Formed in active creeks. Represents fast deposition, intense bioturbation, or too weathered to see sedimentary features.	Fine-Very Coarse sand	3mm-1cm	2cm-5m

Table 1 (continued).

Facies No.	Lithofacies	Sedimentary Structures	Interpretation	Grain Size of matrix	Clast Size in diameter	Thickness Range
L-7	Cross Bedded and Planar Laminated Sandstone	Deposits may contain cross-bedded sands, be well sorted or poorly sorted with angular grains. Scour- and-fill structures are common in normal stream flow. May be normal graded, and can resemble high density turbidites (Smith and Lowe, 1991)	Formed in active creeks during normal stream flow and hyperconcentrated flow. Normal stream flows are turbulent, with deposition by traction.	Fine-very coarse sand		2cm-1m
L-8	Mudstone	May have ripples, massive	Flood deposits	Mud-silt	2mm-2cm	1cm-2m

L-2: Breccia, Clast-Supported Lithofacies

L-2 (Figure 9) beds are thinner than L-1 with a thickness range of 0.5 to 5 meters. Bedding of L-2 on Musty Buck Ridge is generally thin, reaching a maximum thickness of 0.5 meters. The adjacent Highway 32 Ridge consists of thicker L-2, reaching a maximum thickness of 5 meters. Additionally, Highway 32 Ridge consists of larger, poor-well sorted clasts, up to 1 meter in diameter. Musty Buck Ridge clasts are poorly sorted, averaging in size from 1 centimeter to 1 meter.

Figure 8. Breccia, matrix-supported (L-1).

Large breccia composed of a coarse sandy-ashy matrix. Boulders can be up to 3 meters in diameter. Figure from section 13, 39°49'9.36"N, 121°44'0.06"W.

L-3: Reworked Tuff Deposits

L-3 is a deposit of reworked volcanic sandstone, silt and air-fall pumice. Volcanic clasts and pumice are rounded-subrounded, .05 to 6 centimeters in diameter. The Ishi Tuff (Figure 10) and Nomlaki Tuff are the two main tuffaceous deposits of L-3 in the Tuscan Formation. The Ishi Tuff is located between the two youngest breccia beds on Musty Buck Ridge. It is light grey-pink in color. The Nomlaki Tuff is white-light grey in color, and has been mapped by Doukas (1983) at the basal section of the Tuscan Formation. Thin, laterally continuous beds (4 centimeters to 0.5 meters) of angular, pumiceous layers are found close to the basal section of the Tuscan Formation. Due to the angularity of clasts, deposits do not resemble a true reworked tuff.

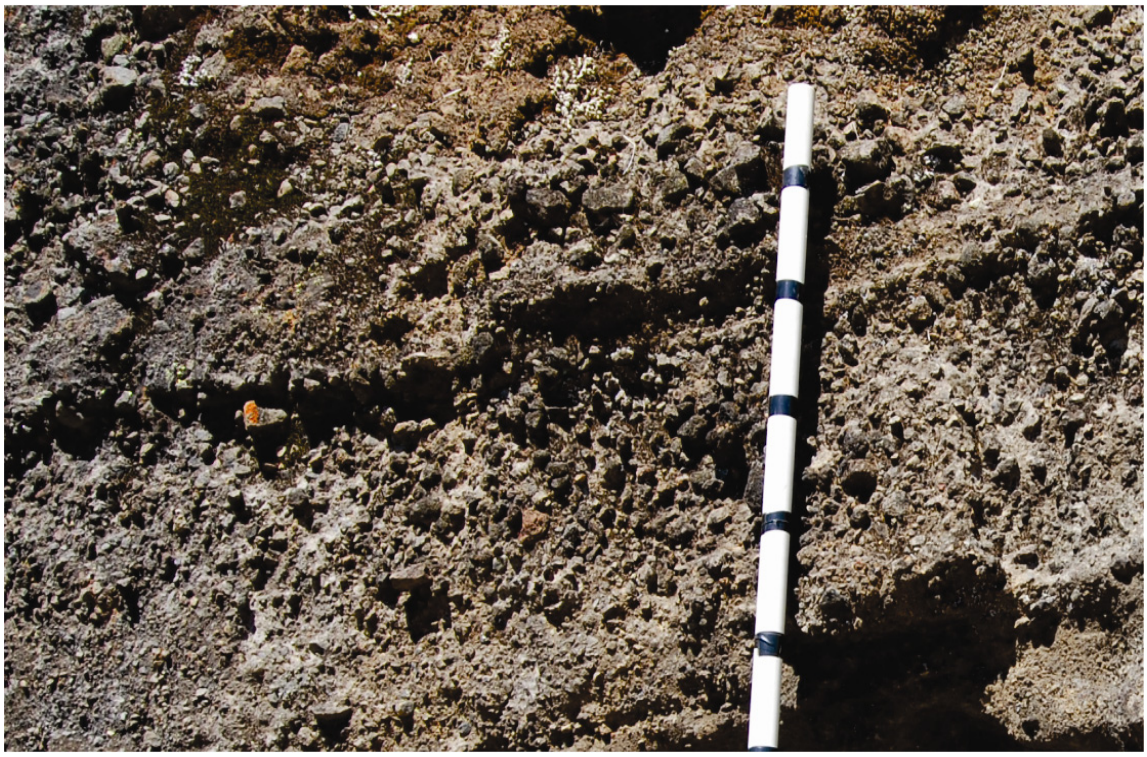

Figure 9. Breccia, clast-supported (L-2).

Deposit of a clast-supported breccia. Figure from section 13, 39°49'4.13"N, 121°43'52.11"W.

L-4: Conglomerate, Matrix-Supported

Volcanic basalt and andesitic basalt make up the primary clasts in L-4 (Figure 11). However, some metamorphic clasts occur at the base of the section. Clasts are poorly sorted, normally graded, rounded to sub-rounded, and 5 millimeters to 10 centimeters in diameter. Thickness of bedding is 2 centimeters to 3 meters. The matrix of L-4 is medium to coarse sand and can contain interbedded lenses of sandstone, cross bedded sandstone, mud, and ash.

Figure 10. Reworked tuff deposits (L-3).

Tuff deposits from the Ishi Tuff. Figure from section 9, 39°47'26.85"N, 121°44'45.44"W.

L-5: Conglomerate, Clast-Supported

Volcanic basalt and andesitic basalt are the dominant clast type in L-5 (Figure 12). Clasts are rounded to sub-rounded, and 1 centimeter to 0.5 meters in diameter. Clast-supported conglomerates contain less than 15% medium sand-to-ashy matrix. Thickness of bedding is 10 centimeters to 9 meters. Thick beds of L-5 are commonly found between contacts of large volcanic breccia beds. Imbrication of clasts is common.

Figure 11. Conglomerate, matrix-supported (L-4).

L-4 beds consist of rounded to sub-rounded clasts. Matrix can be very fine sands or ashy to coarse grained sands. Figure from section 2, 39°46'32.14"N, 121°45'14.65"W.

L-6: Massive Sandstone

Massive sandstone (*L-6*) can be found throughout the Tuscan Formation and lack any sedimentary structures (Figure 13). *L-6* is composed of well to poorly sorted, fine - coarse ashy sand and is white - grey in color. Small white grains of pumice, 3 millimeters to 1centimeters can be found in *L-6*. Thickness of bedding ranges from small centimeter scale lenses (1 to 2 centimeters) to 5 meter beds though the thicker beds are not well indurated. Weathering of *L-6* produces rocks that break into blocky fragments. The lack of sedimentary structures could represent fast deposition, intense bioturbation, or instense weathering. Thicker deposits of L-6 are often found at the base of conglomerates.

Figure 12. Conglomerate, clast-supported (L-5).

L-5 beds consist of rounded to sub-rounded clasts. Imbricated clasts near the top 20 centimeters of the Jacobs staff has a 150° SE paleocurrent. Photo from section 13, 39°49'2.97"N, 121°43'47.94"W.

L-7: Cross-Bedded and Planar Laminated Sandstone

L-7 sands consist of ashy, and fine-coarse grained sands and characteristically contain cross-bedding (Figure 14) or planar laminations (Figure 15). They can be well sorted or poorly sorted with angular grains. Typically L-7 is found on top of massive sands or lenses in conglomerates. Scour-and-fill structures are common. Normal grading of *L-7* sands in the Tuscan Formation can resemble high-density turbidites (Smith and Lowe, 1991). Bedding thickness ranges from 2 centimeters to 1 meter are often associated with *L-4* and *L-1* as thin lenses. *L-7* is more cemented than *L-6* and does not display blocky weathering.

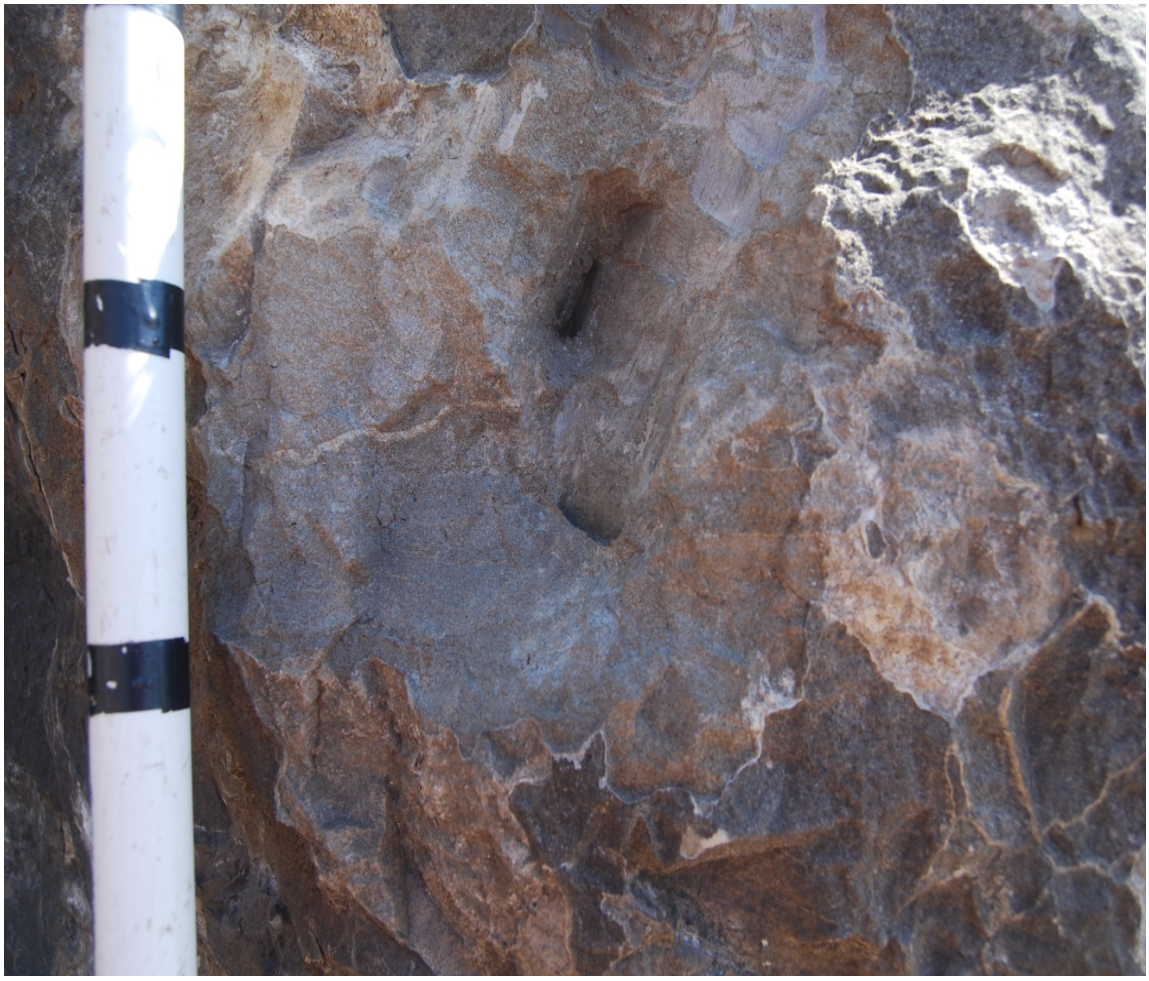

Figure 13. Sandstone (L-6).

Massive sandstones in the Tuscan are composed of fine-coarse grained sand. Weathering produces fragmented blocky sands. Figure is from Section 8, 39°47'0.11"N, 121°44'58.93"W.

L-8: Mudstone

L-8 beds (Figure 16) consist of mud or siltstone with occasional ripples, laminations, mud cracks and root burrows. Bedding thickness of *L-8* ranges from 1 centimeter to 2 meters. *L-8* can contain small fragments of pumice (2 millimeters to 2 centimeters in diameter) and can appear as thin lenses associated with L-4, L-6, and L-7.

Figure 14. Cross bedded sandstone (L-7).

L-7 beds contain cross-bedded sandstone, originally deposited in normal stream flows and channels. Sands range from very-fine to coarse-grained sands. Figure from section 7, 39°46'46.44"N,121°45'8.35"W.

Facies Association Descriptions

Facies Associations is a summary of characteristics and interpretations of the Tuscan Formation's lithofacies. Multiple lithofacies may be grouped together to define a facies association with the goal of determining the volcaniclastic depositional facies similar to those defined by Vessell and Davies (1981).

The Tuscan Formation has been divided into six main facies associations and assigned a facies association number Table 2.

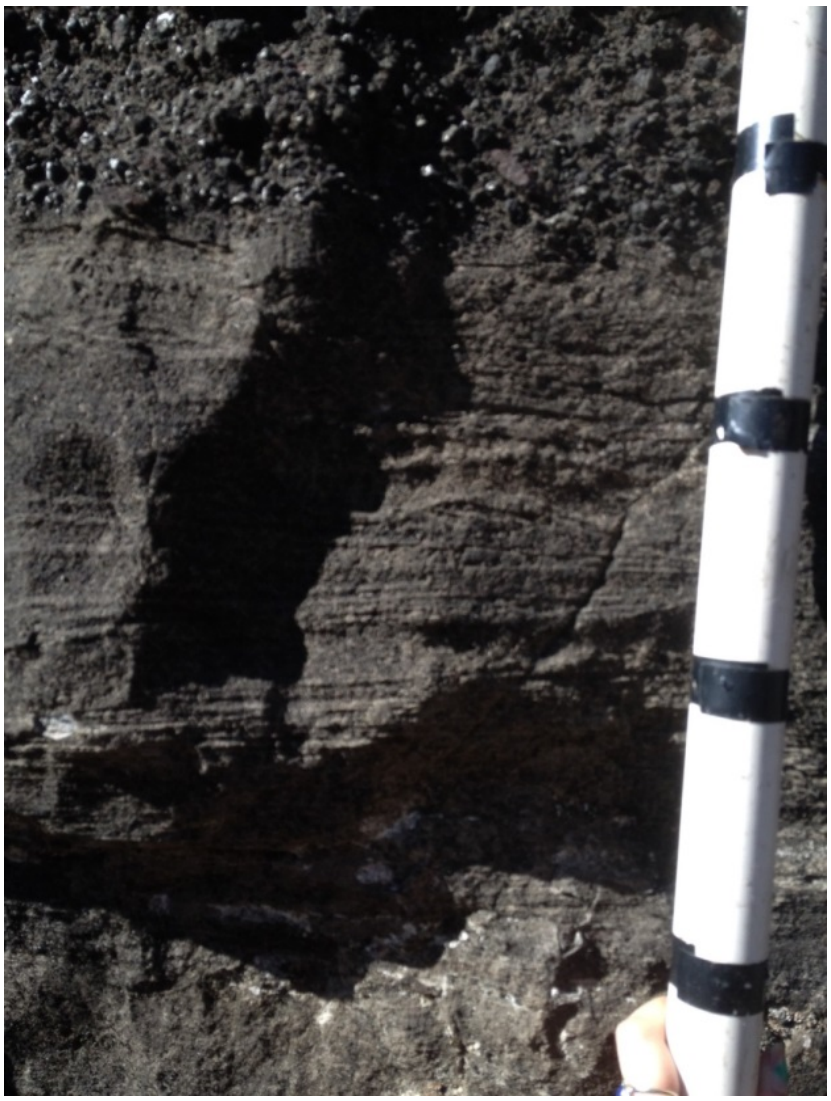

Figure 15. Cross-bedded and planar laminated sandstone (L-7).

L-7 beds contain cross-bedded and planar-laminated sandstone, originally deposited in normal stream flows and channels. Grains size range from very-fine to coarse grained sands. Figure from section 12, 39°47'53.34"N, 121°44'26.82"W.

FA-1: Volcanic Debris Flow

FA-1 deposits (Figure 17) form L-1 (for example see Section 13, Figure A-1; starting at the base of section-28 meters, marked with red arrow) and clasts supported L-2

Figure 16. Mudstone (L-8).

L-8 mudstone can contain small fragments of pumice. Beds can contain planar laminations and ripples. Figure from section 7, 39°46'49.85"N, 121°45'6.10"W.

breccia (for example see Section 7, Figure A-1; 117 meters above base of section, marked with red arrow). *FA-1* is predominantly composed of the lithofacies *L-1* but can be composed of *L-2* as well (Figure 16). *FA-1* forms thick massive beds up to 35 meters thick on Musty Buck Ridge. *FA-1* bedding becomes thinner (2 meters to 10 meters) moving laterally southwest down canyon along Musty Buck Ridge (Figure A-1). Younger deposits of *FA-1* form steep cliffs, but older deposits form rolling hills of variable and differential slopes. Bifurcation and benches may form in FA-1 (for example see Section 6 (Figure A-1; 79 to 99 meters above base of section, marked with red

TABLE 2. FACIES ASSOCIATION

Facies Association No.	Description	Facies No.
FA-1	Volcanic debris flow deposits: matrix supported and clast supported	L-1, L-2
FA-2	Hyperconcentrated flow deposits: intermediate between fully turbulent normal stream flow and viscous non-turbulent debris flows (Smith and Lowe, 1991). Often normal graded, coarse grained, poorly sorted and can often resemble high density turbidites (Smith and Lowe, 1991).	L-1, L-4, L-5, L-6
FA-3	Normal stream flow deposits: deposits may contain cross-bedded sands, planar laminated sandstone, and conglomerates. Scour-and-fill structures are common in normal stream flow.	L-4, L-5, L-6, L-7, L-8
FA-4	Distal debris flow and pyroclastic deposits: matrix supported breccia. Can contain pumice and ashy matrix. Clasts size range from 0.5cm- 5 cm.	L-1, L-3
FA-5	Flood deposits and inter-channel deposits: deposits may contain well-sorted and fine grained sandstone, siltstones and mudstones.	L-1, L-4, L-6, L-7, L-8
FA-6	Reworked tuff	L-1, L-3, L-4

arrow)). Due to modern erosion and landslides, *FA-1* benches can appear laterally discontinuous.

FA-1 deposits comprised of L-1 or L-2 is interpreted as debris flow deposits. Flows are viscous and deposit *en masse*. Debris flows are capable of transporting large, angular to sub-angular boulders, which are found in the FA-1, through a combination of a cohesive matrix, buoyancy and dispersive pressure (Smith, 1986).

FA-2: Hyperconcentrated Flow Deposits

A good example of FA-2 (Figure 18) is in Section 6, 116.5-121.5 meters from base of section (Figure A-1, marked with red arrow). FA-2 in section 6 transitions

Figure 17. Facies association 1, volcanic debris flow.

Volcanic debris flow, composed of matrix supported breccia. Cobbles in this debris flow are large, up to a meter in diameter and angular to sub-angular. FA-1 can contain lithofacies: L-1, L-2. Photo from section 13, 39°49'6.83"N, 121°43'52.45"W.

Figure 18. Facies association 2, hyperconcentrated flow.

Hyperconcentrated flows are often normal graded, coarse grained, poorly sorted. Because hyperconcentrated flows are in the transition stage between normal stream flow and debris flows, it can often be hard to interpret depositional environment. FA-2 can contain lithofacies: L-1, L-4, L-5, L-6. Figure from section 10, 39°47'18.15"N, 121°44'36.82"W.

vertically adjacent from a normally graded, angular to sub-rounded breccia (L-1) to planar laminated sandstone (L-7) and subsequently a sub-rounded, matrix supported conglomerate (L-4). In section 6, 125 meters from base of section (Figure A-1, marked with red arrow), a sub-rounded clast supported conglomerate (L-5) overlays a sandstone (L-6) vertically. From field observations and Smith and Lowe's (1991) hyperconcentrated flow deposit descriptions, lithofacies that have been categorized to define *FA-2* are *L-1*, *L-4*, *L-5*, *L-6* and *L-7*.

In the Tuscan, Section FA-2 is typically more indurated in comparison to deposits that are strictly derived from normal stream flows. L-6 sand grains in FA-2 can range from fine to very coarse but are typically planar laminated and stack vertically adjacent to L-1 (Figure A-1: 121.5 meters from base of section 6, marked with red arrow). Coarser grained sands comprise the matrix of L-5 in FA-2.

FA-2 is most consistent with hyperconcentrated flow deposits which are intermediate between fully turbulent normal stream flow and viscous non-turbulent debris flows (Smith and Lowe, 1991). FA-2 does not deposit *en masse like FA-1*. Due to the transitional nature of *FA-2*, it may be difficult to distinguish *FA-2* from debris flows (*FA-1*) or normal stream flow (*FA-3*).

FA-3: Normal Stream Flow Deposits

An example of FA-3 (Figure 19) in the Tuscan is in Section 8, 45 to 50 meters from base of section (Figure A-1, marked with red arrow) which transitions from a poorly sorted medium-grained sandstone (L-6) to a clast supported conglomerate (L-5), to a laminated mudstone (L-7), followed by a conglomerate (L-4) (Figure 18). In section

Figure 19. Facies association 3, normal stream flow deposits.

Deposits found in active creeks and channels. Deposits include lithofacies: conglomerates both matrix and clast supported, sandstone, cross-bedded and planar laminated sandstone. FA-3 can contain lithofacies: L-4, L-5, L-6, L-7, L-8. Figure from Section 9, 39°47'19.49"N, 121°44'43.80"W.

9, 108 meters from base of section (Appendix A-1, marked with red arrow) is an example of cross bedded and planar laminated sandstone (L-7) commonly found in FA-3. FA-3 deposits are represented by the lithofacies that form in active creeks: *L-4*, *L-5*, *L-6*, *L-7*, and *L*-8. Lithofacies in FA-3 are generally interbedded and vertically stacked. Typically, FA-3 form channel fills underlying FA-1; see Section 8 for example (Figure A-1, 133-141 meters from base of section, marked by red arrow). *FA-3* bedding is thicker, up to 40 meters thick, moving laterally southwest down canyon along Musty Buck Ridge (Figure A-1).

FA-3 has characteristics of deposits from active creeks and rivers. Depositional fabrics such as planar laminated sandstone, cross-bedding, and imbrication in conglomerates is governed by sediment transport and transport mechanisms which are driven by fully turbulent flow. Consequently, laminated sandstone, cross-bedded sandstone, and imbrication in conglomerates can be well developed in FA-3. Medium to fine grained cross-bedded sands are typical in systems that are slowly aggrading or in incised.

FA-4: Distal Debris Flow and Pyroclastic Deposits

An example of FA-4 (Figure 20) is in Section 10, 0 to 6 meters from base of section (Figure A-1, marked with red arrow) comprised of breccia-matrix supported (L-1) and tuff (L-3). FA- 4 shares lithofacies characteristics similar to FA-1. *FA-4* contains angular to sub-angular pumice and volcanic fragments. Clasts size range from 0.5 centimeters to 5 centimeters with fine-grained sand to ashy matrix. *FA-4* is laterally continuous on Musty Buck Ridge. *FA-4* bedding is thicker, up to 20 meters thick, moving

Figure 20. Facies association 4, distal debris flow and pyroclastic deposits.

Distal debris flow and pyroclastic deposits are composed of matrix supported breccias. containing angular-subangular pumice and volcanic fragments. FA-4 can contain lithofacies: L-1, L-3. Figure from section 12, 39°47'57.75"N, 121°44'11.22"W.

laterally southwest down canyon along Musty Buck Ridge. Lithofacies that define *FA-4* are *L-1*, *L-3*. FA-4 is typically laterally continuous and found in the older, basal deposits of the Tuscan Formation.

Lydon (1969) hypothesized that these deposits are microbreccias, deposited in a similar fashion to debris flow breccias. FA-4's smaller clasts indicate that the deposits may have been transported some distance from origin. Although the matrix has high

concentrations of ash and pumice similar to tuffaceous deposits, FA-4 does not display characteristics of being reworked (e.g., rounded clasts).

FA-5: Flood Deposits and Inter-Channel Deposits

An example of FA-5 (Figure 21) is in Section 8, 27 meters from base of section. It contains well-sorted and fine grained sandstone, siltstones and mudstones, which are typically deposited vertically, adjacent to rounded, smaller clast (0.5 to 5 centimeter) conglomerates (Figure A-1). Bedding thickness is 1 centimeter to 2 meters

Figure 21. Facies association 5, flood deposits and inter-channel deposits.

Flood deposits and inter-channel deposits. FA-5 can contain lithofacies: L-4, L-6, L-7, L-8. Figure from section 7, 39°46'49.85"N, 121°45'6.10"W.

and can contain small fragments of pumice. Lithofacies that define FA-5 are L-1, L-4, L-6, L-7, and L-8. Deposits of FA-5 are more prevalent in basal to mid-sections on Musty Buck Ridge, but thin lenses can be found throughout the Tuscan.

Flood deposits and inter-channel deposits are a result channel deposits and overbank deposits associated with a possible increase in river discharge (e.g., melted ice during eruption) (Aslan et al., 2003). Bioturbation, root burrows and mud cracks can often be found in FA-5. Finer grained muds and sands in FA-5 are indicative of a low energy depositional environment.

FA-6: Reworked Tuff

The Ishi Tuff is an example of FA-6. It can be seen in Section 9, 135 meters from base of section (Figure A-1, marked by red arrow). Lithofacies that define FA-6 are L-1, L-3 and L-4. FA-6 contains reworked volcanic sandstone, silt and air-fall pumice. The Ishi Tuff and Nomlaki Tuff are the two main tuffaceous deposits of FA-6 in the Tuscan Formation but other thinner tuff deposits are found throughout the Tuscan. The Ishi Tuff is located between the two youngest debris flows on Musty Buck Ridge and pinches out up canyon northeast on Musty Buck Ridge. Commonly, the Ishi FA-6 is re-worked.

Stratigraphic Surfaces of the Tuscan on Musty Buck Ridge

Rather than using the standard ABCD method of defining the Tuscan Formation on Musty Buck Ridge (Harwood and Helley, 1981), Tuscan deposits were defined by depositional facies (interpreted from facies associations) separated into major

timeline intervals to provide a more detailed geological history. Eleven major time correlative events have been described in the Tuscan Formation on Musty Buck Ridge (Figure B-1) and labeled chronologically as Musty Buck Ridge 1 through Musty Buck Ridge 11 (MBR 1-11), with MBR 1 representing the oldest flow event and MBR 11 representing the youngest flow event. Surfaces are defined by laterally continuous changes in composition and depositional environments.

Time correlative surfaces may only apply to Musty Buck Ridge. Detailed flow-by-flow mapping, employing methodologies similar to this study, will elucidate significant surfaces that may or may not correlate to Must Buck Ride.

Musty Buck Ridge 1 Through 2 (MBR 1-2)

The oldest of the Tuscan Formations timeline surfaces is MBR 1. MBR 1 is laterally continuous through stratigraphic sections 1-13 (Figure 22) and is the Tuscan Formation-Lovejoy Basalt contact. The Tuscan Formation-Lovejoy Basalt contact is intermittently continuous in nearby locations. In Big Chico Creek Canyon, this surface abruptly pinches out, placing Tuscan Formation on top of Chico Formation.

Between timeline surfaces MBR1 and MBR 2 (MBR1-2) (Figure B-1) is a debris flow, consisting of mixed metamorphic brecciated basement rock and volcanic rock. Thin bedded matrix conglomerates composed of metamorphic and volcanic rock can also be found throughout MBR 1-2. Metamorphic rocks are rare in the Tuscan Formation on Musty Buck Ridge

After the deposition of the debris flow, and fluvial channel, a thick bed of distal debris flow deposition ensued. Characteristics of the distal debris flow unit include

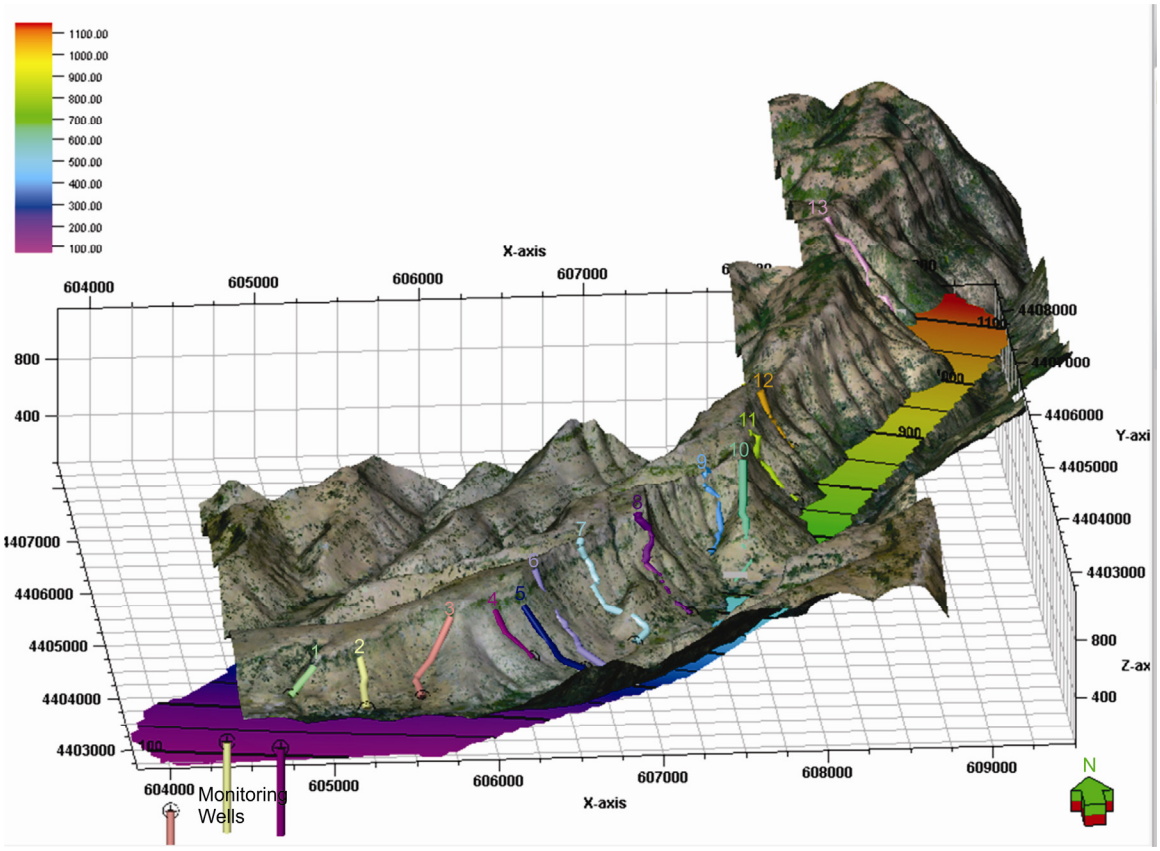

Figure 22. MBR 1.

MBR 1 mappable time surface created from collected GPS data points along contact, imputed into the 3-D modeling program Petrel. MBR1 is the Lovejoy Basalt-Tuscan Formation contact and it laterally continuous. DEM of Musty Buck Ridge has been vertically exaggerated 3x's. Colored pipes represent stratigraphic sections 1-13. X-Y grid is in NAD1927 UTM-11N meters.

small centimeter scale, laterally extensive, brecciated volcanic pebbles and angular pumice.

Previously, Doukas (1983) mapped this unit as Nomlaki Tuff. However, more geochemical analyses may be in order to determine if it truly is the Nomlaki (based on geochemical fingerprinting) as it lacks features of a reworked tuff (e.g., rounded pumice, ashy matrix).

Musty Buck Ridge 2 Through 3
(MBR 2-3)

MBR 2 time surface marks the change from a distal debris flow dominated system to a normal stream flow system. Betweem timeline surfaces MBR 2 (Figure 23) and MBR 3 (MBR 2-3) is a period dominated by active creeks that were deposited during an interval between periods of large debris flow deposition. During MBR 2-3, interbedding of normal stream deposits, hyperconcentrated flow deposits, flood and inter-

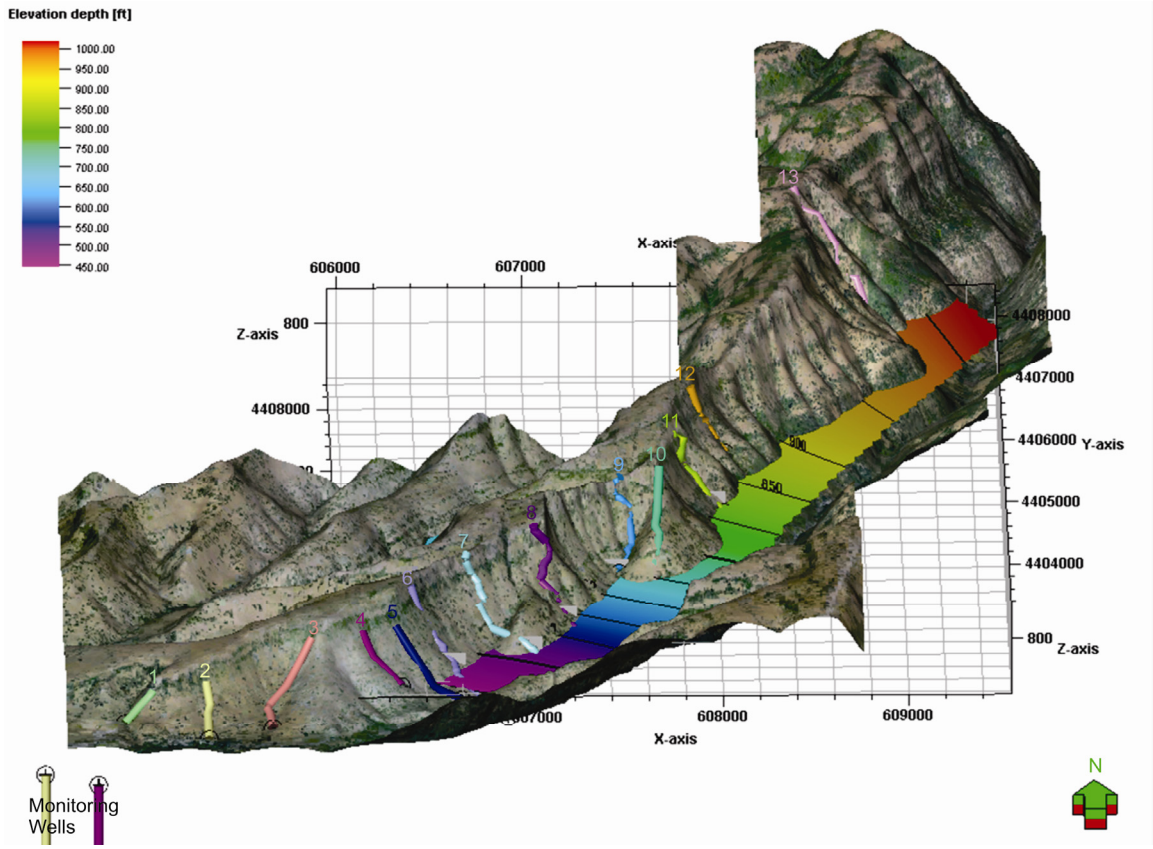

Figure 23. MBR 2.

MBR 2 a mappable time surface created from collected GPS data points along contact, imputed into the 3-D modeling program Petrel. Along the contact of MBR2, compostion of the Tuscan Formation changes from a distal debris flow and pyroclastic deposits to a3x's. Colored pipes represent stratigraphic sections 1-13. X-Y grid is in NAD1927 UTM-11N meters.

channel deposits occur (Figure B-1). MBR 2-3 is likely sourced from the medial or distal volcaniclastic facies. Deposition of MBR 2-3 thins laterally moving northeast.

Musty Buck Ridge 3 Through 4 (MBR 3-4)

MBR 3 marks the contact where deposition changes from a normal stream flow system to a large volcanic debris flow system. Between timeline surfaces MBR 3 (Figure 24) and MBR 4 (MBR 3-4) a thick volcanic brecciated debris flow was deposited, reaching a maximum thickness of 30 meters (Figure B-1). MBR 3-4 thins laterally southwest moving down canyon, where it bifurcates into two flows that thin to interbedded sand and mudstone (Figure 25). The thick continuous northern section of the large debris flow may represent a medial volcaniclastic facies that shifts to a more distal facies in the southward direction. The large debris flow deposit contained within MBR 3-4, forms large, gently sloping surfaces rather than the more typical steep cliffs of the younger Tuscan debris flow units (Figure 26).

Musty Buck Ridge 4 Through 5 (MBR 4-5)

The timeline surface of MBR 4 (Figure 27) marks the contact between the underlying large debris flow and a return to a normal stream flow system. MBR 4-5 consists of interbedded deposits from normal stream flows, hyperconcentrated flows, and flood and inter-channel deposits. MBR 4-5 is medial to distal volcaniclastic facies dominated. Hyperconcentrated flows are more dominant northwest in the down canyon direction. Members 4 and 5 thin out between sections 12 and 13. Both members appear to be a ruminant of a distal flow or an erosional surface. Due to the uncertainty of MBR 4-5, contact lines have been dashed in Figure B-1.

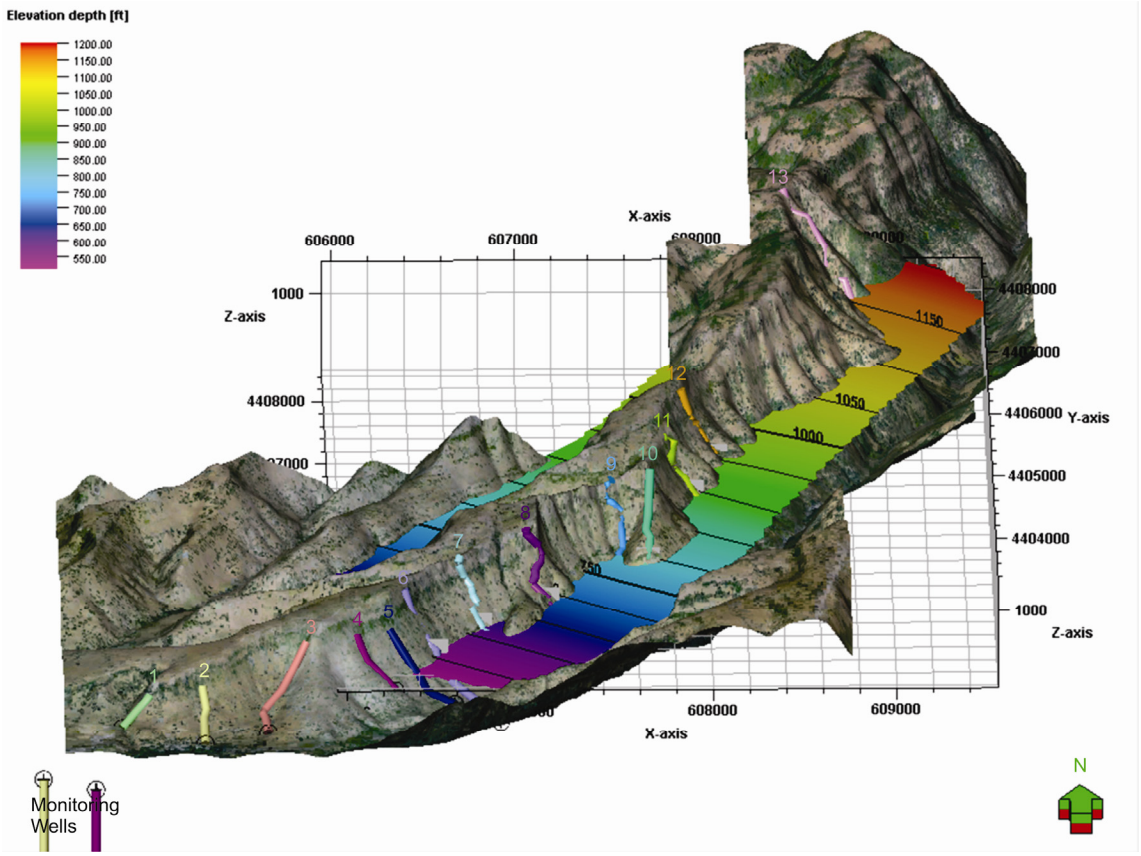

Figure 24. MBR3.

MBR 3 a mappable time surface created from collected GPS data points along contact, imputed into the 3-D modeling program Petrel. MBR 3 is the contact where deposition changes from a normal stream flow system to a large volcanic debris flow system. DEM of Musty Buck Ridge has been vertically exaggerated 3x's. Colored pipes represent stratigraphic sections 1-13 X-Y grid is in NAD1927 UTM-11N meters.

There is a slight drop in elevation and thickening of MBR 4-5 in section 10 (Figure B-1), likely due to an erosional surface created by a paleochannel.

Musty Buck Ridge 5 Through 6 (MBR 5-6)

MBR 5 (Figure 28) marks a change from a normal stream flow system to a volcanic debris flow. Between section 12 and section 13, MBR 5 is difficult to define.

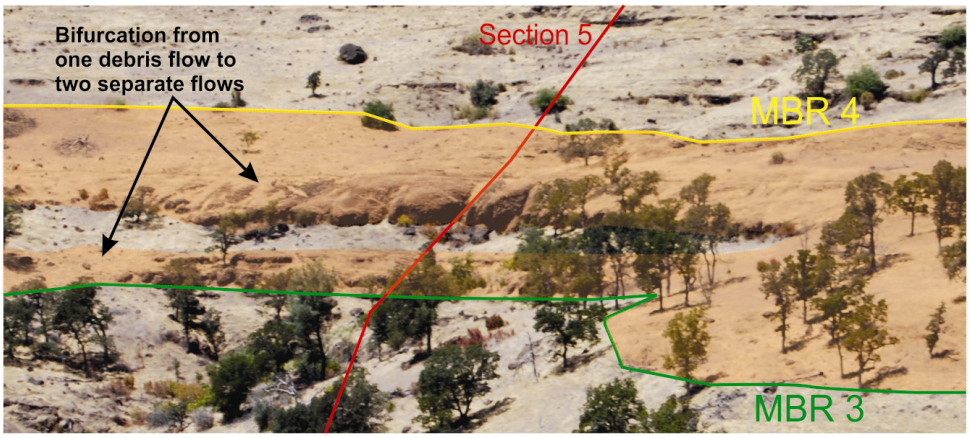

Figure 25. High resolution aerial photo of bifurcating distal debris flow (MBR 3-4).

High resolution aerial photo of the large distal debris flow in MBR 3-4 bifurcating into two separate debris flows. Photo is from section 5.

Figure 26. High resolution aerial photo of debris flow deposits with gently sloping topography (MBR 3-4).

High resolution aerial photo of the large debris flow in MBR 3-4 is, forming large, gently sloping surfaces rather than steep cliffs. Photo is from between sections 6 and 7.

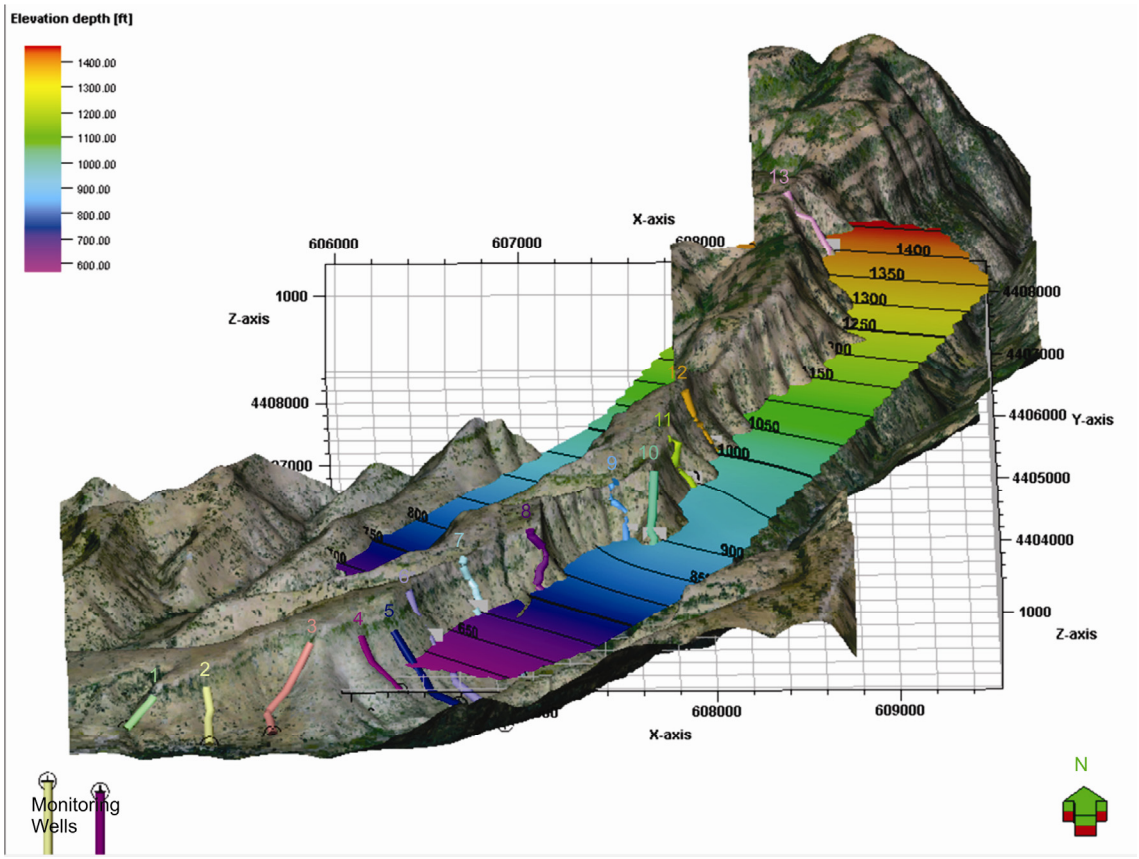

Figure 27. MBR 4.

MBR 4 a mappable time surface created from collected GPS data points along contact, imputed into the 3-D modeling program Petrel. MBR4 marks the contact between large debris flow and a return to a normal stream flow system. DEM of Musty Buck Ridge has been vertically exaggerated 3x's. Colored pipes represent stratigraphic sections 1-13. X-Y grid is in NAD1927 UTM-11N meters.

The volcaniclastic facies of MRB 5-6 transitions from medial to distal moving laterally southwest down canyon, thinning to just 2 to 3 meters thick (Figure B-1). Northern sections of the volcanic debris flow in MBR 5-6 form sharp cliffs and thicken to almost 30 meters.

Slight drop in elevation and thickening of MBR 5-6 deposits continues in section 10 (Figure 29), likely due to an erosional surface created by a paleochannel.

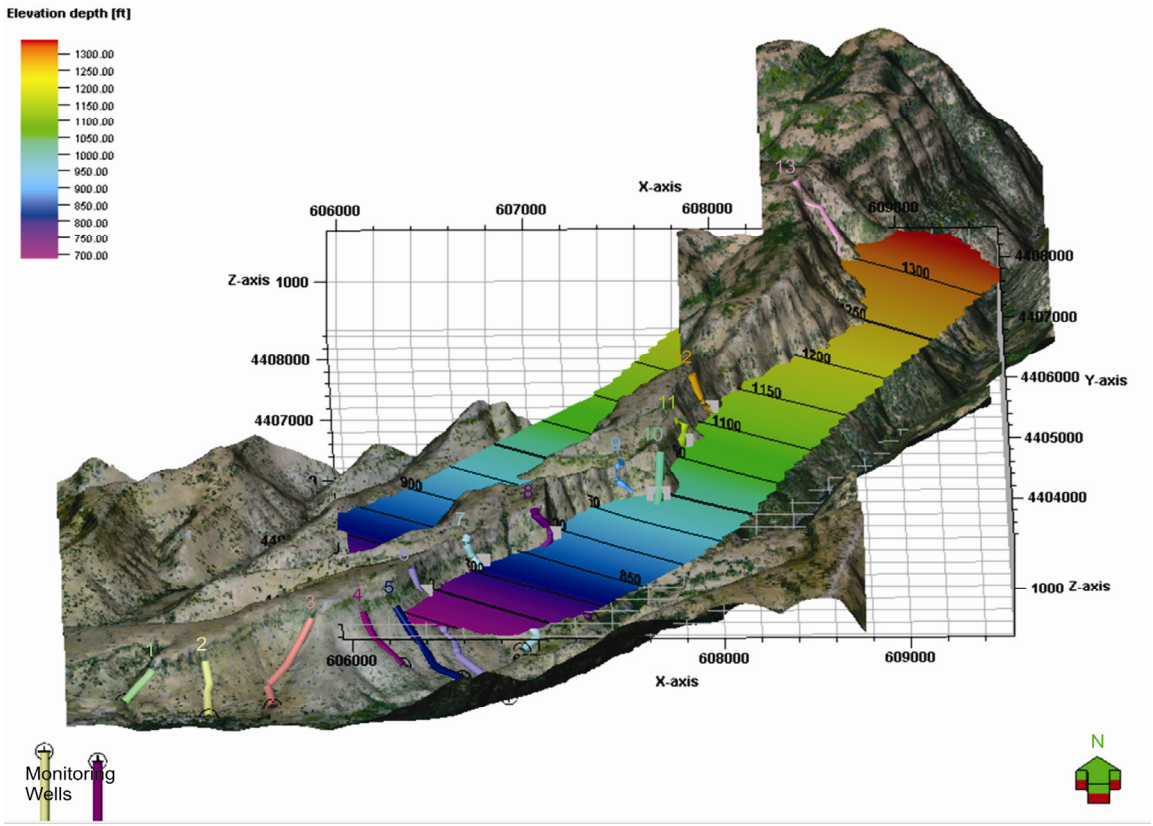

Figure 28. MBR 5.

MBR 5 a mappable time surface created from collected GPS data points along contact, imputed into the 3-D modeling program Petrel. MBR5 marks the contact between normal steam flow and base of a debris flow. DEM of Musty Buck Ridge has been vertically exaggerated 3x's. Colored pipes represent stratigraphic sections 1-13. X-Y grid is in NAD1927 UTM-11N meters.

Musty Buck Ridge 6 Through 7 (MBR 6-7)

MBR 6 marks the contact between a debris flow and the return to a normal stream flow system (Figure 30). MBR 6-7 consist of normal stream flow deposits containing laterally continuous clast-supported conglomerate, with thin sandstone lenses (Figure B-1). The volcaniclastic facies could exist in a medial to distal position of Vessell and Davies (1981). The conglomerate in MBR 6-7 pinches out toward the northeast in section 13.

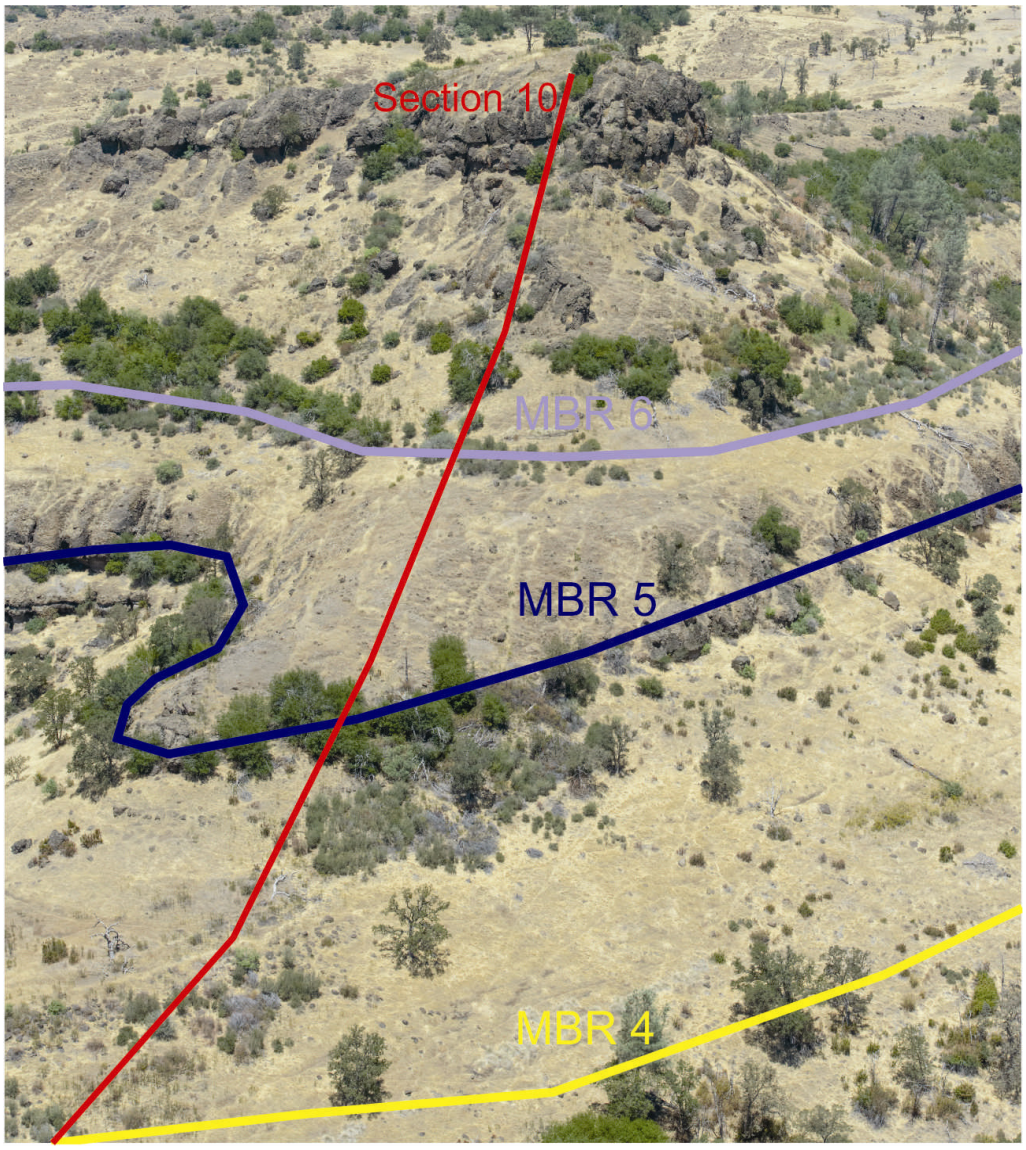

Figure 29. High resolution aerial photo of thickening MBR 5-6 deposits.

Thickening of deposits in MBR 5-6 from a paleochannel in section 10 is visible from high resolution aerial photo.

Musty Buck Ridge 7 Through 8 (MBR 7-8)

MBR7 marks the contact between normal stream flow deposits and the base of a debris flow (Figure 31). MBR 7-8 is dominated by a laterally continuous brecciated volcanic debris flow deposits. Southeast sections of the debris flow thin to 3 to 5 meters

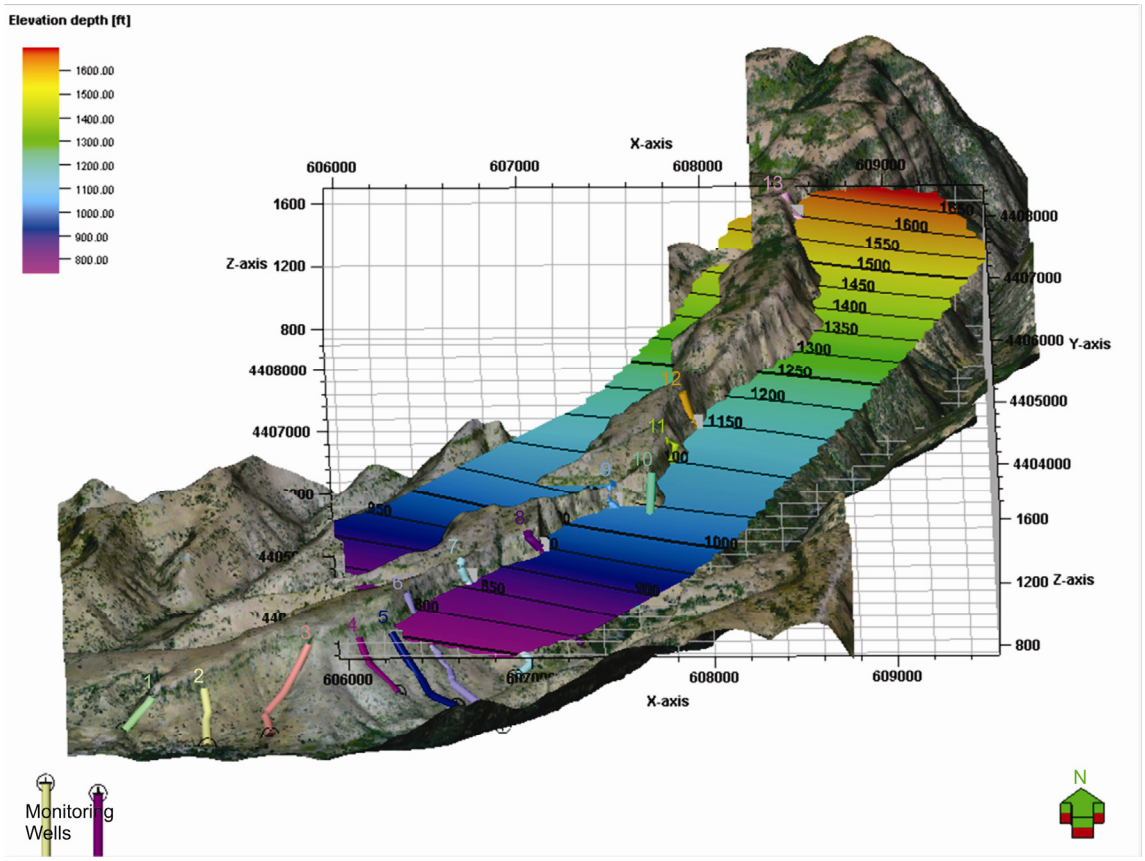

Figure 30. MBR 6.

MBR 6 a mappable time surface created from collected GPS data points along contact, imputed into the 3-D modeling program Petrel. MBR 6 marks the contact between a debris flow and the return to a normal stream flow system. DEM of Musty Buck Ridge has been vertically exaggerated 3x's. Colored pipes represent stratigraphic sections 1-13. X-Y grid is in NAD1927 UTM-11N meters.

thick (Figure B-1). The volcanic debris flow in MBR 7-8 can be placed in the medial to distal volcaniclastic facies (Vessell and Davies, 1981), transitioning from medial to distal moving laterally southwest down canyon. Section 6 consists of the thickest deposit of MBR 7-8 (~27 meters) (Figure 32), likely due an erosional channel creating more accommodation space.

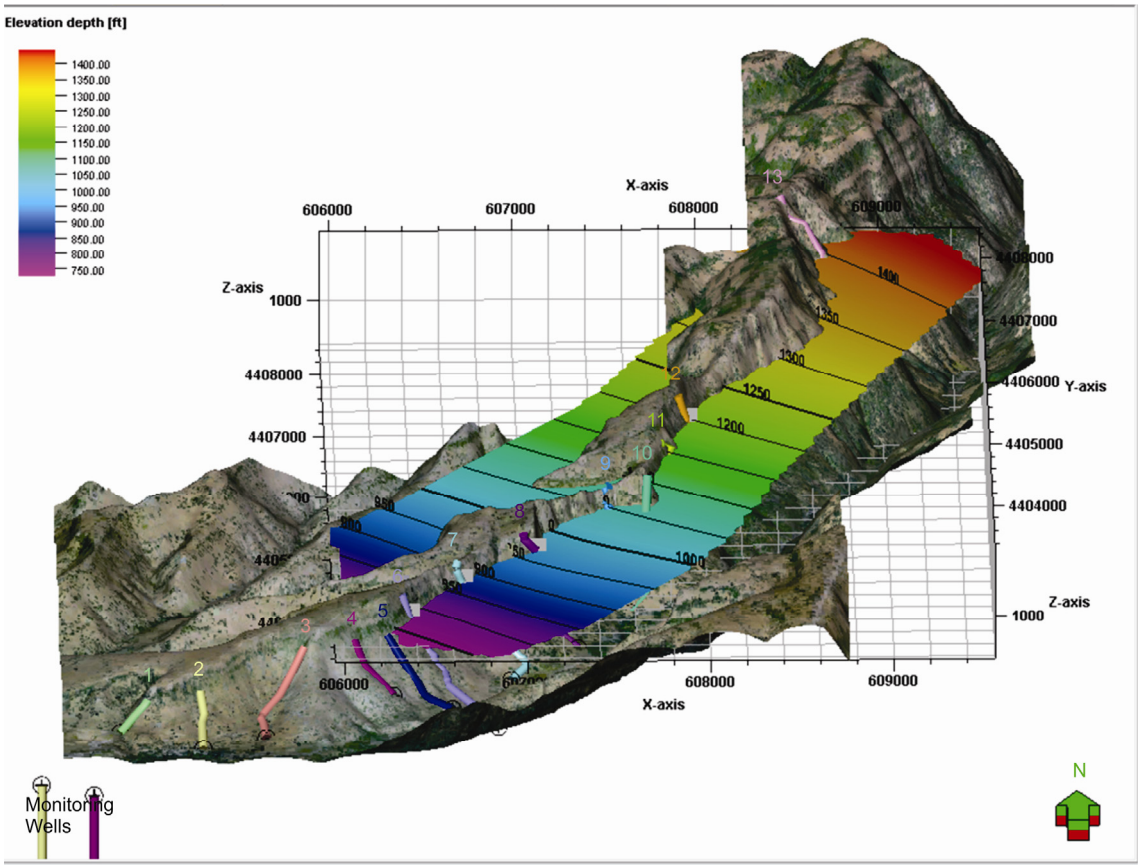

Figure 31. MBR 7.

MBR 7 a mappable time surface created from collected GPS data points along contact, imputed into the 3-D modeling program Petrel. MBR7 marks the contact between normal stream flow deposits and the base of a debris flow. DEM of Musty Buck Ridge has been vertically exaggerated 3x's. Colored pipes represent stratigraphic sections 1-13. X-Y grid is in NAD1927 UTM-11N meters.

Musty Buck Ridge 8 Through 9 (MBR 8-9)

MBR 8 marks the contact between a debris flow and a return to normal stream flow deposits (Figure 33). Dominated by active creeks, MBR 8-9 consists of clast-supported conglomerate interbedded with thin sandstone lenses (Figure B-1). Volcaniclastic facies of Vessell and Davies (1981) is medial to distal. The conglomerate in MBR 8-9 pinches out in the northeast sections.

Figure 32. High resolution aerial photo of thickening MBR 7-8 deposits.

Thickening of deposits in MBR 7-8 from a paleochannel in section 6 is visible from high resolution aerial photo.

Musty Buck Ridge 9 Through 10 (MBR 9-10)

Between timeline surfaces MBR 9-10 is the Ishi Tuff. The Ishi Tuff pinches out up canyon in the northeast sections (Figure B-1). The Ishi Tuff is a reworked tuff, with rounded pumiceous clasts, placing it in the medial to distal volcaniclastic facies. MBR 9 (top of the Ishi tuff) deposits are too thin to get an accurate GPS surface, but it follows a similar trend to MBR10 (Figure 34).

Musty Buck Ridge 10 Through 11 (MBR10-11)

Between timeline surfaces MBR 10 (Figure 34) and MBR 11 (Figure 35) is the youngest of the large volcanic debris flows on Musty Buck Ridge, consisting of one, or possibly two debris flow deposits. Southwest sections of MBR 10-11 are thinner (3 to 4 meters thick) and thicken moving up canyon, reaching a maximum thickness of approximately 30 meters (Figure B-1). However, thickness is variable in MBR 10-11 due to an erosional surface at the base and the modern weathered surface at the top of Musty Buck Ridge. The farthest northeast contact of MBR 10 in section 13 is ambiguous either due to cover of the contact or MBR 10-11 may have been completely eroded. A thin,

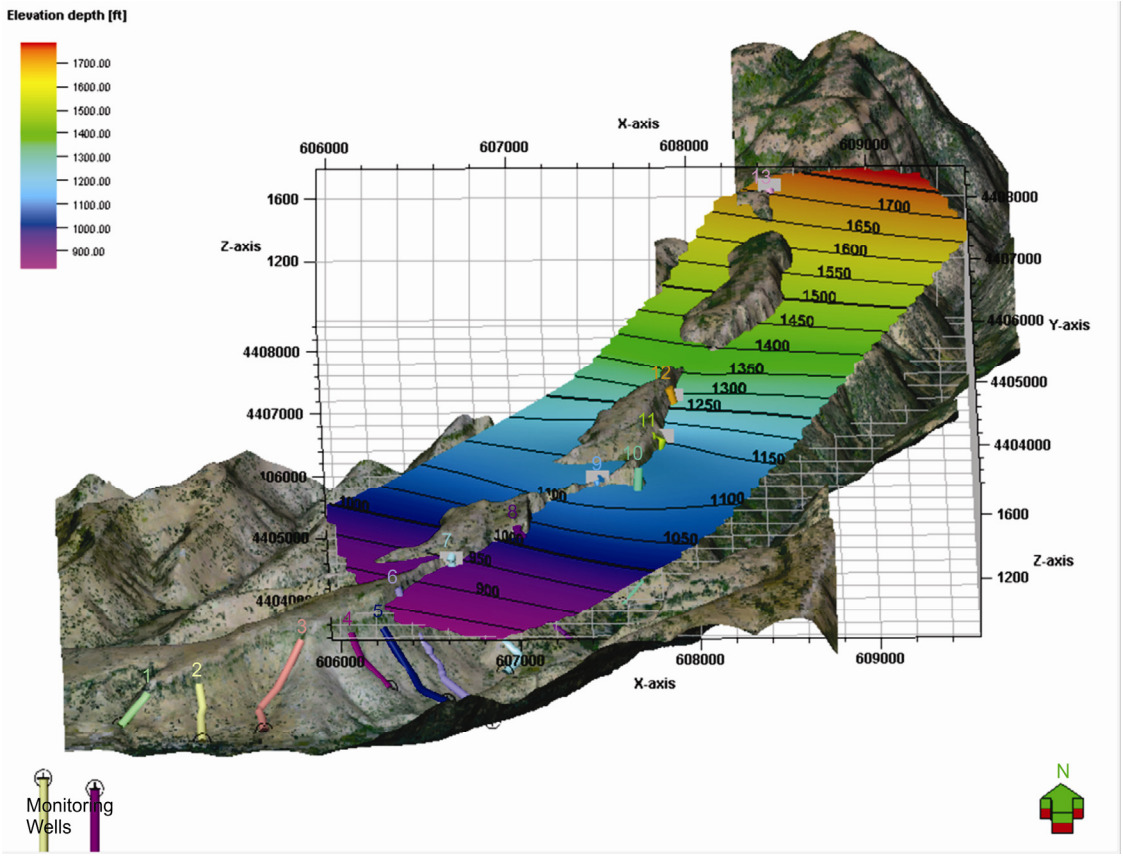

Figure 33. MBR 8.

MBR 8 a mappable time surface created from collected GPS data points along contact, imputed into the 3-D modeling program Petrel. MBR 8 marks the contact between a debris flow and a return to normal stream flow deposits. DEM of Musty Buck Ridge has been vertically exaggerated 3x's. Colored pipes represent stratigraphic sections 1-13. X-Y grid is in NAD1927 UTM-11N meters.

younger debris flow is located stratigraphically above the large debris flow deposit but the contact is only visible in section 10 (Figure 36) and not the other sections due to pinching out or erosion. Volcaniclastic facies is medial to distal.

Petrographic Analysis

It is important to gain a greater understanding of the Red Bluff Formation- top Tuscan Formation boundary because the city of Chico gets its water both above and

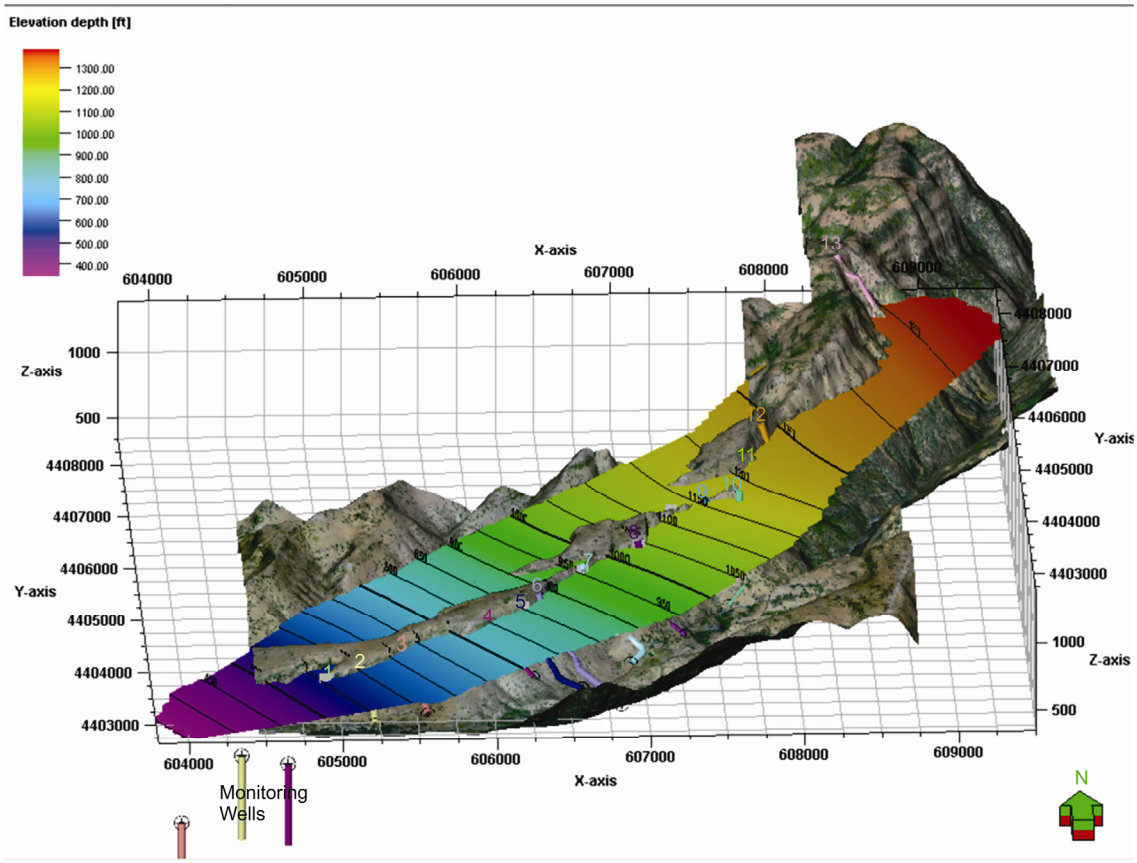

Figure 34. MBR 10.

MBR 10 a mappable time surface created from collected GPS data points along contact, imputed into the 3-D modeling program Petrel. MBR 10 marks the contact between the Ishi Tuff and a volcanic debris flow. DEM of Musty Buck Ridge has been vertically exaggerated 3x's. Colored pipes represent stratigraphic sections 1-13. X-Y grid is in NAD1927 UTM-11N meters.

below this boundary. This boundary, while in the past has been studied texturally; it has not been defined geologically or by composition. Once the top-Tuscan surface has been established, data can be combined with MBR surfaces to construct preliminary framework of individual flows within the Tuscan aquifer system.

A total of 79 thin sections were analyzed from 3 wells, MW9, MW11, and MW13. Using a cross-polarized microscope, a point count method was used to identify

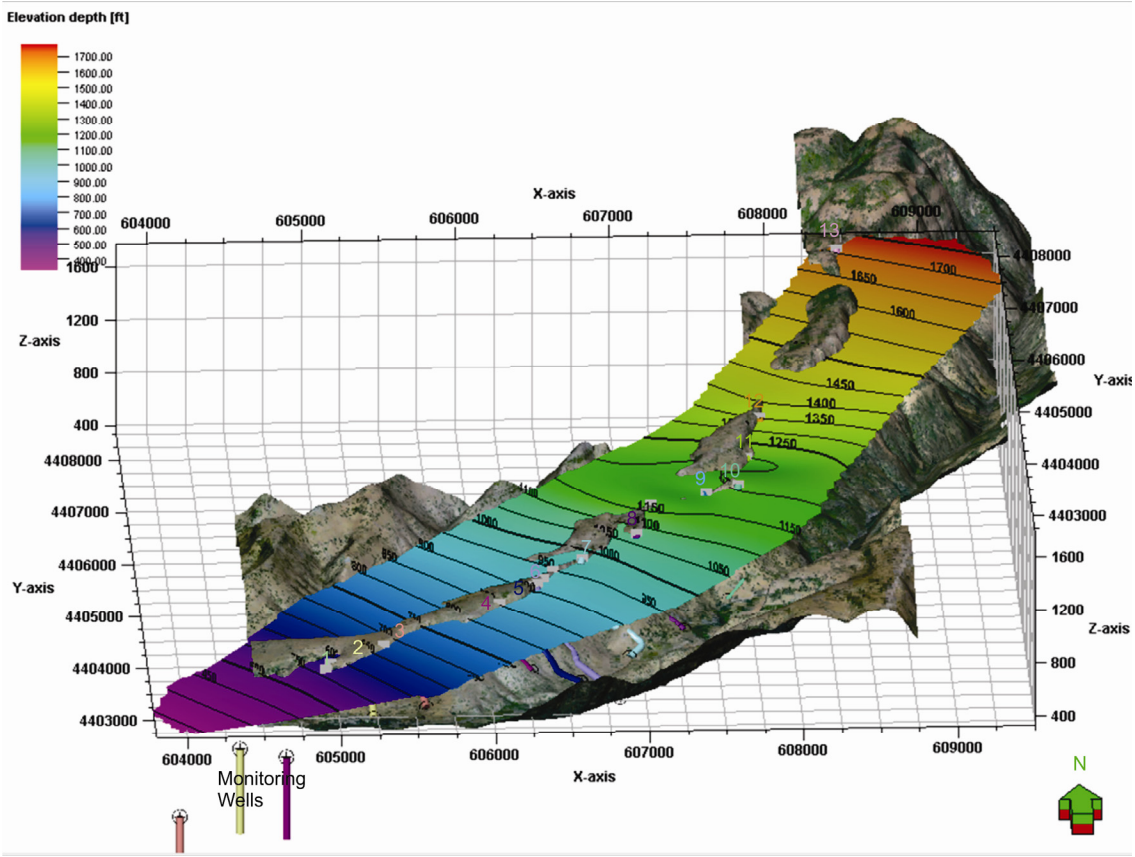

Figure 35. MBR 11.

MBR 11 a mappable time surface created from collected GPS data points along contact, imputed into the 3-D modeling program Petrel. MBR 11 marks top of the youngest debris flow in Musty Buck Ridge. DEM of Musty Buck Ridge has been vertically exaggerated 3x's. Colored pipes represent stratigraphic sections 1-13. X-Y grid is in NAD1927 UTM-11N meters.

and record compositions of 300 sand sized grains per sample. Key diagnostic minerals that dominate the Tuscan Formation are volcanic minerals such as plagioclase (plag), potassium feldspar (k-spar), pyroxene/olive (Py/Ol), glass pumice fragments and volcanic lithics (Lv) (Figure 37). Although metamorphic lithics (Lm) (Figure 38, Figure 39) are not typical in the Tuscan Formation, some Lm can be found at deeper depths, closer to the Sierran basement source. Because the Red Bluff Formation west of the Sacramento

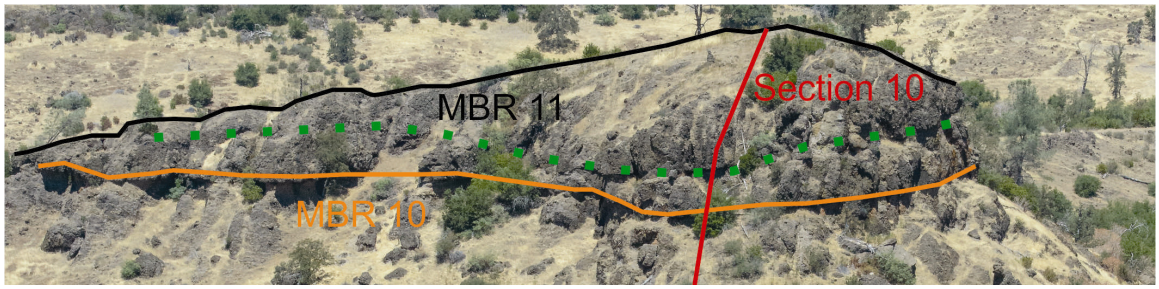

Figure 36. High resolution aerial photo of youngest debris on Musty Buck Ridge.

The youngest debris flow, located only in section 10 is stratigraphically above the larger laterally continuous debris flow in MBR 10-11. Green dashed line marks the contact between the two youngest debris flows.

River is derived from a mixture of metamorphic rocks off the Coast Ranges and Klamath Mountains (Buer, 2007), minerals and lithics typically found in the Red Bluff Formation are monocrystalline quartz (Qm), polycrystalline quartz (Qp), and metamorphic lithics (Lm) and volcanic lithics (Lv). Sedimentary lithics (Ls) are also found in the Red Bluff Formation, but are rare. Sedimentary lithics have rounded quartz grains and can easily be misinterpreted as intraclasts (Figure 40). Therefore, it is hypothesized that a sharp change in metamorphic lithics is indicative of the Red Bluff Formation-Tuscan Formation. The sharp change in composition from Tuscan Formation to Red Bluff Formation most likely occurred during the ~1 m.y. unconformity between the two formations.

Tabulated data from all three wells were normalized as a relative percentage of volcanic to metamorphic lithics and then plotted against correlating well depth (Figure C-1) to determine significant patterns that could indicate a change in composition from Red Bluff Formation to Tuscan Formation deposits. The formula places volcanic-related grains in the numerator and metamorphic/plutonic-related grains in the denominator.

$$\%\ \text{Volcanic Grains} = \frac{(\text{Plag}+\text{Lv}+\text{Py}+\text{Ol})}{(\text{Qm}+\text{Op}+\text{kspar}+\text{Lm}+\text{Ls}+\text{Plag}+\text{Lv}+\text{Py}+\text{Ol})}$$

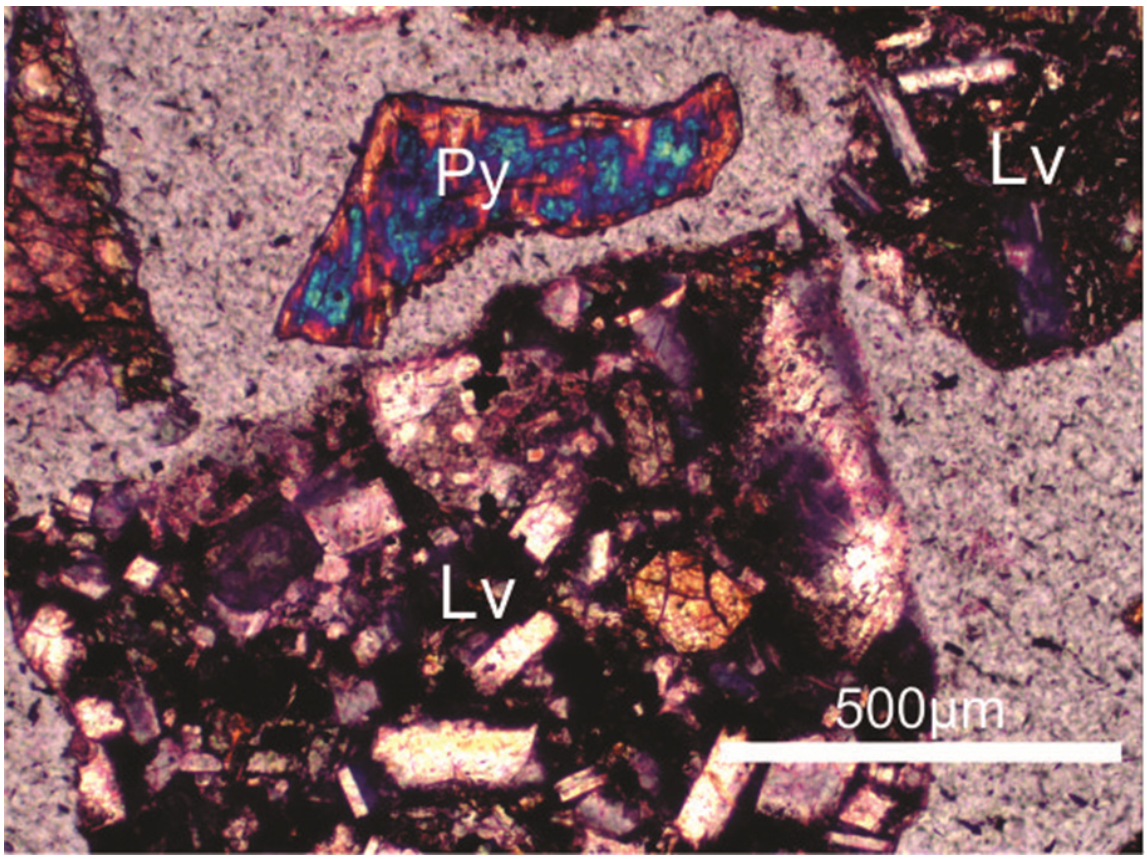

Figure 37. Volcanic lithic.

Volcanic lithics are dominated by euhedral shaped minerals, predominantly plagioclase, potassium feldspar and pyroxene. From MW11, 239 feet in drillers depth. Lv=volcanic lithic; Py=pyroxene. Cross-polarized light, 10X.

Well MW9 Petrographic Analysis

In well MW9 there is an abrupt change from metamorphic/volcanic lithics to volcanic mineral/lithics at a depth of ~136 to 138 feet below ground surface (bgs) (Table 3) indicating a possible Red Bluff Formation-Tuscan Formation boundary. Although MW9 has a steady amount of volcanics throughout the entire well (Figure 40), metamorphic lithics, monocrystalline, and polycrystalline quartz numbers decline below ~136ft. Metamorphic lithics at deeper depths in the Tuscan Formation may have a Sierran

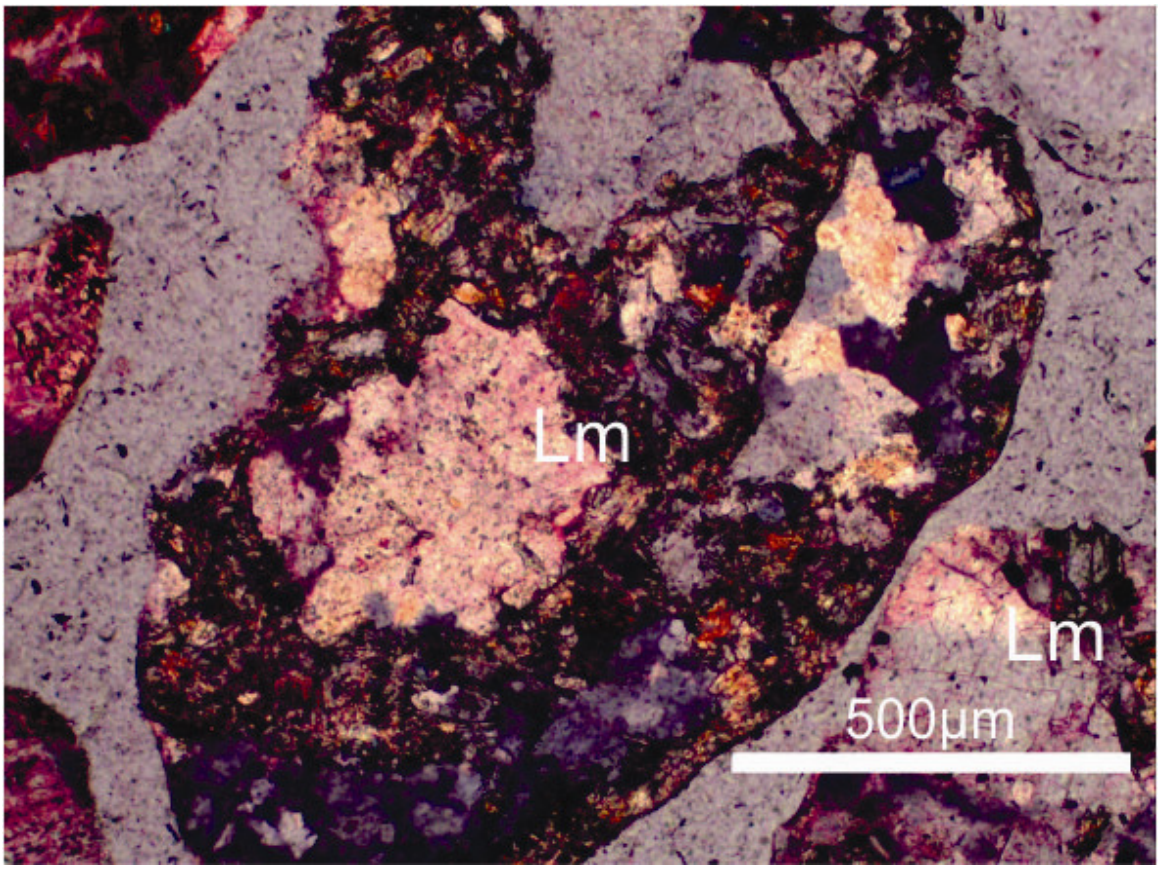

Figure 38. Metamorphic lithic from basement source.

Located in deeper depths, metamorphic lithics can be found in the Tuscan Formation. These metamorphic basement lithics are often composed of monocrystalline and polycrystalline quartz. From MW11, 239 feet in drillers depth. Lm=metamorphic lithic. Cross-polarized light, 10X.

Basement origin. Depths 114 to 146 feet bgs and 180 to 185 feet bgs have an influx of intraclast, indicating a potential paleochannel. Calculated volcanic lithic to metamorphic lithic percentage places the boundary in well MW9 at ~136.60 feet (bgs) (Figure C-1).

Well MW11 Petrographic Analysis

Well MW11 displays an abrupt change from a mixed source of metamorphic lithics/volcanic lithics to predominantly volcanic lithics below ~142 to 147 feet bgs

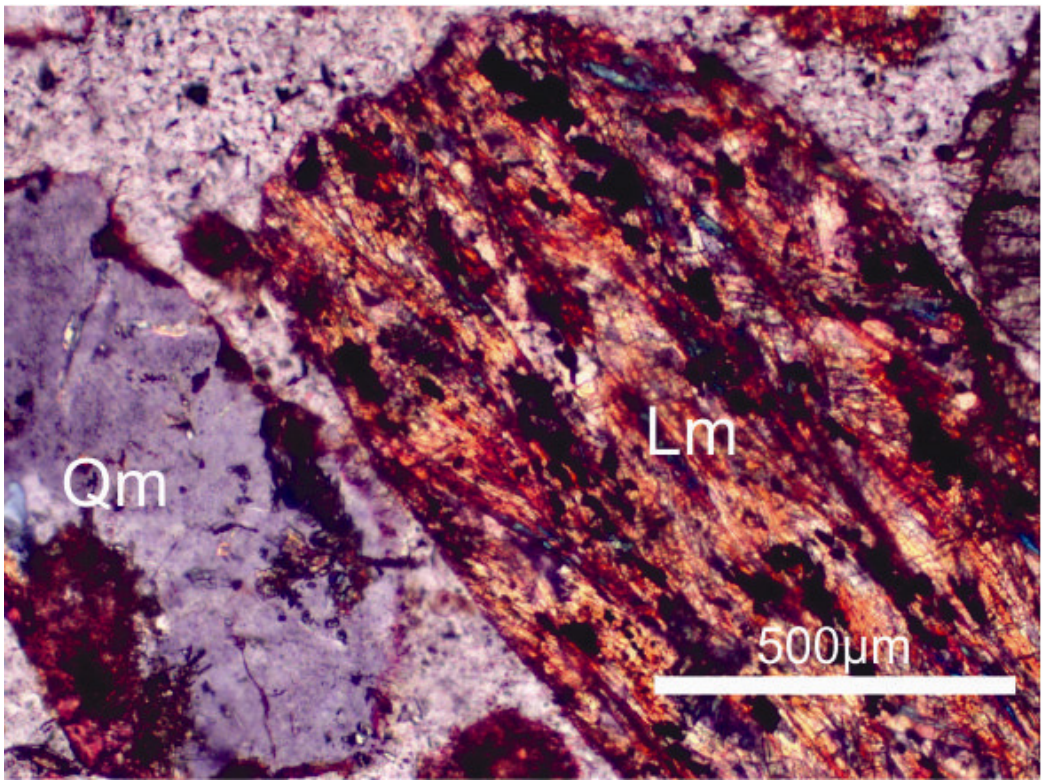

Figure 39. Metamorphic lithic and monocrystalline quartz

The appearance of weak to moderate foliation, strained, stretched, or flattened minerals defines metamorphic lithics. The appearance of monocrystalline or polycrystalline quartz is also an indicator of a metamorphic source. Lm=metamorphic lithic; Qm=monocrystalline quartz. From well MW13, 87 feet in drillers depth. Cross-polarized light, 10X.

(Table 4). The decline of metamorphic indicates a possible Red Bluff Formation-Tuscan Formation boundary (Figure 41). At depths 139.5 to 164.5 feet bgs, there is an influx of intraclast, and decrease of volcanic lithics. Increasing of intraclast could be indicative of a paleochannel reworking of recently deposited volcanic grains.

Calculated volcanic lithic to metamorphic lithic percentage places the boundary in well MW11 at ~144.5 feet (bgs) (Figure C-1).

TABLE 3. MW9 POINT COUNTS

Below Ground Surface (ft)	Qm	Qp	Kspar	Plag	Lm	Ls	Lv	Py/ Ol	Int	Micas	pumice	heavy minerals	total
114	34	2	0	5	134	0	81	25	19	0	0	0	300
120	14	1	3	9	67	0	161	25	19	0	1	0	300
124	56	6	0	10	74	0	106	38	10	0	0	0	300
126	11	0	2	7	22	0	191	28	39	0	0	0	300
128	18	6	3	7	31	0	168	29	37	0	1	0	300
130	3	1	0	4	14	0	181	57	40	0	0	0	300
132	11	2	0	5	25	0	166	44	47	0	0	0	300
134	18	5	0	7	25	0	171	45	29	0	0	0	300
136	23	2	0	2	25	0	118	22	108	0	0	0	300
138	0	0	0	3	1	0	35	36	225	0	0	0	300
140	0	0	0	20	0	0	139	65	76	0	0	0	300
142	0	0	0	11	2	0	103	38	146	0	0	0	300
146	0	0	0	2	4	0	45	16	233	0	0	0	300
148	0	0	0	25	0	0	208	58	9	0	0	0	300
150	1	0	0	14	0	0	212	61	12	0	0	0	300
156	0	0	0	20	1	0	223	55	1	0	0	0	300
158	0	0	0	22	1	0	234	40	2	0	0	1	300
160	0	0	0	14	0	0	257	29	0	0	0	0	300
162	0	0	0	29	0	0	240	29	2	0	0	0	300
166	0	0	0	23	1	0	230	44	1	0	0	1	300
168	0	0	0	28	1	0	233	33	5	0	0	0	300

Table 3 (continued).

Below Ground Surface (ft)	Qm	Qp	Kspar	Plag	Lm	Ls	Lv	Py/ Ol	Int	Micas	pumice	heavy minerals	total
174	0	0	0	23	0	0	251	22	4	0	0	0	300
180	2	1	0	1	1	0	183	63	49	0	0	0	300
182	0	0	0	20	3	0	206	55	15	0	0	1	300
184	0	1	0	18	3	0	145	84	44	0	0	5	300
185	0	0	0	8	1	0	192	67	31	0	0	1	300
187	0	0	0	23	1	0	219	53	3	0	0	1	300
189	0	0	0	24	0	0	228	39	7	0	0	2	300
191	0	0	0	11	0	0	263	21	5	0	0	0	300
195	0	0	0	18	0	0	261	15	6	0	0	0	300
197	0	0	0	13	0	0	271	14	2	0	0	0	300
199	0	0	0	13	0	0	278	9	0	0	0	0	300
230	0	0	0	9	9	0	195	82	5	0	0	0	300
232	0	0	0	10	3	0	238	46	1	0	0	2	300
258	0	0	0	18	2	0	220	57	3	0	0	0	300
262	0	0	0	23	1	0	223	52	0	0	0	1	300

Note: 300 mineral point counts were tabulated from each thin section from well MW11. The red line represents the Red Bluff Formation-Tuscan Formation boundary (depth 136-138 feet), where Red Bluff dominant minerals cease (Lm, Qm, Qp).

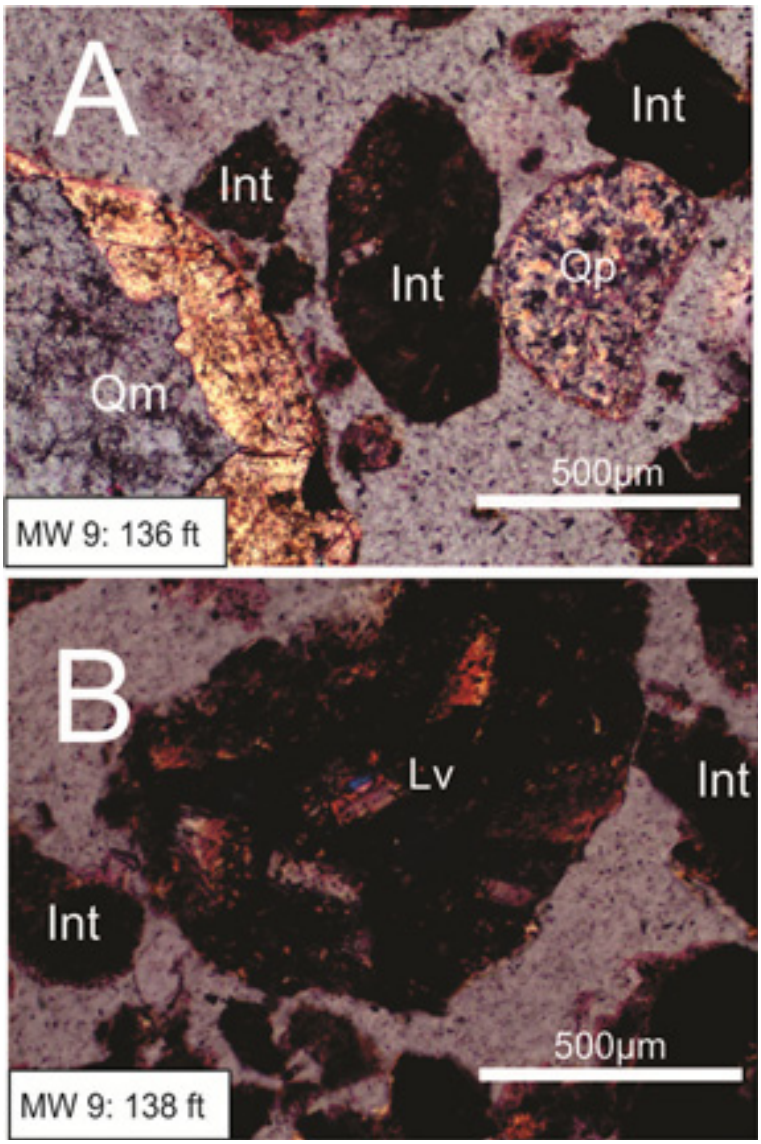

Figure 40. Red Bluff Formation-Tuscan Formation boundary

Compositional change from metamorphic lithics/ monocrystalline quartz (A), to predominantly volcanic lithics (B), suggest a Red Bluff Formation-Tuscan Formation boundary at a depth range of (136-138 feet). Qm=monocrystalline quartz; Qp= polycrystalline quartz; Lv= volcanic lithics; Int=intraclast. Cross-polarized light, 10X

TABLE 4. MW11 POINT COUNTS

Below Ground Surface (ft)	Qm	Qp	Kspar	Plag	Lm	Ls	Lv	Py/Ol	Int	Micas	pumice	heavy minerals	total
122	10	2	0	2	34	7	182	5	47	0	0	11	300
124.5	30	1	0	5	110	0	66	25	51	0	0	12	300
129.5	42	0	0	4	97	0	62	17	72	0	0	6	300
130	108	0	4	112	34	0	9	23	7	0	0	3	300
132	22	2	0	1	83	0	110	13	69	0	0	0	300
134.5	26	18	0	0	98	0	82	3	73	0	0	0	300
139.5	25	4	0	0	13	0	50	0	206	0	2	0	300
142	12	1	0	0	39	0	96	0	152	0	0	0	300
147	0	0	0	0	0	0	22	1	270	0	7	0	300
149.5	2	0	0	0	3	0	39	6	245	0	5	0	300
154.5	0	0	0	0	1	0	65	2	232	0	0	0	300
159.5	0	0	0	0	3	0	124	10	163	0	0	0	300
164.5	0	0	0	0	0	0	51	31	218	0	0	0	300
194.5	0	0	0	13	1	0	250	36	0	0	0	0	300
209	0	0	0	11	2	0	211	74	2	0	0	0	300
210	0	0	0	0	0	0	0	0	0	0	0	0	0
219.5	0	0	0	17	0	0	224	58	1	0	0	0	300
239.5	0	0	0	8	2	0	219	70	1	0	0	0	300

Note: 300 mineral point counts were tabulated from each thin section from well MW11. The red line represents the Red Bluff Formation-Tuscan Formation boundary (depth 142-147 feet), where Red Bluff dominant minerals cease (Lm, Qm, Qp).

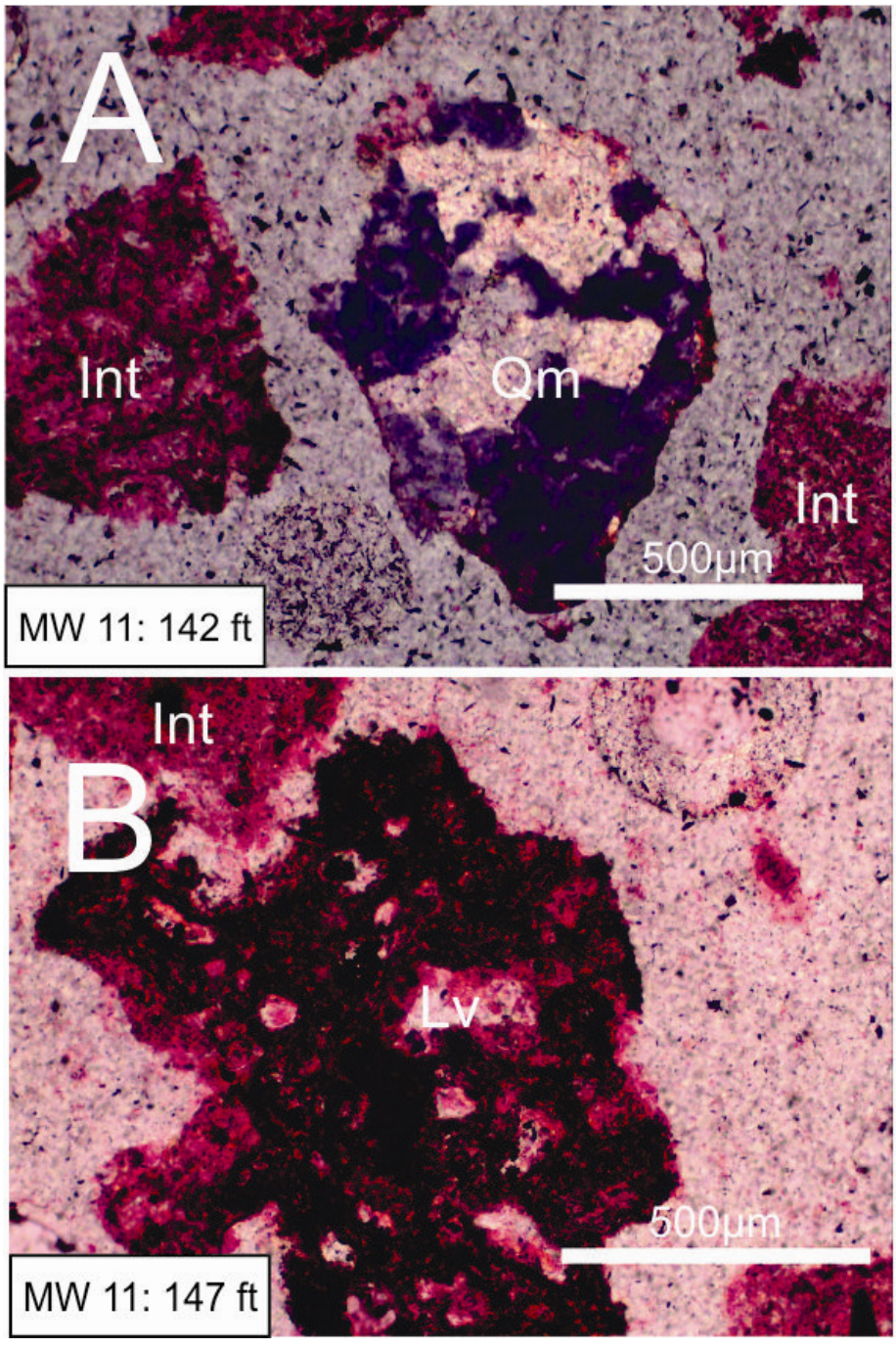

Figure 41. MW11 Red Bluff Formation-Tuscan Formation boundary

Compositional change from metamorphic lithics/monocrystalline quartz (A), to predominantly volcanic lithics (B), suggest a Red Bluff Formation-Tuscan Formation boundary at a depth range of (142-147 feet). Qm=monocrystalline quartz; Lv= volcanic lithics; Int=intraclast. Cross-polarized light, 10X.

Well MW13 Petrographic Analysis

Well MW13 displays a decline of metamorphic lithics/minerals (Lm, Qm, Qp) at ~147 to 152 feet bgs (Table 5) indicating a possible Red Bluff Formation-Tuscan Formation boundary (Figure 42). Concentrations of volcanic vary drastically in MW13, depleting between depths~197 to 152 feet bgs with an increase of intraclasts. A paleochannel may be indicated by a decrease of volcanic lithics, and an increase in intraclasts.

Calculated volcanic lithic to metamorphic lithic percentage places the boundary in well MW13 at ~149.10 (bgs) (Figure C-1).

Red Bluff Formation-Top Tuscan Formation Subsurface Correlation

Petrographic analysis data as well as well completion reports (Appendix E) from driller's logs provide a method to correlate Red Bluff-top Tuscan boundary to the wireline logs of water wells. Once a Red Bluff-top Tuscan baseline boundary was established, pattern recognition was used to identify the surface in adjoin wells without sandstone data. By combining the well depth placement of the boundary from all of the wells, it is possible to produce cross-sections as well as a 3D representation of the surface using the Petrel software (Figure 43). Three cross sections were produced along strike and dip of the Red Bluff Formation- top Tuscan Formation surface: Cross Section 1 (Figure C-1) displays the MW wells, including MW9, MW11, and MW13; Cross Section 2 (Figure C-2) is along strike of the surface and Cross Section 3 (Figure C-3) is along dip of the surface. Dip averages of the top Tuscan surface were calculated, both in the subsurface and in the outcrop. The average Red Bluff Formation- top Tuscan Formation

TABLE 5. MW13 POINT COUNTS

Below Ground Surface (ft)	Qm	Qp	Kspar	Plag	Lm	Ls	Lv	Py/Ol	Int	Micas	pumice	heavy minerals	total
87	28	2	0	5	45	1	155	45	19	0	0	0	300
97	28	1	0	7	49	1	164	25	25	0	0	0	300
127	33	2	0	4	60	1	107	55	38	0	0	0	300
137	36	0	0	7	29	0	173	44	11	0	0	0	300
147	28	1	0	36	16	0	167	34	18	0	0	0	300
152	4	0	0	0	4	0	57	19	216	0	0	0	300
159.5	1	1	0	2	10	0	61	7	218	0	0	0	300
167	1	0	0	1	2	0	23	2	271	0	0	0	300
179.5	3	0	0	10	0	0	52	12	223	0	0	0	300
182	1	0	0	0	0	0	12	8	279	0	0	0	300
184.5	2	0	0	0	1	0	50	2	245	0	0	0	300
187	2	0	0	0	1	0	44	10	243	0	0	0	300
189.5	1	0	0	3	0	0	58	4	234	0	0	0	300
192	0	0	0	5	1	0	143	13	138	0	0	0	300
194.5	0	0	0	8	1	0	85	39	167	0	0	0	300
197	0	0	0	2	1	0	107	49	141	0	0	0	300
199.5	1	0	0	36	0	0	221	41	0	0	1	0	300
202	0	0	0	30	0	0	240	30	0	0	0	0	300
207	0	0	0	40	0	0	229	31	0	0	0	0	300
214.5	0	0	0	43	0	0	224	33	0	0	0	0	300
227	0	0	0	46	1	0	204	41	8	0	0	0	300
229.5	0	0	0	29	0	0	227	44	0	0	0	0	300

Table 5 (continued)

Below Ground Surface (ft)	Qm	Qp	Kspar	Plag	Lm	Ls	Lv	Py/Ol	Int	Micas	pumice	heavy minerals	total
234.4	0	0	0	18	1	0	220	56	4	0	0	1	300
240	1	0	0	42	0	0	224	33	0	0	0	0	300
250	0	0	0	38	0	0	231	31	0	0	0	0	300

Note: 300 mineral point counts were tabulated from each thin section from well MW13. The red line represents the Red Bluff Formation-Tuscan Formation boundary (depth 147-152 feet), where Red Bluff dominant minerals cease (Lm, Qm, Qp).

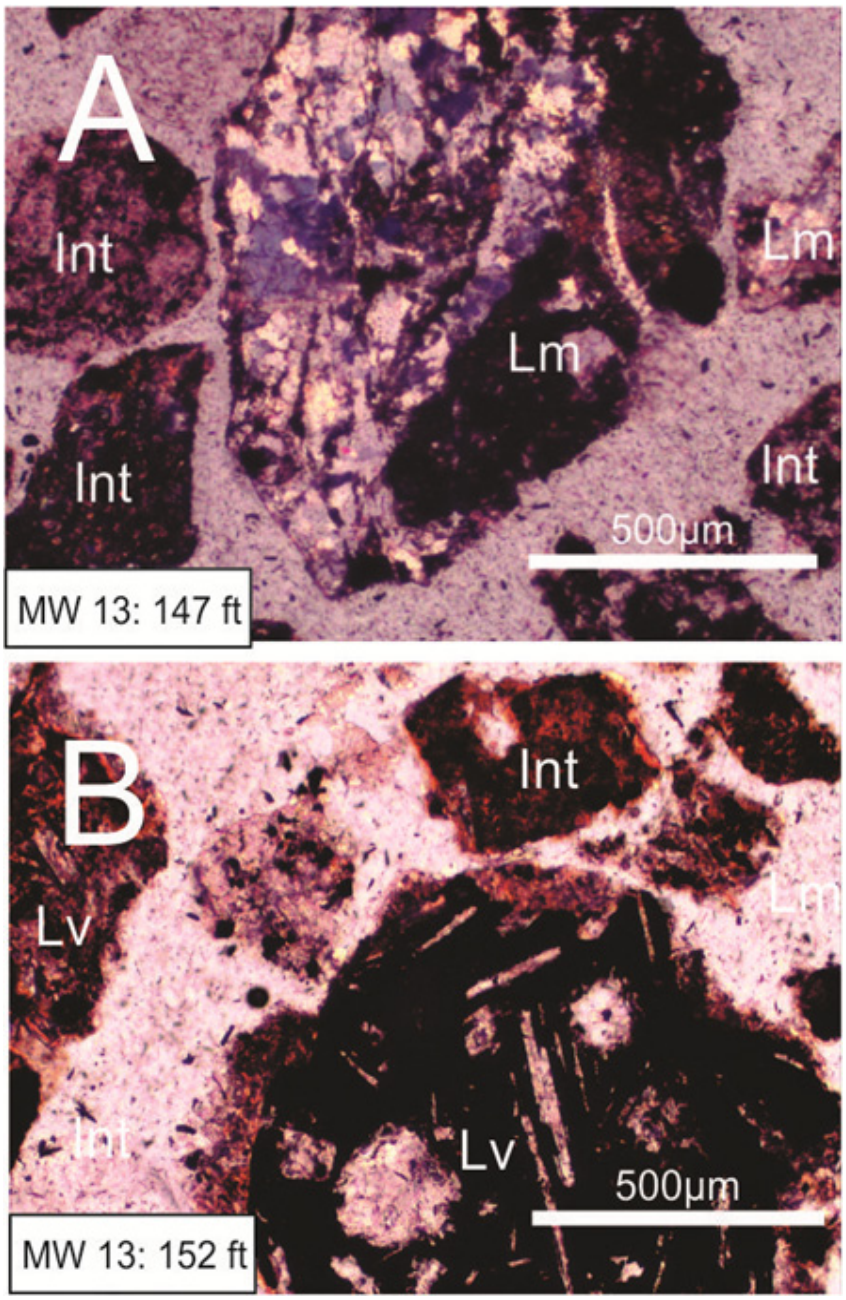

Figure 42. MW13 Red Bluff Formation-Tuscan Formation boundary.

Compositional change from metamorphic lithics/monocrystalline quartz (A), to predominantly volcanic lithics and intraclast (B), suggest a Red Bluff Formation-Tuscan Formation boundary at a depth range of (147-152 feet). Lm=metamorphic lithic; Lv=volcanic lithics; Int=intraclast. Cross-polarized light, 10X.

dip in the subsurface was calculated with a calculated average dip of 1.13°. In outcrop, the average Red Bluff Formation-top Tuscan Formation dip is 3.74°. Specific features of this surface along with their interpretations will be discussed in the following chapter.

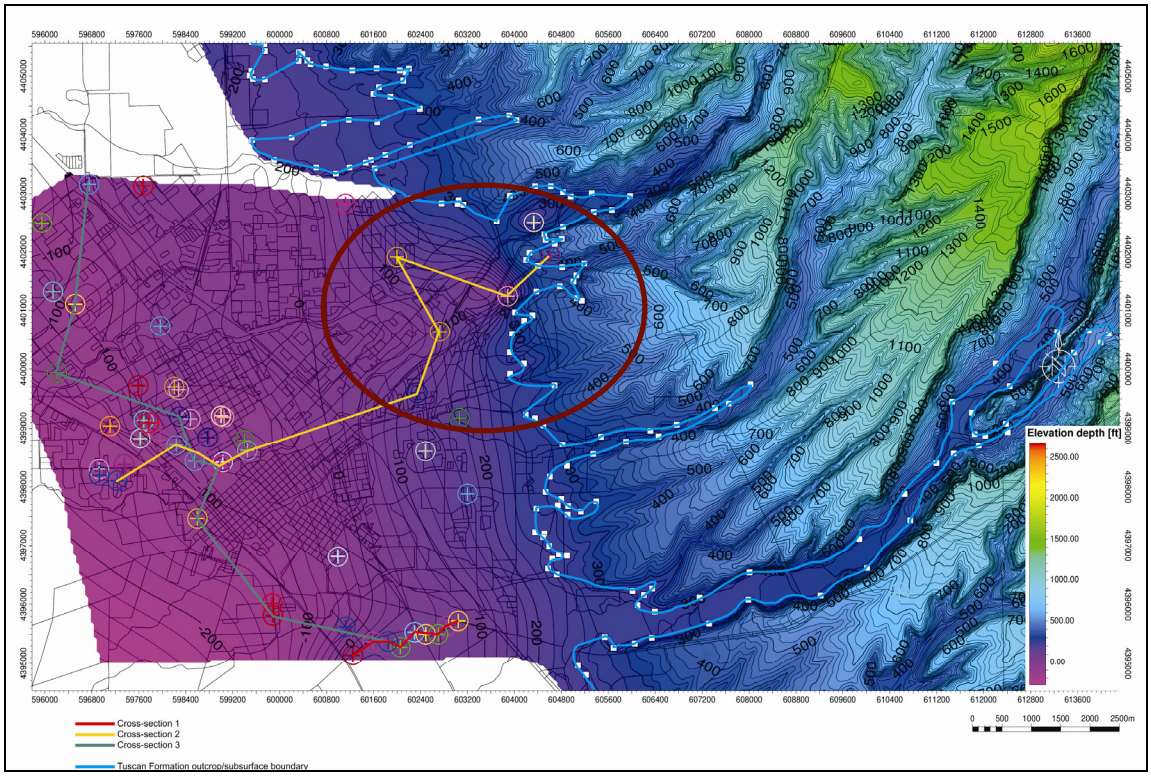

Figure 43. 3D representation of Red Bluff Formation-top Tuscan Formation surface.

3D representation of the Red Bluff Formation-top Tuscan Formation surface using the Petrel software. The light blue line marks GPS Tuscan Formation outcrop/subsurface boundary. Three cross sections were produced along strike and dip of the Red Bluff Formation- top Tuscan Formation surface: Cross-section 1 (red line) displays the MW wells, including MW9, MW11, and MW13; Cross-section 2 (yellow line) is along strike of the surface and Cross-section 3 (green line) is along dip of the surface. Inside the red circle appears to be an erosional-valley where the now modern day Horse-Shoe Lake resides.

CHAPTER V

DISCUSSION

Timelines in Tuscan Formation Outcrop

By determining facies (Table 1) and facies associations (Table 2) in the Tuscan Formation, time-correlative surfaces were mapped on Musty Buck Ridge. These surfaces were designated based on identification of synchronous stratigraphic surfaces which represent a major change in depositional environment (e.g. normal stream flows and active creeks, debris flows, hyperconcentrated flows, distal debris flow, pyroclastic deposits and flood deposits) and/or major change in composition. The most common timeline type was interpreted to be at the base of large debris flow deposits because the flows were quickly emplaced and non-erosive in their distal settings.

Depositional Processes and Preferred Depositional Model

Between each timeline surface is a complex sedimentary depositional history consisting of interbedded debris flows, normal stream flows, distal debris flows, hyperconcetrated flows, reworked tuff, flood deposits and inter-channel deposits. The complexity of how the volcaniclastic facies are arranged in sequences are dependent on flow types and the variety of ways in which sediment and water mixtures are triggered (Smith and Lowe, 1991). The concentration of sediment, sediment transport, flow rheology, and depositional mechanics may vary spatially or temporally at a fixed

depositional site due to sediment bulking into the flow and additional water being added, causing complex lateral and vertical facies sequences produced by single events (Smith and Lowe, 1991). These complex facies sequences, defined as facies associations (Table 2) are definable in the Tuscan Formation outcrops.

Smith (1991) attributes the variation in facies sequences (facies associations) to two generalized conditions of sedimentation using the syneruption versus inter-eruption model. Syneruption periods occur during explosive volcanic eruptions, causing influxes of pyroclastic material to be produced. Rivers and channels are transformed to wider, often braided, aggrading streams that are affected by hyperconcentrated flows and debris flows. Facies during syneruption conditions tend to be brecciated flow deposits, pyroclastic-fall deposits, overbanked flood deposits and inter-channel deposits. Syneruption deposition can occur for years to decades after volcanic cessation until loose sediment and debris have been completely removed from hill slopes, or until vegetation stabilizes the debris. Eventually, restoration of pre-eruption, inter-eruption conditions will be restored. Inter-eruption periods are considered “normal conditions,” when volcanism has little to no effect on the fluvial system, and normal stream flow and dilute stream flow processes are the dominant depositional mechanism. During the inter-eruption period, stream beds typically become incised, forming narrower, more sinuous channels (Figure 44). Facies during inter-eruption conditions are controlled by rates of lateral migration of channels, whereas vertical aggradation is the primary control during syneruption. Deposition during normal stream flow typically occurs on point bars, depositing medium to fine grain sands. Channel scouring of loose grains can develop due

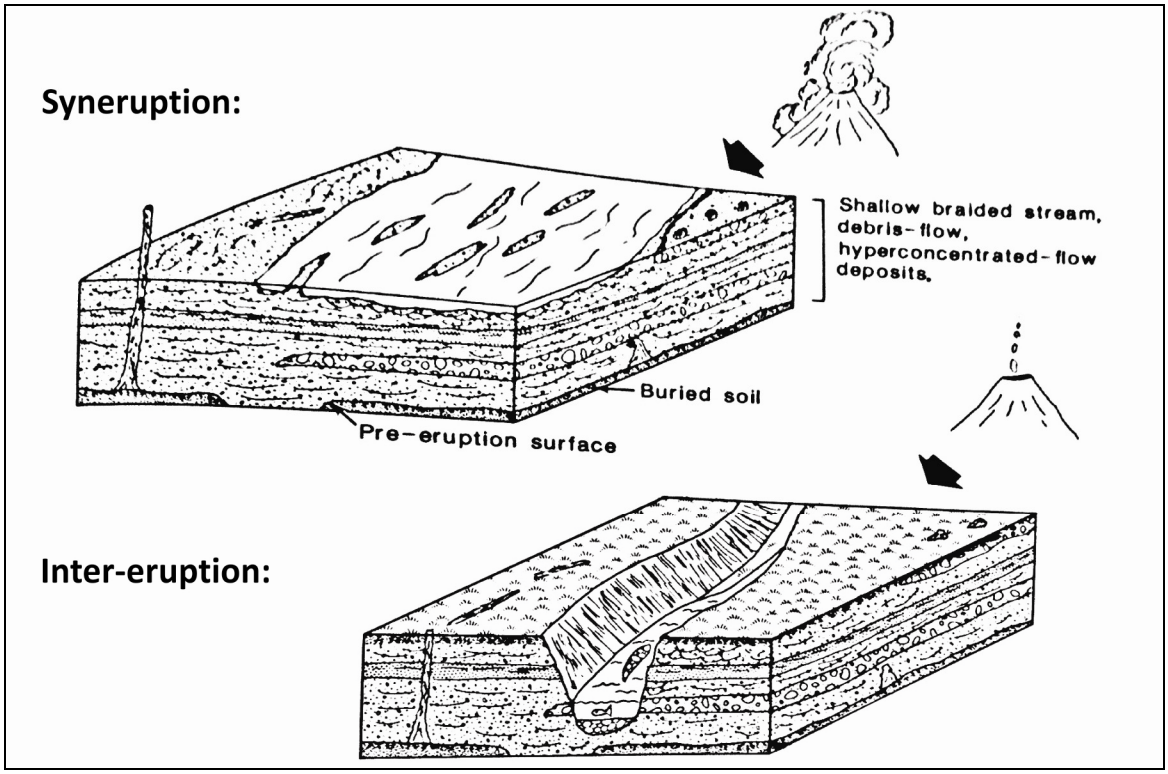

Figure 44. Syneruption versus Inter-eruption Model.

Schematic representation of geomorphic and stratigraphic characteristics of syneruption and inter-eruption. Syneruption is brought on by eruptive activity, creating an influx of sediment and water, leading to transformations of wider, aggrading braided streams, which are impacted by hyperconcentrated and debris flows. Under normal conditions, with little to no influence from volcanic activity, inter-eruption conditions develop, producing deposits and facies associated with normal stream flow. Modified from Smith, A.G., 1991, Facies sequences and geometries in continental volcaniclastic sediments: Sedimentation in Volcanic Settings, SEPM Special Publication No. 45 (fig 3).

to lateral erosion. Typical facies found in inter-eruption are poorly sorted sandstone, cross-bedded and planar laminated sandstone, and both matrix (poorly sorted) and clast supported conglomerates.

The syneruption versus inter-eruption model may be applicable to the Tuscan. For example, the Tuscan's volcanic derived facies association (e.g. volcanic debris flow,

hyperconcentrated flow, distal debris flow, pyroclastic deposits and flood deposits) are intercalated with normal stream flow facies association on the Tuscan. This could represent a period of sedimentation influences from active volcanic eruption followed by restoration to normal stream flow conditions once volcanic activity has ceased.

In addition to depositional environment, lithofacies can be influenced by physical confinement. According to Palmer *et al*. (1991) physiographic barriers generally confine debris flows. Major flow direction is downstream, and dominant direction of lithofacies development is parallel to flow. Spatial arrangement of lithofacies in the resulting deposits is a proximal (axial a) to medial (axial b) to distal (marginal) arrangement (Figure 45). Development of a minor flow component oblique to the dominant flow direction can occur in some cases if the valley floor is large enough. In an unconfined setting, deposits fan out, producing rapid, lateral facies changes (Figure 45).

Deposits on Musty Buck Ridge have apparent deposition in a predominantly confined system. Spatial lithofacies arrangements appear to follow medial to distal deposits as you move down stream rather than oblique, rapid, lateral facies changes. North-east deposits on Musty Buck Ridge exhibit Thick deposits (up to 35 meters) of debris flow become thinner (2-3 meters) laterally, south-west down canyon (Figure A-1) and normal stream deposits are more prevalent on Musty Buck Ridge. Further evidence for a confined system is the dissimilarity of stratigraphy in adjacent Ridges to Musty Buck Ridge. Typically in an unconfined system, approximal ridges would share the same or very similar stratigraphy, yet this is not the case with ridges surrounding Musty Buck Ridge. Stratigraphic sections created by Greene (2014) on the Chico overlook, south-east

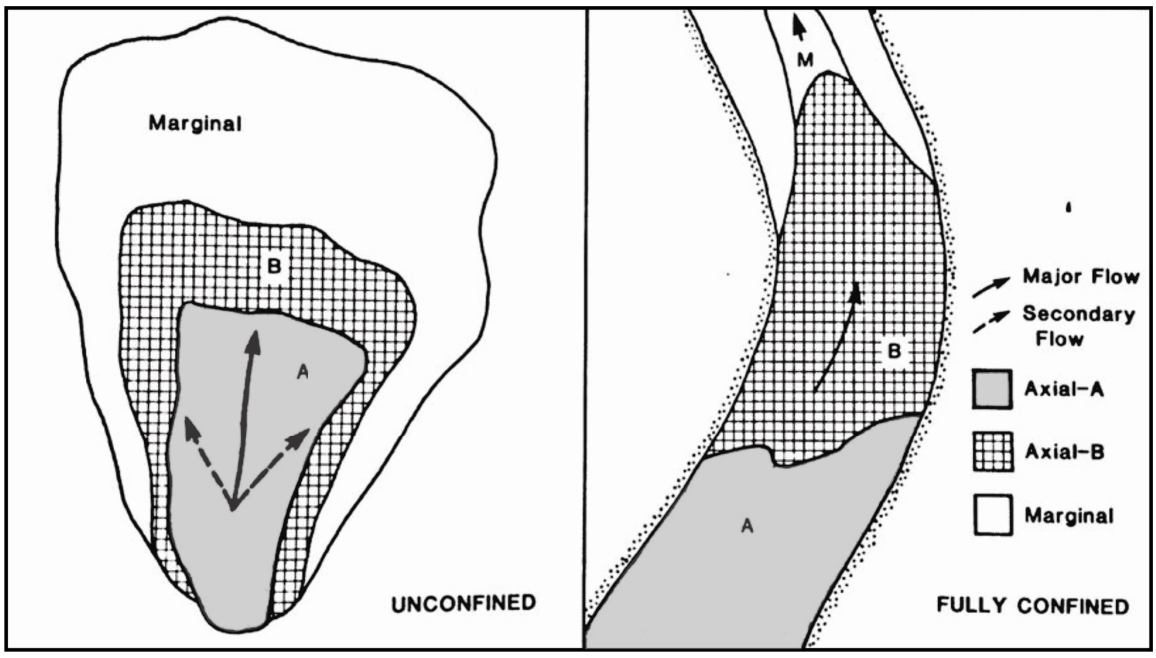

Figure 45. Generalized lithofacies relationship in confined and unconfined debris avalanche/debris flow deposits.

Modified from Palmer, B.A., Alloway, B.V., and Neall, V.E., 1991, Volcanic-debris-avalanche deposits in New Zealand: Lithofacies organization if unconfined, wet-avalanche flows: Sedimentation in Volcanic Settings, February 1, 2010, v. 1, p. 89-98. (fig 8).

Highway 32 ridge, have a different depositional history than Musty Buck Ridge (Figure 46). While lithofacies are similar on both ridges, they do not correlate across canyon. For example, absent from Musty Buck Ridge, but found on Highway 32 Ridge, are massive (up to 60 meters thick) brecciated debris flow deposits, while the maximum thickness of brecciated debris flow deposits on Musty Buck Ridge is 35 meters. Although evidence points to a confined system, further study and stratigraphic sections on nearby ridges is needed to make a definitive conclusion. A summarized series of events with interpreted depositional geometries for each of the MBR units are shown in Figure 47.

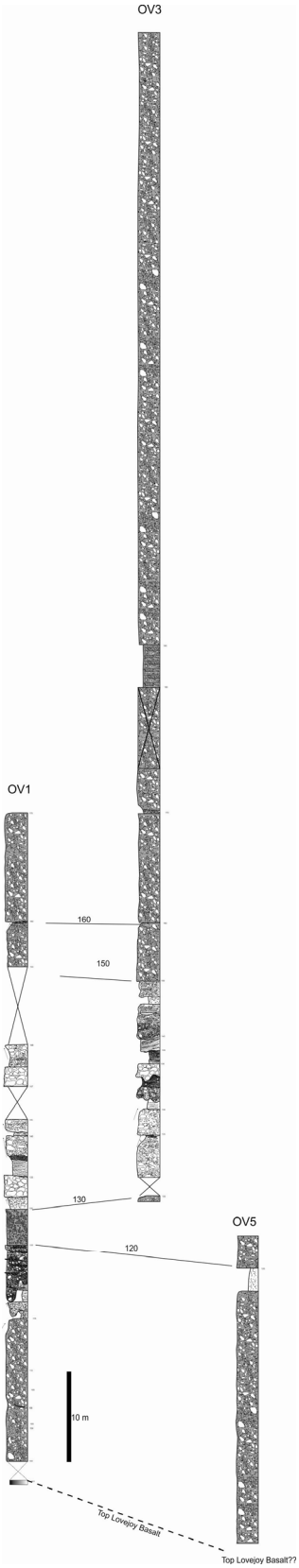

Figure 46. Stratigraphic section measured on HW 32 Ridge

Stratigraphic section from south, across canyon of Musty Buck Ridge on HWY 32 Ridge.
Figure modified from Todd Greene, unpublished 2014.

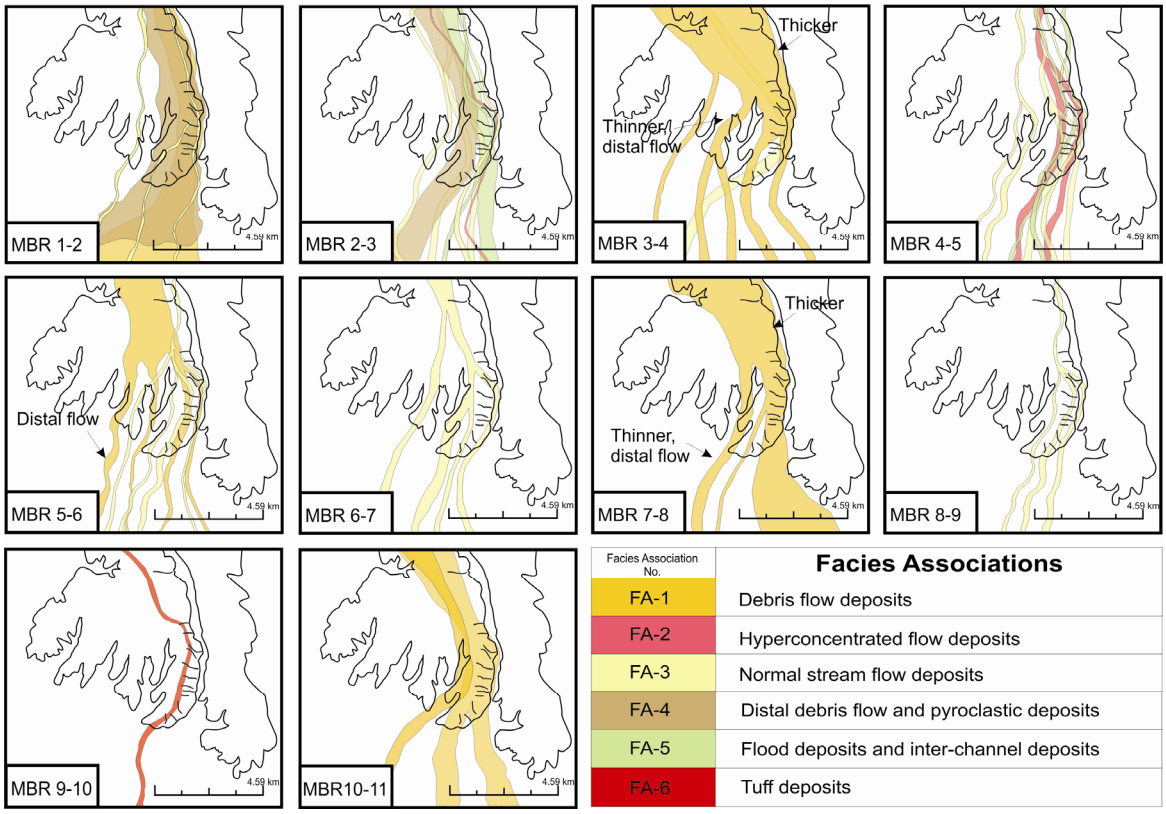

Figure 47. Major time correlative events in order of deposition

Panels depict what depositional facies association may have looked like on Musty Buck Ridge between major time correlative events. Time correlative events are based on major changes in depositional environment and/or major change in composition.

Idealized Tuscan Sedimentation Cycle: Creating an Idealized Aquifer System

Understanding an idealized Tuscan sedimentation cycle may provide some insight on how it relates to how the sedimentologic structure of an effective aquifer may be created. The Tuscan Formation's sedimentation appears to occur in cycles similar to those of modern volcanoes (as discussed in Modern Analogs section) controlled by volcanic activity, glaciations, and climate (Vessell and Davies, 1981). Though no attempt at statistically representing cyclic deposition has been attempted on the Tuscan, vertically

repeating facies associations in outcrop are good evidence of sedimentation cycles. During the late Pliocene, the paleo-valley had alternating periodic influxes of sedimentation from normal stream flow deposits, channels, and debris flow deposits flowing westward off ancestral volcanoes onto the valley floor. During normal stream flow, rivers and creeks flowed downslope over the debris flows, forming channels that were then infilled with reworked volcanic sands and gravel sediments. After burial, the porous volcanic sands and gravel act as a good aquifer capable of storing and transmitting fresh groundwater (California Department of Water Resources, 2014). Subsequent debris flows were deposited over the reworked sediment creating a confining layer over the sand and gravel leading to an eventual aquiclude or aquitard when buried.

Petrology and Subsurface Analysis

In order to determine the connectivity of various porous zones in the local aquifer it is important to locate the Red Bluff Formation-top Tuscan Formation boundary. It not only represents an unconformity surface but compositional differences between the Red Bluff Formation and the Tuscan Formation could also alter the permeability and transmissivity of the formations, affecting the groundwater flow. A maximum soil profile developed on the Red Bluff Formation forms hardpans that are aquicludes (Olmsted and Davis, 1961). The aquicludes could prevent the percolation of surface waters into the subsurface aquifer (Olmsted and Davis, 1961).

Ingersoll and Steinpress (2007) first demonstrated that is possible to use a petrographic sand provenance analysis to determine these types of stratigraphic

boundaries by exploiting differences in the various formations' source rocks. Using tabulated data of sand grains from monitoring wells MW9, MW11 and MW13, the location of the Red Bluff Formation-Tuscan Formation boundary in all three wells was determined to be: MW9 is ~136.60 feet bgs, MW11 is ~144.5 feet bgs, and MW13 is ~149.10 feet bgs. Future production of a hydraulic model on the local aquifer relies on accurately identifying the Tuscan Formation-Red Bluff Formation boundary, as water will transmit differently between the two media. By understanding the Tuscan Formation and Red Bluff Formation in the subsurface, future groundwater models can help constrain flowpaths and storage volumes of the local aquifer (Greene and Teasdale, 2008).

Data from the three wells was used as a baseline to find the Red Bluff Formation-Tuscan Formation boundary to correlate to nearby wells as well as data from well completion reports and GPS data of top Tuscan outcrops, and hand samples from MW35, MW18, CMW 112, and CMW 121C (Figure 43). The mapped surface provides a picture of what the topography may have looked like prior to deposition of the Red Bluff Formation. For example, a subsurface valley-shaped feature occurs in the central portion of the map indicating a possible paleo-valley prior to Tuscan deposition. In addition, the shallow slope of the top Tuscan Formation in the western portion of the map may not be an actual change in dip of the Tuscan layers, but it may reflect the erosional nature of the top-Tuscan surface (Figure 48). For example, in central Chico, the dip is fairly shallow relative to the rest of the map. This change in dip may affect where groundwater will travel in response to groundwater pumping either through municipal pumping or pumping related to water treatment projects monitoring contaminant plumes.

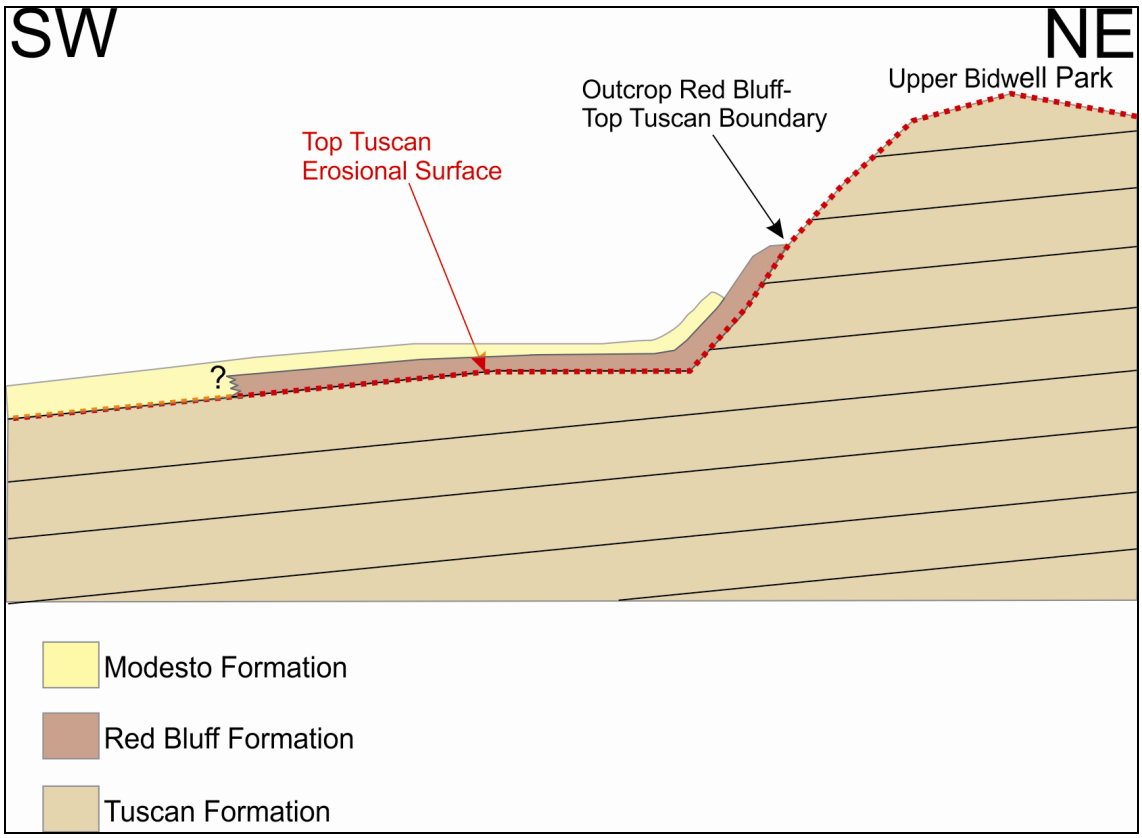

Figure 48. Idealized cross-section of Red Bluff Formation-Tuscan Formation surface.

Cross-section depicts an idealized schematic of the Red Bluff Formation-top Tuscan Formation surface. The red dotted line represents the surface mapped in figure 43. Black lines represent dip of Tuscan layers. The question mark depicts the uncertainty in the boundary between the Red Bluff and Modesto formations.

Correlation of Major Outcrop Surfaces Into the Subsurface

While it is possible to determine the top Tuscan Formations boundary in the subsurface, MBR surfaces from outcrop in this study could not be distinguished in the subsurface. Projection of MBR surfaces do not intersect with the wells because the MBR surfaces either pinch out before projecting into the subsurface or they have been eroded by the top-Tuscan erosional surface. However, from well completion reports and drill

cores, large thick volcanic debris flows have been identified in the subsurface. Unfortunately it is difficult to ascertain if they originated from the same source as the flows on Musty Buck Ridge or from other debris flow events (e.g., Highway 32 Ridge). It appears more likely that the MBR flows traveled westward and would now be encountered in the subsurface north of the well data control area. Nevertheless, future outcrop studies of the flows along the Highway 32 Ridge may relate more directly to the Tuscan deposits seen in the well data control area from this study.

CHAPTER VI

CONCLUSIONS

Combined study of outcrop characterization and subsurface analysis provide insight on establishing a geologic history and framework of the Tuscan Formation on Musty Buck Ridge and the local aquifer. This study provides a methodology for mapping individual flow types, depositional facies, and correlation of flow types based on eight stratigraphic sections (Section 6-13) and five additional stratigraphic sections (Sections 1-5) mapped by Alward and Springhorn (2006). In addition to field work, petrographic analysis of wells MW9, MW11, MW13, as well as utilization of GPS to mark key surfaces of Tuscan outcrops, provide the framework to map the Red Bluff-Top Tuscan Formation boundary in the subsurface.

Previous interpretations of the Tuscan are based off of Harwood and Helley's (1981) ABCD model which only divides the Tuscan on a regional scale rather than individual units established on flow-by-flow basis. In this study, detailed stratigraphic mapping of individual flow units on Musty Buck Ridge, allowed for recognition of major lithofacies in the Tuscan: breccia matrix-supported (L-1), breccia clast-supported (L-2), tuff (L-3), conglomerate matrix-supported (L-4), conglomerate clast-supported (L-5), massive sandstone (L-6), cross-bedded and planar laminated sandstone (L-7), and mudstone (L-8). Environmental interpretations of Tuscan lithofacies were then grouped together and correlated to define facies associations: volcanic debris flow (FA-1),

hyperconcentrated flow deposits (FA-2), normal stream deposits (FA-3), distal debris flow and pyroclastic deposits (FA-4), flood deposits and inter-channel deposits (FA-5) and tuff (FA-6).

In order to provide a more detailed geological history of the Tuscan, major changes of facies associations were used to create broken out timelines that bounded correlative packages on Musty Buck Ridge, from oldest to youngest (MBR 1-11). Older deposits near the base of sections on Musty Buck Ridge reflect a distal environment, with higher concentrations of distal debris flow and pyroclastic deposits, followed by an inter-eruption period dominated by active creeks and normal stream flow deposits. Younger deposits of the Tuscan are dominated by massive debris flows interbedded with normal stream flows. It should be noted that time correlative surfaces presented in this study do not correlate across canyon to adjacent ridges and should only be used to interpret the geologic history of Musty Buck Ridge.

In addition to field work, a petrographic analysis of wells MW9, MW11, MW13 using a point count method of individual sand grains was conducted to establish the Red Bluff-top Tuscan boundary. Higher concentrations of metamorphic lithics and metamorphic minerals are indicative of the Red Bluff Formation. Increased percentage of volcanic lithics, volcanic minerals are indicative of the Tuscan Formation. After a Red Bluff-Top Tuscan baseline was established in the subsurface, additional data such as driller completion reports, hand samples from core, and resistivity pattern recognition were utilized to complete a 3D map of the surface as well as three cross-sections. Due to

the erosional nature of the top-Tuscan Formation surface, attempts of correlating additional outcrop surfaces into the subsurface could not occur.

Outcrop and subsurface results in this study provide methods and data for creating a depositional interpretation and depositional model for the Tuscan; however, further development of the spatial geometry along multiple Tuscan cliffs via additional measured sections still needs to be completed. In addition, because time correlative surfaces do not correlate across canyon, it is crucial to map adjoining ridges and outcrops of Tuscan deposits. Finally, the petrographic analysis method provided in this study to establish the top-Tuscan surface should be applied to more wells across a broader area of the aquifer. While this study hypothesizes that the Red Bluff Formation-top Tuscan contact is identified by the abrupt change from volcanic dominated to metamorphic dominated lithics, recreating the same petrographic analysis in a stratigraphic column on the surface, where the contact can be directly observed, will provide more conclusive results. Finally, collecting additional drill cores samples and well data will aid in identifying other key surfaces in the Tuscan Formation and add to a growing database that could eventually be used to create an accurate subsurface model of the Tuscan Aquifer system.

REFERENCES CITED

REFERENCES

Alward, R., and Springhorn, S.T., 1996, Fluvial channel architecture and depositional setting of the Tuscan Formation, Chico, California: Abstracts with Programs - Geological Society of America, May, 2006, v. 38, no 5, pp.32.

Aslan, A., White, W.A., Warne, A.G., and Guevara, E.H., 2003, Holocene evolution of the western Orinoco Delta: Venezuela. Geological Society of America Bulletin, v. 115, no. 4, p. 479-498.

Brunkal, H.A. (2004), A stratigraphic and sedimentological evaluation of the Tuscan Formation, Northern California.

Buer, K. (2007), Sacramento River Fluvial Geomorphology-Red Bluff –Tehama, http://www.sacramentoriver.org/articles/Float.pdf

California Department of Water Resources, Northern Region Office Groundwater and Geologic Investigations Section, 2014, Geology of the Northern Sacramento Valley, California, http://www.water.ca.gov/pubs/geology/geology_of_the_northern_sacramento_valley__california__june_2014web/geology_of_the_northern_sacramento_valley_california_june_2014.pdf

Cande, S.C., and Kent, D.V., 1995, Revised calibration of the geomagnetic polarity timescale for the Late Cretaceous and Cenozoic: Journal of Geophysical Research, v.100, p. 6093-6095.

Carlton, A.E., Wohletz, A., Greene, T.J., and Teasdale, R., 2008, Volcaniclastic debris flow processes inferred from sedimentary textures of the southern Tuscan Formation, California: Abstracts With Programs - Geological Society Of America, v. 40, no. 1, p. 93.

Cecil, M.R., Rotberg, G.L., Ducea, M.N., Saleeby, J.B., and Gehrels, G.E., 2012, Magmatic growth and batholithic root development in the northern Sierra Nevada, California: Geosphere, v. 8, no. 3, p. 592-606, doi:10.1130/GES00729.1

Chen, J.H., and Tilton, G.R., 1982, Applications of lead and strontium isotopic relationships to the petrogenesis of granitoid rocks, central Sierra Nevada batholith, California: Geological Society of America Bulletin, v. 103, p.439-447.

Christiansen, R.L., Foulger, G.R., and Evans, J.R., 2002, Upper mantle origin of the Yellowstone hot spot: Geological Society of America Bulletin, v. 114, p. 1245-1256.

Crandell, D.R., 1987, Deposits of pre-1980 pyroclastic flows and lahars from Mount St. Helens Volcano: Washington. U.S. Geological Survey Professional Paper, 1444, 91 p., http://pubs.er.usgs.gov/publication/pp1444

Creely, R.S., 1965, Geology of the Oroville Quadrangle, California: California Division of Mines and Geology Bulletin 184, 86 p.

Day, H.W., Moores, E.M., and Tuminas, A.C., 1985, Structure and tectonics of the Northern Sierra Nevada: Geol. Soc. Am. Bull., 96, p. 436-450.

Dilek, Y., and Moores, E.M., 1989, Island-arc evolution and frature zone tectonics in the Mesozoic Sierra Nevada, California, and implications for transform offset of the Sierran/Klammath convergent margins: Salt Lake City, Utah, International Basement Tectonics Association, Inc.

Doukas, M., 1983,Volcanic geology of Big Chico Creek area, Butte County, California [Masters thesis]: San Jose, University of California, 157 p.

Duncan, J.A. (2005). Sedimentologic analysis of the pleistocene Red Bluff Formation[Masters thesis]: Chico, University of California, 266 p.

Evernden, J.F., Curtis, G., James, G., and Savage, D., 1964, Potassium-argon dates and the Cenozoic mammalian chronology of North America: American Journal of Science, v. 262, p. 145-198.

Fulton, A., Dudley, T., and Staton, K., 2012, Incentives for groundwater management in the northern Sacramento Valley: UC Irrigation and Water Resources Farm Advisors, University of California.

Garrison, N.J., Busby, C.J., Gans, P.B., Putirka, K., and Wagner, D.L., 2008, A mantle plume beneath California? The mid-Miocene Lovejoy flood basalt, Northern California, *in* Wright, J.E. and Shervais, J.W., eds., Ophiolites, arcs, and batholiths: A tribute to Cliff Hopson: Geological Society of America Special Paper 438, p. 551-572.

Greene, T.J., 2014, Stratigraphic section on Highway 32 Ridge, The Overlook, Chico California, unpublished raw data.

Greene, T.J., 2010, Proposal to analyze well-cuttings and well-logs from the Stony Creek fan conjunctive water management (SCF) program test wells installed near Hamilton City, CA.

Greene, T.J., and Teasdale, R., 2008, Geology tour of Big Chico Creek Canyon: The Miocene Lovejoy Basalt and Pliocene volcaniclastic Tuscan Formation: Department of Geological and Environmental Sciences, CSU-Chico, National Association of Geoscience Teachers-Far Western Section, Fall 2008 Conference.

Griscom, A., and Jachens, R.C., 1989, Tectonic history of the north portion of the San Andreas Fault system, California, inferred from gravity and magnetic anomalies: Journal of Geophysical Research 94, doi: 10.1029/88JB03834.

Haggart, J. W., and Ward, P. D., 1984, Late Cretaceous (Santonian-Campanian) stratigraphy of the northern Sacramento Valley, California: Geological Society of America Bulletin, v. 95, no. 5, p. 618-627.

Hall, J., 2011, Thin-section analysis to define the Tuscan/Red Bluff boundary from sonic drilling core samples near Chico, CA: Poster for the Department of Geological and Environmental Sciences, California State University Chico.

Harwood, D., Helley, E. and Doukas, M., 1981, Geologic map of the Chico monocline and northeast part of the Sacramento Valley: California. U.S. Geological Survey Miscellaneous Investigation Map, I-1238.

Harwood, D., and Helley, E., 1987, Late Cenozoic tectonism of the Sacramento Valley, California: Washington DC: U.S. Geological Survey.

Helley, E., and Harwood, D., 1985, Geologic map of the late Cenozoic deposits of the Sacramento Valley and northern Sierran foothills, California: U.S. Geological Survey Miscellaneous Field Studies Map MF-1790: 24 pp., 5 sheets, scale 1:62,500.

Helley, E., and Jaworowski, C., 1985, The Red Bluff Pediment-A datum plane for locating quaternary structures in the Sacramento Valley, California: Bulletin 1628. Menlo Park: U.S. Geological Survey.

Henry, C.D., and Perkins, M.E., 2001, Sierra Nevada-Basin and Range transition near Reno, Nevada: Two-stage development at 12 and 3 Ma: Geology v. 29, p. 719-722.

Ingersoll, R.V., and Steinpress, M., 2007, Northern Sacramento Valley sand provenance study, summary of petrographic results: Report prepared for the Department of Water Resources-Northern District, 43 p.

Janda, R.J., Scott, K.M., Nolan, K.M., H.A. and Martinson, H.A., 1981, Lahar movement, effects, and deposits, *in* Lipman, P.W. and Mullineaux, D.R., eds., The 1980 eruptions of Mount St. Helens: Washington, DC: Geological Survey Professional Paper 1250, p. 461-478.

Keiffer, S.W., 1981, Fluid dynamics of May 18 blast at Mount St. Helens, The 1980 eruption of Mount St. Helens, Washington: U.S. Geological Survey Professional Paper 1250, p. 379-400.

Kerle, N. N., Froger, J. L., Oppenheimer, C. C., and van Wyk de Vries, B. B., 2003, Remote sensing of the 1998 mudflow at Casita Volcano, Nicaragua: International Journal of Remote Sensing, v. 24, no. 23, p. 4791-4816.

Larsen, E., Anderson, E., Avery, E., Dole, K., 2002, The controls on and evolution of channel morphology of the Sacramento: Report to the Nature Conservancy, Sacramento River, California, Chico Landing Study Reach Meander Migration Report.

Lindberg, E., Teasdale, R., and Clynne, M., 2006, Characterization of the Yana volcanic center: Geological Society of America, Cordilleran Section, 102nd Annual Meeting; Abstracts with Programs, v. 38, p. 94.

Lydon, P.A., 1968, Geology and lahars of the Tuscan Formation: Northern California. Geological Society of America Memoir, p. 441-475.

Major, Jon J., Pierson, Thomas C., and Scott, Kevin M., 2005, Debris flows at Mount St. Helens, Washington, USA, Chapter 27 *in* Jakob, M., and Hungr, O.. eds, Debris-flow Hazards and Related Phenomena: Chichester, UK, Springer/Praxis, p. 685-731.

Moody, J.D., and Teasdale, R., 2006, Geologic mapping and descriptions of Pliocene Tuscan Formation lahar flows, Chico, California: Geological Society of America, Cordilleran Section, 102nd Annual Meeting; Abstracts with Programs, v. 38, p. 94.

Mullineaux, D.R., and Crandell, D.R., 1962, Recent lahars from Mount St. Helens, Washington: Bulletin of the Geological Society of America, v. 73, p. 855-870.

National Oceanic and Atmospheric Administration, 2014, What is LIDAR? LIDAR—light detection and ranging—is a remote sensing method used to examine the surface of the Earth, http://oceanservice.noaa.gov/facts/lidar.html

Nilsen, T. H., Barats, G. M., Imperato, D. P., Moore, D. W., and Serena, D. B., 1990, Upper Cretaceous hydrocarbon-rich depositional systems of the Sacramento Basin, California: AAPG Bulletin, v. 74, no. 5, p. 731, doi:10.1306/44B4B743-170A-11D7-8645000102C1865D

Olmstead, F. H., and Davis, G. H., 1961, Geologic features and ground-water storage capacity of the Sacramento Valley, California: U.S. Geological Survey Water-Supply Paper 1497, 241 p.

Palmer, B.A., Alloway, B.V., and Neall, V.E., 1991, Volcanic-debris-avalanche deposits in New Zealand: Lithofacies organization if unconfined, wet-avalanche flows: Sedimentation in Volcanic Settings, February 1, 2010, v. 1, p. 89-98.

Pierson, T.C., 1985, Initiation and flow behavior of the 1980 Pine Creek and Muddy River lahars, Mount St. Helens: Washington, DC: Geological Society of America Bulletin, v. 96, p. 1056-1069.

Redwine, L.E., 1972, The Tertiary Princeton submarine valley system beneath the Sacramento Valley, California [Ph.D. thesis]: Los Angeles, University of California, 480 p.

Russell, R., and Vanderhoof, V., 1931, A vertebrate fauna from a new pliocene formation in Northern California: Berkeley: University of California Press.

Schoenborn, W.A., and Fedo, C.M., 2012, Geochemical evidence for a glaciogenic origin of the Cryogenian Wildrose Diamictite, upper Kingston Peak Formation, Goler Wash, Death Valley, California: Abstracts With Programs - Geological Society Of America v. 44, no. 7, p. 36.

Schweickert, R.A., Bogen, N.L., Girty, G.H., Hansen, R. E., Merguerian, C., 1984, Timing and structural expression of the Nevadan Orogeny, Sierra Nevada, California: Geological Society of America Bulletin, v. 95, p. 967-979.

Scott, W.E., 1989, Volcanic and related hazards, Ch. 2, *in* Tilling, R.I., ed., Volcanic Hazards: Short Course in Geology, v. 1, p. 9-23.

Scott, K. M., Vallance, J. W., Kerle, N., Macias, J., Strauch, W., Devoli, G., 2004, Catastrophic precipitation-triggered lahar at Casita Volcano, Nicaragua; occurrence, bulking and transformation: Earth Surface Processes and Landforms, v. 30, no. 1, p. 59-79.

Siemers, C. T., Tillman, R. W., 1981, Recommendations for the proper handling of cores and sedimentological analysis of core sequences, *in* Siemers, C. T., Tillman, R. W., Williamson, C. R., eds., Deep-Water Clastic Sediments—A Core Workshop: SEPM Core Workshop, n. 2, p. 20–44.

Skartvedt-Forte, M., 2006, A hydrostratigraphic study of the Tuscan Formation: Abstracts with Programs - Geological Society of America, v. 38, no. 5, p. 32.

Smith, M.R., Greene, T.J., and Teasdale, R., 2008, Geologic mapping and flow identification of the Tuscan Formation, northern California: Geological Society of America, Cordilleran Section, 104th Annual Meeting; Abstracts with Programs, v.40, p. 43.

Smith, A.G., 1986, Coarse-grained nonmarine volcaniclastic sediment; terminology and depositionsl process: Geological Society of America Bulletin, v. 97, no. 1, p. 1-10.

Smith, A.G., 1991, Facies sequences and geometries in continental volcaniclastic sediments: Sedimentation in Volcanic Settings, SEPM Special Publication No. 45.

Smith, A.G., and Lowe, R.D., 1991, Lahars: Volcano-hydrologic events and deposition in the debris flow-hyperconcentrated flow continuum, *in* Fisher, R.V., and Smith, G.A., eds., Sedimentation in Volcanic Settings, v. 45, p. 59-70.

Vallance, J. W., Gardner, C., Scott, W. E., Iverson, R., and Pierson, T., 2010, Mount St. Helens: A 30-Year legacy of volcanism: EOS, v. 91, p. 169-170, http://www.agu.org/pubs/crossref/2010/2010EO190001.shtml

Vallance, J.W., Schilling S.P., Devoli, G., Reid, M.E., Howell, M.M., and Brien, D.L., 2004, Lahar hazards at Casita and San Cristóbal volcanoes, Nicaragua: U.S. Geological Survey Open-File Report 01-468.

Vallance, J. W., 2000, Lahars, *in* Sigurdsson, H., ed., Encyclopedia of Volcanoes, San Diego, Academic Press, p. 601-616

Vessel, R.K., and Davies, D.K., 1981, Nonmarine sedimentation in an active fore arc basin: Soc. Econ. Paleont. Mineral. Publ. 31, p. 31-45.

Wagner, H. W., Saucedo, G.J., 1981, Age and Stratigraphic Relationships of Miocene volcanic rocks along the eastern margin of the Sacramento Valley, CA, *in* Ingersoll, R.V., and Nilsen, T.H., eds., Sacramento Valley Symposium and Guidebook: Society of Economic Paleontologist and Mineralogist, Pacific Section, v. 65, p. 143-151.

Walton, A. W., and Palmer, B. A., 1988, Lahar facies of the Mount Dutton Formation (Oligocene-Miocene) in the Marysvale volcanic field, southwestern Utah: Geological Society of America Bulletin, v. 100, no. 7, p. 1078-1091, doi:10.1130/0016-7606(1988)100<1078:LFOTMD>2.3.CO;2

APPENDIX A

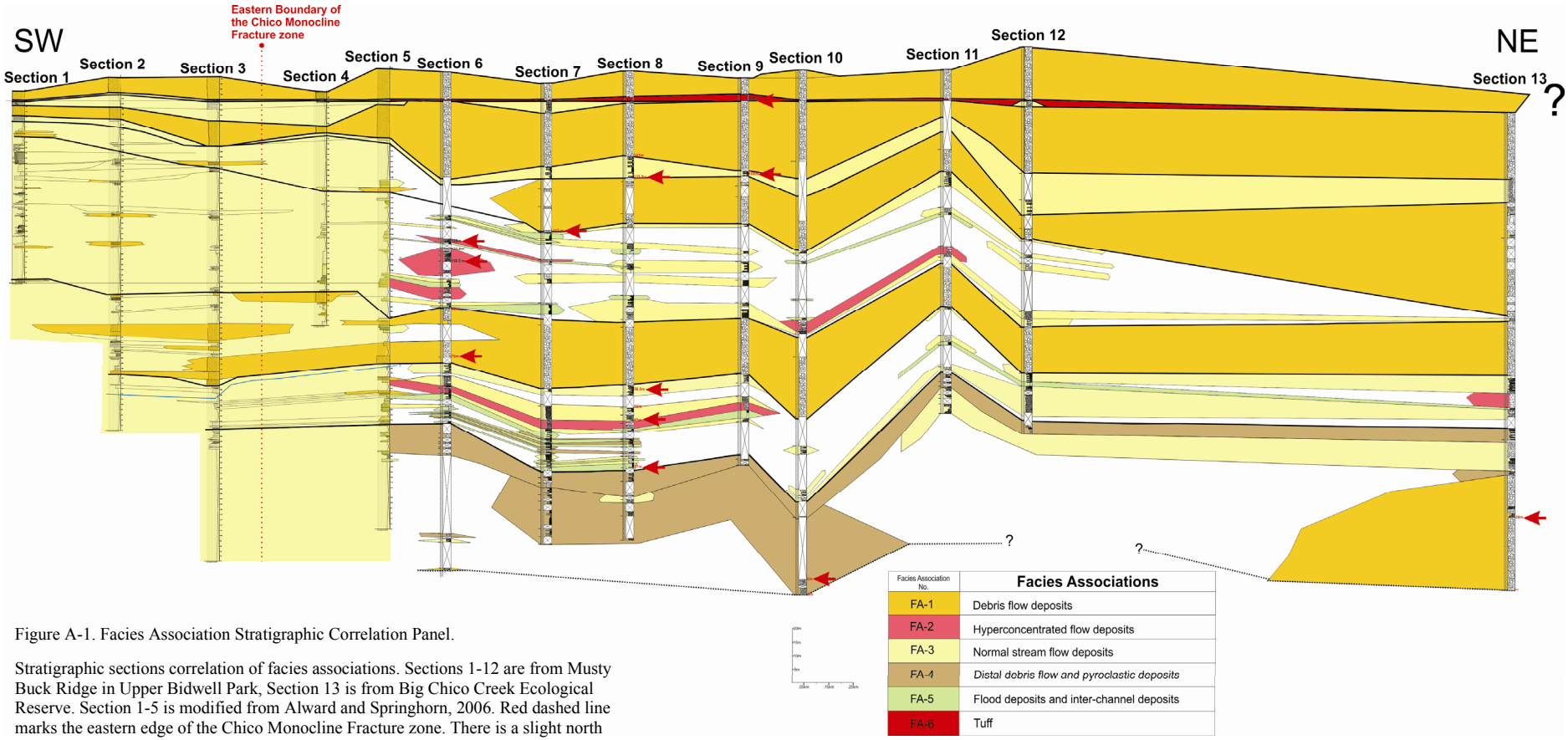

Figure A-1. Facies Association Stratigraphic Correlation Panel.

Stratigraphic sections correlation of facies associations. Sections 1-12 are from Musty Buck Ridge in Upper Bidwell Park, Section 13 is from Big Chico Creek Ecological Reserve. Section 1-5 is modified from Alward and Springhorn, 2006. Red dashed line marks the eastern edge of the Chico Monocline Fracture zone. There is a slight north eastward dip in Sections 1-7, possibly resulting from the Chico Monocline.

APPENDIX B

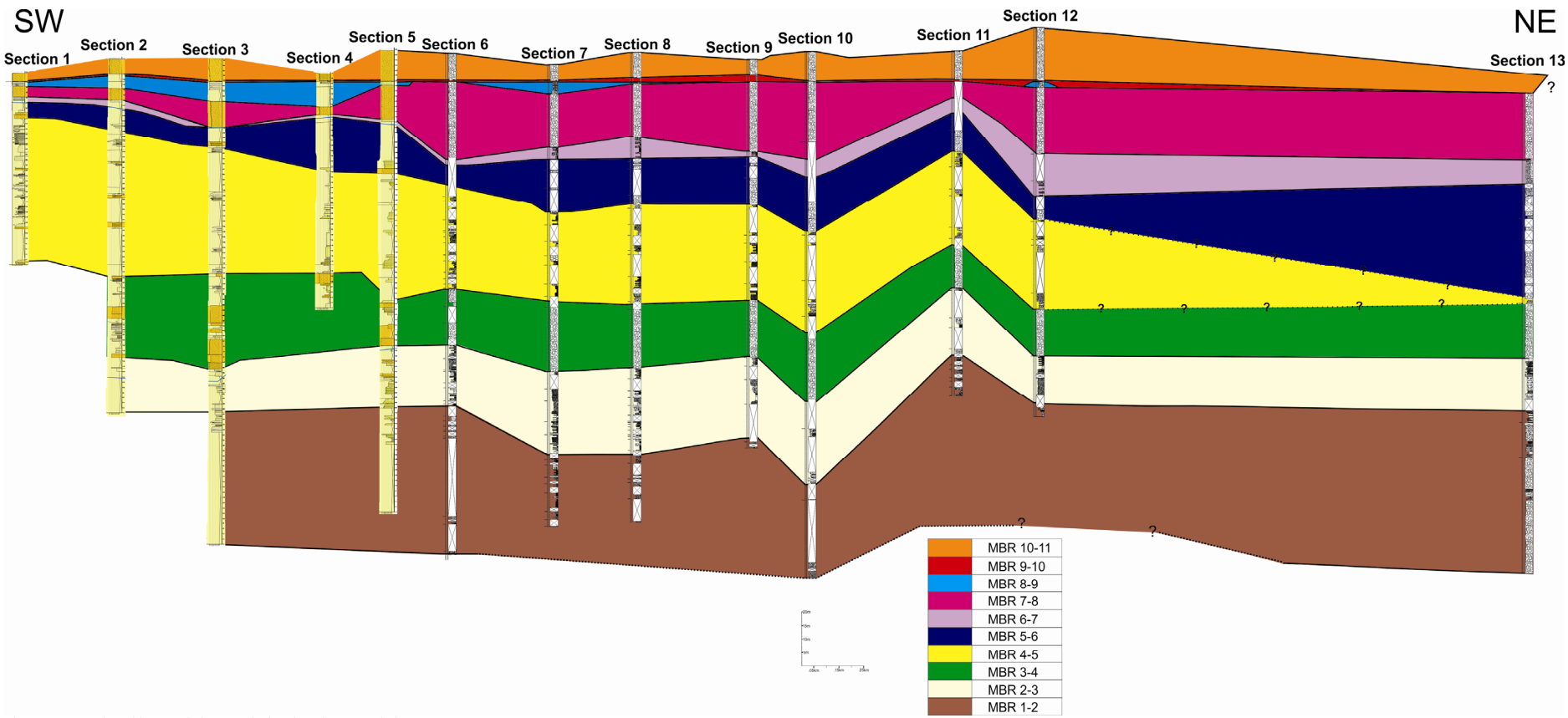

Figure B-1. Stratigraphic Correlation Panel of Major Time Correlative Events

Eleven distinct laterally continuous major time correlative events (Musty Buck Ridge events: MBRs) are defined based on changes in composition and depositional environments and labeled chronologically as Musty Buck Ridge 1 through Musty Buck Ridge 10 (MBR 1-11), with MBR 1 representing the oldest flow event and MBR 11 representing the youngest flow event. Colors represent periods in between these major events. Sections 1-12 are from Musty Buck Ridge in Upper Bidwell Park, Section 13 is from Big Chico Creek Ecological Reserve. Section 1-5 is modified from Alward, R., and Springhorn, S.T., 1996, Fluvial channel architecture and depositional setting of the Tuscan Formation, Chico, California. Abstracts with Programs - Geological Society of America, May, 2006, v. 38, no 5, pp.32.

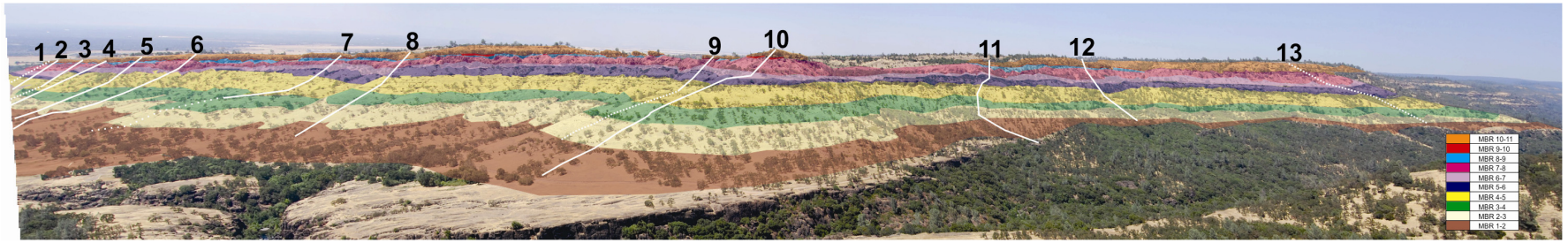

Figure B-2. Correlation Photo Panel of Major Time Correlative Events.

Eleven distinct laterally continuous major time correlative events (Musty Buck Ridge events: MBRs) are defined based on changes in composition and depositional environments and labeled chronologically as Musty Buck Ridge 1 through Musty Buck Ridge 10 (MBR 1-11), with MBR 1 representing the oldest flow event and MBR 11 representing the youngest flow event. Colors represent periods in between these major events. Photo panel was created using aerial geologic photomosaics of the Tuscan rocks. In order to obtain the best perspective of the rocks, the photos have been taken directly perpendicular to the cliff face using a helicopter and high-resolution photography.

APPENDIX C

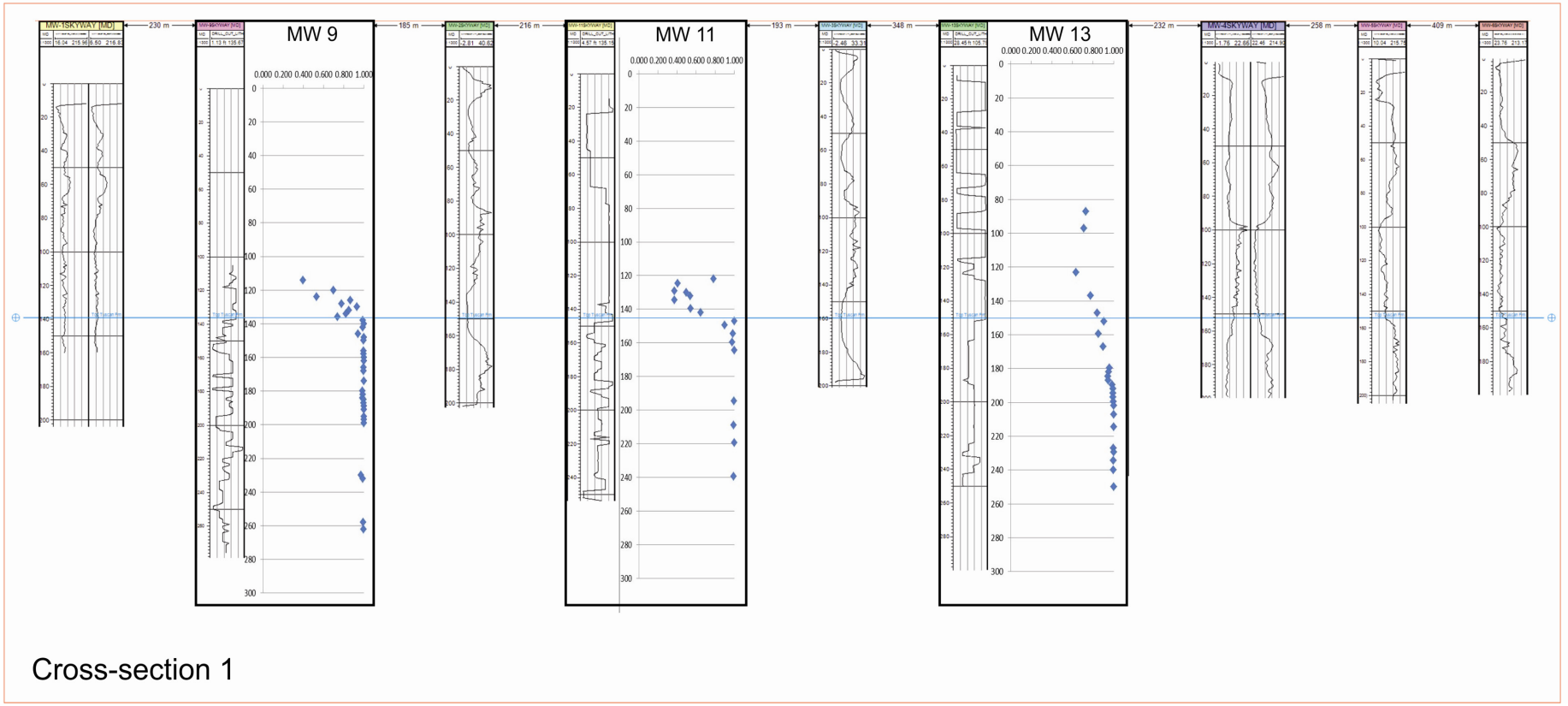

Figure C-1. Cross Section of Monitoring Wells and Graphical Mineral Percentages Plotted Along Depth.

Mineral percentages used to determine a compositional change from the Red Bluff Formation to Tuscan Formation were normalized as a relative percentage of volcanic to metamorphic lithics and then plotted against correlating well depth (MW9, MW11 and MW13). Percentage volcanic lithics represented by horizontal axis against measured vertical depth. Shift away from 100% indicates increased metamorphic content associated with transition to Red Bluff Formation. After a Red Bluff-Top Tuscan baseline was established additional data such as driller completion reports, hand samples from core, and resistivity pattern recognition was used to correlate additional wells in the subsurface. Blue line indicates a change from Red Bluff to Tuscan Formation. Location of cross-section can be found on Figure 43.

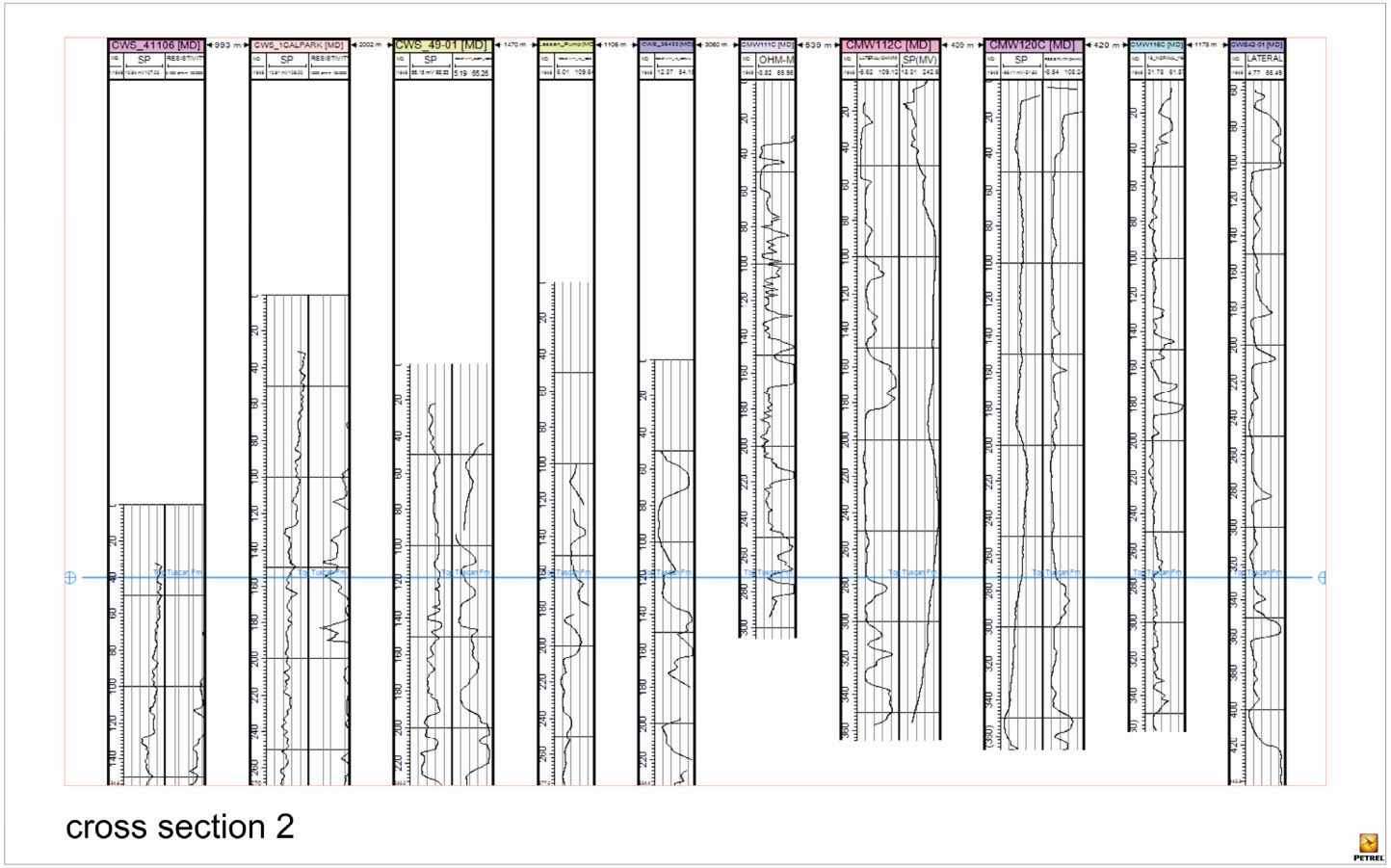

Figure C-2. Cross section 2 along dip of the Red Bluff Formation-top Tuscan Formation boundary surface.

Cross section of wells is along dip of the Red Bluff-top Tuscan boundary (well CWS41106 is the farthest well up dip, progressing down dip as you approach well CWS42-01). Red Bluff-Top Tuscan baseline was established from petrographic analysis of sand grain composition (volcanic vs. metamorphic) additional data such as driller completion reports, hand samples from core, and resistivity pattern recognition was used to correlate additional wells in the subsurface. Blue line indicates a change from Red Bluff to Tuscan Formation. Location of cross-section can be found on Figure 43.

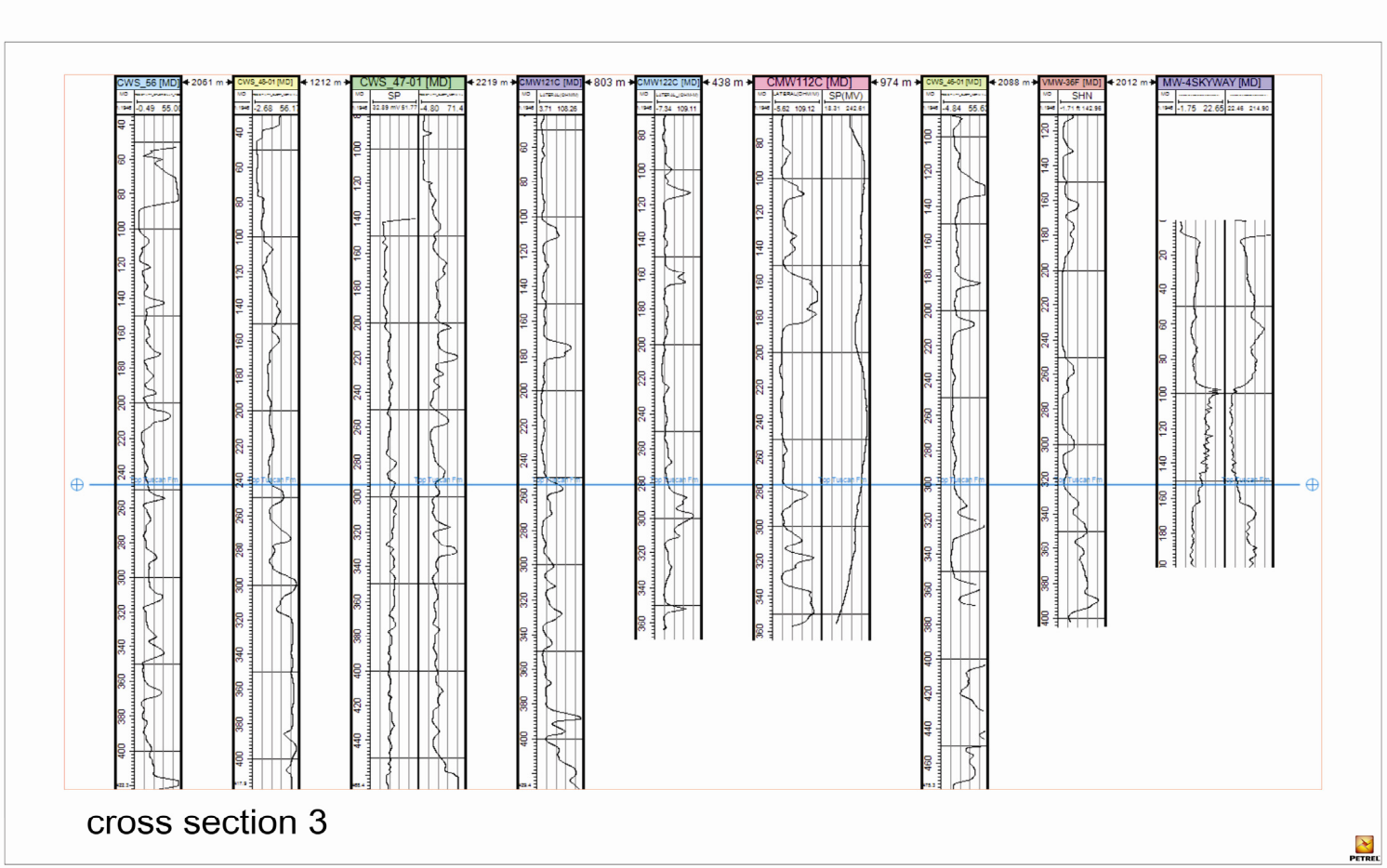

Figure C-3. Cross section 2 along strike of the Red Bluff Formation- top Tuscan Formation boundary surface.

Cross section of wells is along strike of the Red Bluff-top Tuscan boundary (well CWS56 is the farthest northern well in cross-section along strike). Red Bluff-Top Tuscan baseline was established from petrographic analysis of sand grain composition (volcanic vs. metamorphic) additional data such as driller completion reports, hand samples from core, and resistivity pattern recognition was used to correlate additional wells in the subsurface. Blue line indicates a change from Red Bluff to Tuscan Formation. Location of cross-section can be found on Figure 43.

APPENDIX D

DATA TABLES

Table D-1: MBR1

X	Y	Elevation (ft)
606840.1074	4403389.939	301.17944
607586.7264	4404514.01	575.10536
608844.8663	4408014.194	1090.36712

Note: X-Y is in NAD1927 UTM-11N meters

Table D-2: MBR2

X	Y	Elevation (ft)
606556.1246	4403786.453	481.2908
606966.1675	4403946.518	518.84352
607158.9659	4404265.211	588.596
607449.4879	4404736.571	698.312
607984.1405	4405512.142	817.71384

Note: X-Y is in NAD1927 UTM-11N meters

Table D-3: MBR3

X	Y	Elevation (ft)
606498.508	4403863.596	559.79104
606739.1091	4404138.256	619.74288
607114.2251	4404366.459	688.12432
607532.4132	4404899.502	800.42824
607667.2286	4404734.397	795.78704
607916.7319	4405558.485	897.63104
608055.4253	4405976.125	954.73256

Note: X-Y is in NAD1927 UTM-11N meters

Table D-4: MBR4

X	Y	Elevation (ft)
606444.6289	4403907.088	619.63792
606695.3517	4404182.87	697.71504
607525.4857	4404945.864	869.91504
607678.8541	4404818.479	896.51584
607888.1071	4405595.833	947.40176
608006.2558	4406013.681	1008.79352
608684.7649	4408194.576	1398.99544

Note: X-Y is in NAD1927 UTM-11N meters

Table D-5: MBR5

X	Y	Elevation (ft)
606378.6962	4403969.233	734.23456
606692.8279	4404273.297	812.28216
607073.6248	4404538.981	881.88048
607525.9004	4405029.829	985.0332
607669.1456	4404914.615	990.84864
607804.2619	4405600.673	1065.97704
607947.9887	4406034.453	1114.94416

Note: X-Y is in NAD1927 UTM-11N meters

Table D-6: MBR6

X	Y	Elevation (ft)
606651.0274	4404292.344	862.09224
607051.9933	4404570.44	942.82288
607460.4324	4405031.014	1043.43032
607916.6324	4406015.439	1146.18288
608502.748	4408269.757	1597.12384

Note: X-Y is in NAD1927 UTM-11N meters

Table D-7: MBR7

X	Y	Elevation (ft)
606357.345	4403978.586	779.94464
606653.5676	4404278.392	876.53736
607060.0159	4404541.119	968.748
607442.8434	4405043.226	1051.44992
607908.4908	4406043.044	1197.58048

Note: X-Y is in NAD1927 UTM-11N meters

Table D-8: MBR8

X	Y	Elevation (ft)
606626.4474	4404287.95	941.05168
607454.1279	4405085.211	1137.3564
607824.1397	4405700.2	1151.28328
607884.9819	4406038.573	1278.32096
608462.1911	4408338.333	1707.4532

Note: X-Y is in NAD1927 UTM-11N meters

MBR9: NO GPS DATA

Table D-9: MBR10

X	Y	Elevation (ft)
606624.3437	4404288.851	957.22536
607001.5271	4404530.294	1041.00968
604911.3716	4403292.747	555.97968
606226.8702	4403863.282	853.62
607232.2447	4404981.083	1123.02608

Note: X-Y is in NAD1927 UTM-11N meters

TableD-10: MBR11

X	Y	Elevation (ft)
604927.9785	4403305.819	563.71392
606322.9876	4403993.068	905.88352
606632.2629	4404315.657	977.40064
606995.2704	4404529.528	1072.21232
607474.2186	4405074.835	1164.6788
605308.6111	4403476.44	675.14864
604958.6525	4403372.738	582.28528
606331.2499	4404022.637	911.74488
606438.5804	4404181.902	946.89992
606373.0492	4404079.799	920.696
606293.5139	4403979.859	907.412
607765.165	4405662.965	1197.29184
607865.6438	4406039.073	1350.90408
608462.1911	4408338.333	1707.4532
607693.985	4406147.463	1329.838406
607842.2365	4406354.052	1374.924241
607990.4881	4406560.641	1420.010076
	Top of small debris flow above youngest MBR 11	
608138.7397	4406767.23	1465.09591
608286.9912	4406973.819	1510.181745

Note: X-Y is in NAD1927 UTM-11N meters

APPENDIX E

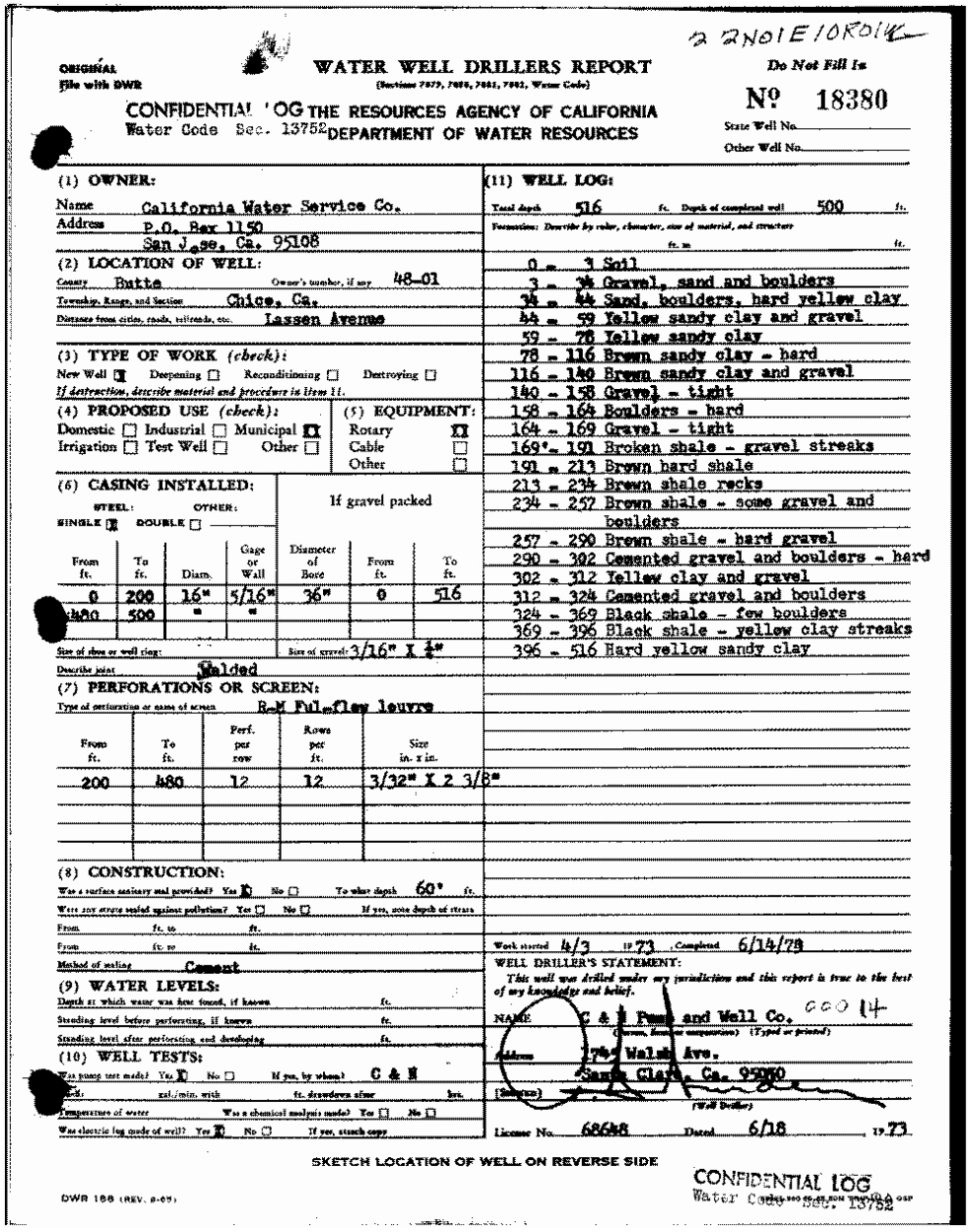

2 2N01E10R01M

ORIGINAL
File with DWR

WATER WELL DRILLERS REPORT
(Sections 7879, 7880, 7881, 7882, Water Code)

CONFIDENTIAL LOG THE RESOURCES AGENCY OF CALIFORNIA
Water Code Sec. 13752 DEPARTMENT OF WATER RESOURCES

Do Not Fill In
№ 18380
State Well No.
Other Well No.

(1) OWNER:
Name California Water Service Co.
Address P.O. Box 1150
San Jose, Ca. 95108

(2) LOCATION OF WELL:
County Butte Owner's number, if any 48-01
Township, Range, and Section Chico, Ca.
Distance from cities, roads, railroads, etc. Lassen Avenue

(3) TYPE OF WORK (check):
New Well ☒ Deepening ☐ Reconditioning ☐ Destroying ☐
If destruction, describe material and procedure in item 11.

(4) PROPOSED USE (check):
Domestic ☐ Industrial ☐ Municipal ☒
Irrigation ☐ Test Well ☐ Other ☐

(5) EQUIPMENT:
Rotary ☒
Cable ☐
Other ☐

(6) CASING INSTALLED:
STEEL: OTHER:
SINGLE ☒ DOUBLE ☐

From ft.	To ft.	Diam.	Gage or Wall	Diameter of Bore	If gravel packed From ft.	If gravel packed To ft.
0	200	16"	5/16"	36"	0	516
480	500	"	"			

Size of shoe or well ring:
Size of gravel: 3/16" X 1"
Describe joint Welded

(7) PERFORATIONS OR SCREEN:
Type of perforation or name of screen R-W Full-flow louvre

From ft.	To ft.	Perf. per row	Rows per ft.	Size in. x in.
200	480	12	12	3/32" X 2 3/8"

(8) CONSTRUCTION:
Was a surface sanitary seal provided? Yes ☒ No ☐ To what depth 60' ft.
Were any strata sealed against pollution? Yes ☐ No ☐ If yes, note depth of strata
From ft. to ft.
From ft. to ft.
Method of sealing Cement

(9) WATER LEVELS:
Depth at which water was first found, if known ft.
Standing level before perforating, if known ft.
Standing level after perforating and developing ft.

(10) WELL TESTS:
Was pump test made? Yes ☒ No ☐ If yes, by whom? C & H
gal./min. with ft. drawdown after hrs.
Temperature of water Was a chemical analysis made? Yes ☐ No ☐
Was electric log made of well? Yes ☒ No ☐ If yes, attach copy

(11) WELL LOG:
Total depth 516 ft. Depth of completed well 500 ft.
Formations: Describe by color, character, size of material, and structure

ft. to	ft.	
0	3	Soil
3	34	Gravel, sand and boulders
34	44	Sand, boulders, hard yellow clay
44	59	Yellow sandy clay and gravel
59	78	Yellow sandy clay
78	116	Brown sandy clay - hard
116	140	Brown sandy clay and gravel
140	158	Gravel - tight
158	164	Boulders - hard
164	169	Gravel - tight
169'	191	Broken shale - gravel streaks
191	213	Brown hard shale
213	234	Brown shale rocks
234	257	Brown shale - some gravel and boulders
257	290	Brown shale - hard gravel
290	302	Cemented gravel and boulders - hard
302	312	Yellow clay and gravel
312	324	Cemented gravel and boulders
324	369	Black shale - few boulders
369	396	Black shale - yellow clay streaks
396	516	Hard yellow sandy clay

Work started 4/3 19 73 Completed 6/14/73

WELL DRILLER'S STATEMENT:
This well was drilled under my jurisdiction and this report is true to the best of my knowledge and belief.

NAME C & H Pump and Well Co. 000 14
(Person, firm, or corporation) (Typed or printed)
Address 1794 Walsh Ave.
Santa Clara, Ca. 95050
(Signature) (Well Driller)

License No. 68648 Dated 6/18 19 73

SKETCH LOCATION OF WELL ON REVERSE SIDE

CONFIDENTIAL LOG
Water Code Sec. 13752

DWR 188 (REV. 8-69)

Figure E-1. CWS 48

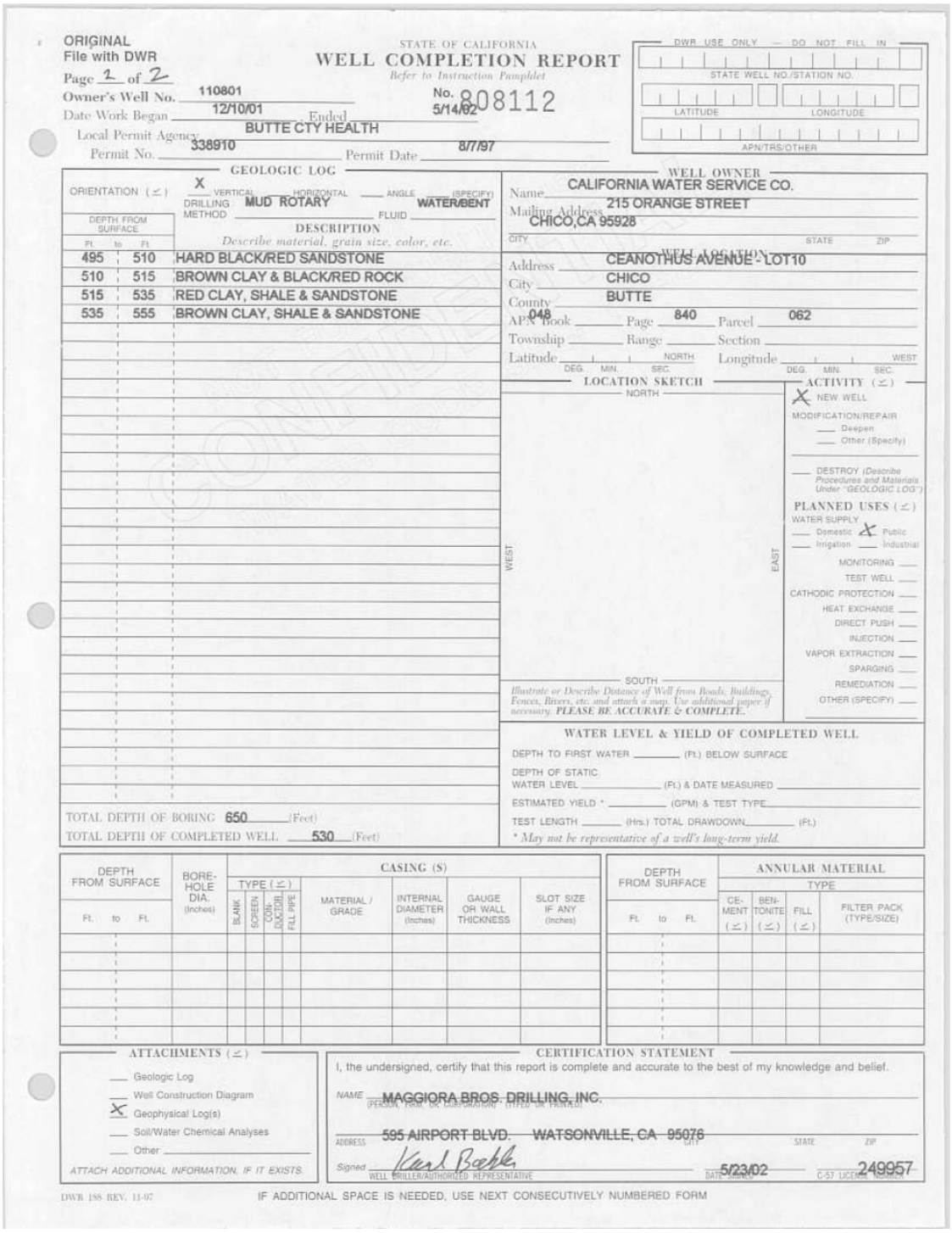

ORIGINAL
File with DWR

Page 1 of 2

STATE OF CALIFORNIA
WELL COMPLETION REPORT
Refer to Instruction Pamphlet

No. 808112

DWR USE ONLY — DO NOT FILL IN
STATE WELL NO./STATION NO.
LATITUDE LONGITUDE
APN/TRS/OTHER

Owner's Well No. 110801
Date Work Began 12/10/01 Ended 5/14/02
Local Permit Agency BUTTE CTY HEALTH
Permit No. 338910 Permit Date 8/7/97

GEOLOGIC LOG

ORIENTATION (✓) X VERTICAL HORIZONTAL ANGLE (SPECIFY)
DRILLING METHOD MUD ROTARY FLUID WATER/BENT

DEPTH FROM SURFACE Ft.	to Ft.	DESCRIPTION Describe material, grain size, color, etc.
495	510	HARD BLACK/RED SANDSTONE
510	515	BROWN CLAY & BLACK/RED ROCK
515	535	RED CLAY, SHALE & SANDSTONE
535	555	BROWN CLAY, SHALE & SANDSTONE

TOTAL DEPTH OF BORING 650 (Feet)
TOTAL DEPTH OF COMPLETED WELL 530 (Feet)

WELL OWNER
Name CALIFORNIA WATER SERVICE CO.
Mailing Address 215 ORANGE STREET
CHICO,CA 95928
CITY STATE ZIP

WELL LOCATION
Address CEANOTHUS AVENUE - LOT10
City CHICO
County BUTTE
APN Book 048 Page 840 Parcel 062
Township Range Section
Latitude DEG. MIN. SEC. NORTH Longitude DEG. MIN. SEC. WEST

LOCATION SKETCH
NORTH
WEST EAST
SOUTH
Illustrate or Describe Distance of Well from Roads, Buildings, Fences, Rivers, etc. and attach a map. Use additional paper if necessary. PLEASE BE ACCURATE & COMPLETE.

ACTIVITY (✓)
X NEW WELL
MODIFICATION/REPAIR
___ Deepen
___ Other (Specify)
___ DESTROY (Describe Procedures and Materials Under "GEOLOGIC LOG")

PLANNED USES (✓)
WATER SUPPLY
___ Domestic X Public
___ Irrigation ___ Industrial
MONITORING ___
TEST WELL ___
CATHODIC PROTECTION ___
HEAT EXCHANGE ___
DIRECT PUSH ___
INJECTION ___
VAPOR EXTRACTION ___
SPARGING ___
REMEDIATION ___
OTHER (SPECIFY) ___

WATER LEVEL & YIELD OF COMPLETED WELL
DEPTH TO FIRST WATER ___ (Ft.) BELOW SURFACE
DEPTH OF STATIC WATER LEVEL ___ (Ft.) & DATE MEASURED ___
ESTIMATED YIELD * ___ (GPM) & TEST TYPE ___
TEST LENGTH ___ (Hrs.) TOTAL DRAWDOWN ___ (Ft.)
* May not be representative of a well's long-term yield.

DEPTH FROM SURFACE Ft.	to Ft.	BORE-HOLE DIA. (Inches)	CASING (S) TYPE (✓) BLANK	SCREEN	CONDUCTOR	FILL PIPE	MATERIAL / GRADE	INTERNAL DIAMETER (Inches)	GAUGE OR WALL THICKNESS	SLOT SIZE IF ANY (Inches)

DEPTH FROM SURFACE Ft.	to Ft.	ANNULAR MATERIAL TYPE CEMENT (✓)	BENTONITE (✓)	FILL (✓)	FILTER PACK (TYPE/SIZE)

ATTACHMENTS (✓)
___ Geologic Log
___ Well Construction Diagram
X Geophysical Log(s)
___ Soil/Water Chemical Analyses
___ Other ___
ATTACH ADDITIONAL INFORMATION, IF IT EXISTS.

CERTIFICATION STATEMENT
I, the undersigned, certify that this report is complete and accurate to the best of my knowledge and belief.
NAME MAGGIORA BROS. DRILLING, INC. (PERSON, FIRM, OR ORGANIZATION) (TYPED OR PRINTED)
ADDRESS 595 AIRPORT BLVD. CITY WATSONVILLE, STATE CA ZIP 95076
Signed Karl Babb (WELL DRILLER/AUTHORIZED REPRESENTATIVE) DATE SIGNED 5/23/02 C-57 LICENSE NUMBER 249957

DWR 188 REV. 11-97
IF ADDITIONAL SPACE IS NEEDED, USE NEXT CONSECUTIVELY NUMBERED FORM

Figure E-2. CWS 72

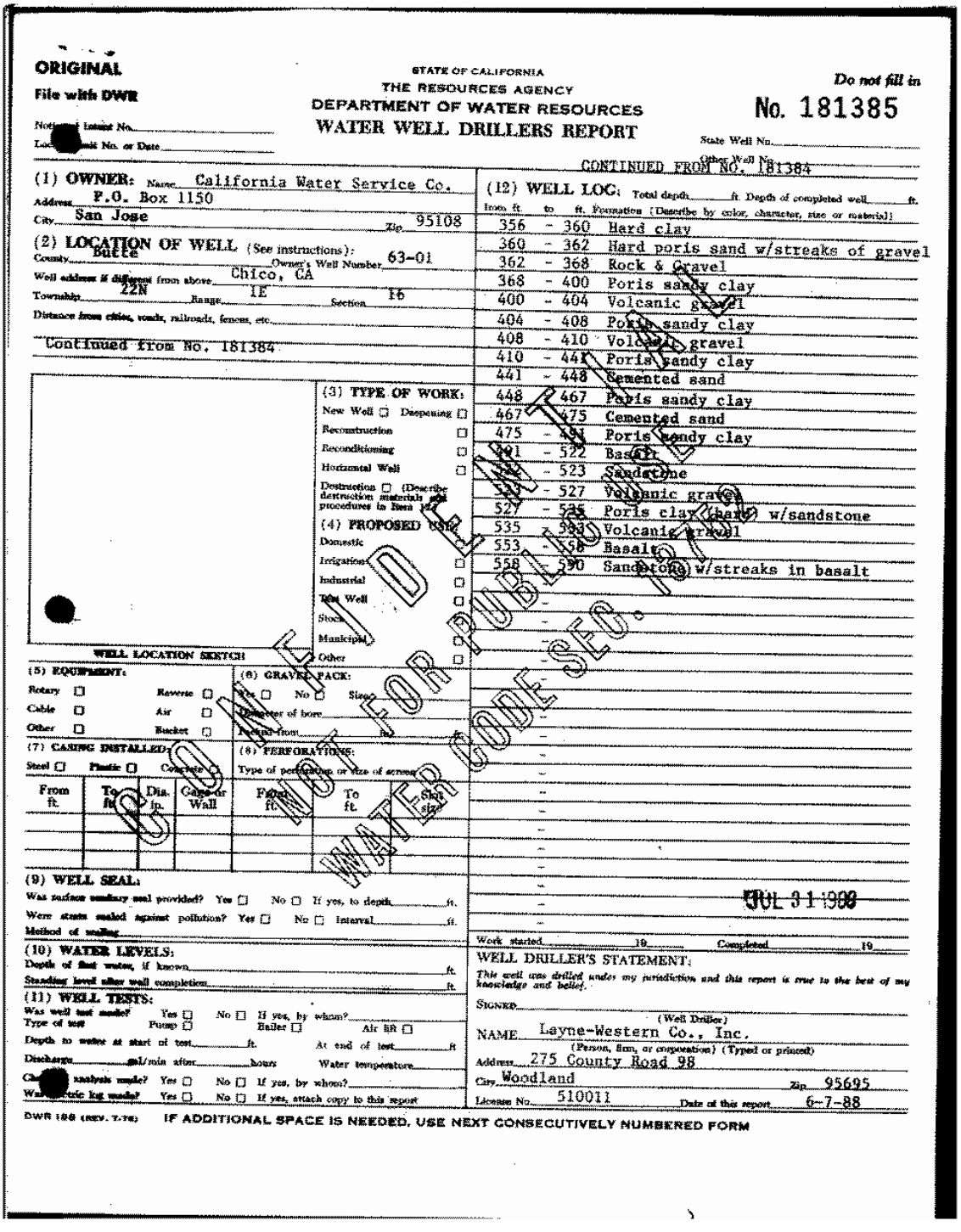

ORIGINAL
File with DWR

STATE OF CALIFORNIA
THE RESOURCES AGENCY
DEPARTMENT OF WATER RESOURCES
WATER WELL DRILLERS REPORT

Do not fill in
No. 181385

Notice of Intent No. [redacted]
Local Permit No. or Date

State Well No.
Other Well No.

CONTINUED FROM No. 181384

(1) OWNER: Name California Water Service Co.
Address P.O. Box 1150
City San Jose Zip 95108

(2) LOCATION OF WELL (See instructions):
County Butte Owner's Well Number 63-01
Well address if different from above Chico, CA
Township 22N Range 1E Section 16
Distance from cities, roads, railroads, fences, etc.
Continued from No. 181384

(3) TYPE OF WORK:
New Well ☐ Deepening ☐
Reconstruction ☐
Reconditioning ☐
Horizontal Well ☐
Destruction ☐ (Describe destruction materials and procedures in Item 12)

(4) PROPOSED USE:
Domestic
Irrigation ☐
Industrial ☐
Test Well ☐
Stock ☐
Municipal ☐
Other ☐

WELL LOCATION SKETCH

(5) EQUIPMENT:
Rotary ☐ Reverse ☐
Cable ☐ Air ☐
Other ☐ Bucket ☐

(6) GRAVEL PACK:
Yes ☐ No ☐ Size
Diameter of bore
Depth from ft. to ft.

(7) CASING INSTALLED:
Steel ☐ Plastic ☐ Concrete ☐

From ft.	To ft.	Dia. in.	Gage or Wall	Perf. ft.	To ft.	Slot size

(8) PERFORATIONS:
Type of perforation or size of screen

(9) WELL SEAL:
Was surface sanitary seal provided? Yes ☐ No ☐ If yes, to depth ft.
Were strata sealed against pollution? Yes ☐ No ☐ Interval ft.
Method of sealing

(10) WATER LEVELS:
Depth of first water, if known ft.
Standing level after well completion ft.

(11) WELL TESTS:
Was well test made? Yes ☐ No ☐ If yes, by whom?
Type of test Pump ☐ Bailer ☐ Air lift ☐
Depth to water at start of test ft. At end of test ft.
Discharge gal/min after hours Water temperature
Chemical analysis made? Yes ☐ No ☐ If yes, by whom?
Was electric log made? Yes ☐ No ☐ If yes, attach copy to this report

(12) WELL LOG: Total depth ft. Depth of completed well ft.

from ft.	to ft.	Formation (Describe by color, character, size or material)
356	360	Hard clay
360	362	Hard poris sand w/streaks of gravel
362	368	Rock & Gravel
368	400	Poris sandy clay
400	404	Volcanic gravel
404	408	Poris sandy clay
408	410	Volcanic gravel
410	441	Poris sandy clay
441	448	Cemented sand
448	467	Poris sandy clay
467	475	Cemented sand
475	491	Poris sandy clay
491	522	Basalt
522	523	Sandstone
523	527	Volcanic gravel
527	535	Poris clay (hard) w/sandstone
535	553	Volcanic gravel
553	558	Basalt
558	590	Sandstone w/streaks in basalt

JUL 31 1988

Work started 19 Completed 19

WELL DRILLER'S STATEMENT:
This well was drilled under my jurisdiction and this report is true to the best of my knowledge and belief.

SIGNED (Well Driller)
NAME Layne-Western Co., Inc. (Person, firm, or corporation) (Typed or printed)
Address 275 County Road 98
City Woodland Zip 95695
License No. 510011 Date of this report 6-7-88

DWR 188 (REV. 7-74) IF ADDITIONAL SPACE IS NEEDED, USE NEXT CONSECUTIVELY NUMBERED FORM

SOLD FOR PUBLICATION ONLY
NOT FOR PUBLICATION
WATER CODE SEC.

Figure E-3. CWS 63

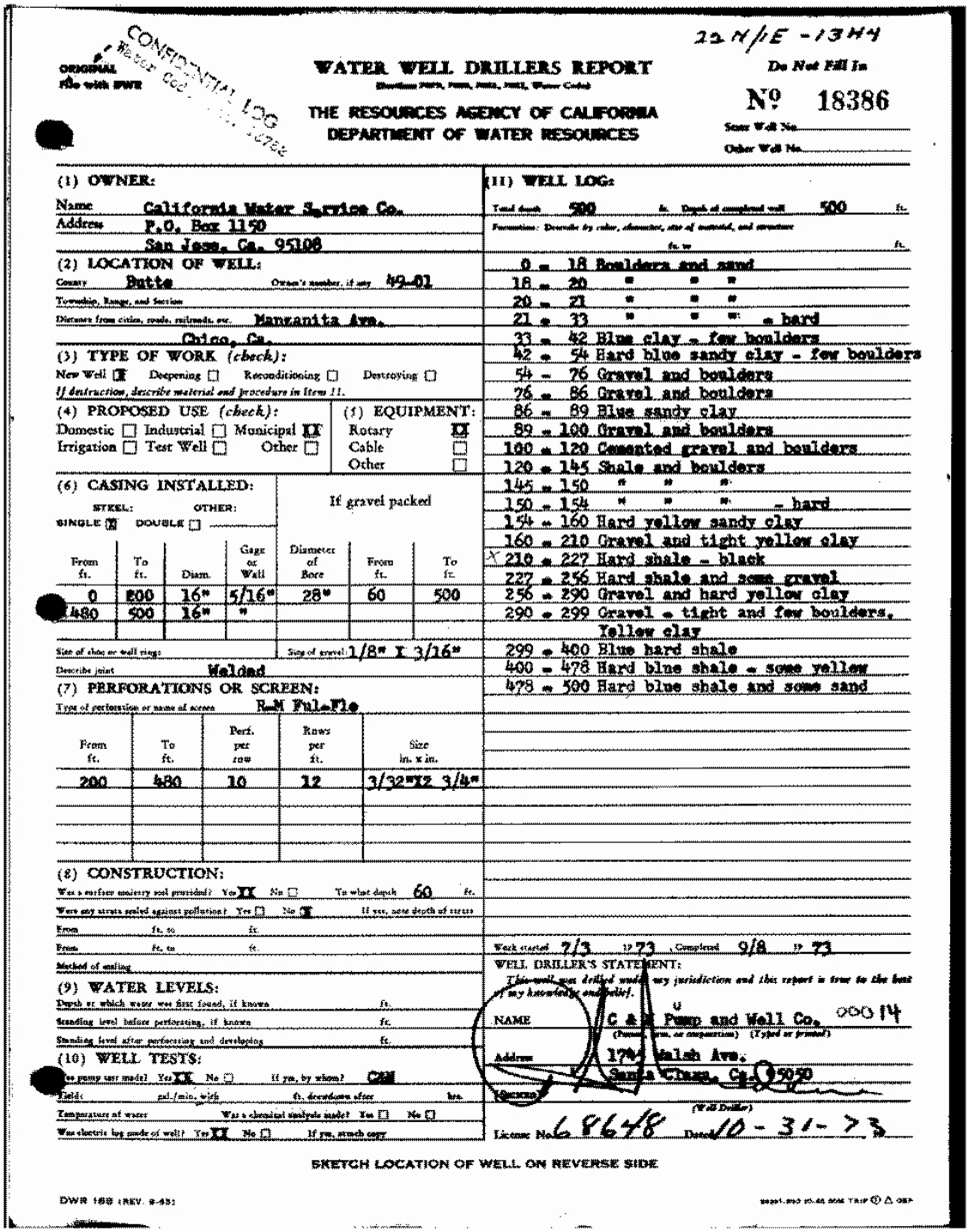

22N/1E-13H4

CONFIDENTIAL LOG Water Code Sec. 13752

ORIGINAL file with DWR

WATER WELL DRILLERS REPORT

THE RESOURCES AGENCY OF CALIFORNIA
DEPARTMENT OF WATER RESOURCES

Do Not Fill In

No 18386

State Well No.

Other Well No.

(1) OWNER:

Name California Water Service Co.
Address P.O. Box 1150
San Jose, Ca. 95108

(2) LOCATION OF WELL:

County Butte Owner's number, if any 49-01
Township, Range, and Section
Distance from cities, roads, railroads, etc. Manzanita Ave.
Chico, Ca.

(3) TYPE OF WORK (check):

New Well X Deepening ☐ Reconditioning ☐ Destroying ☐
If destruction, describe material and procedure in item 11.

(4) PROPOSED USE (check):

Domestic ☐ Industrial ☐ Municipal X
Irrigation ☐ Test Well ☐ Other ☐

(5) EQUIPMENT:

Rotary X
Cable ☐
Other ☐

(6) CASING INSTALLED:

STEEL: OTHER:
SINGLE X DOUBLE ☐

From ft.	To ft.	Diam.	Gage or Wall	Diameter of Bore	If gravel packed From ft.	If gravel packed To ft.
0	500	16"	5/16"	28"	60	500
480	500	16"	"			

Size of shoe or well ring: Size of gravel: 1/8" X 3/16"
Describe joint Welded

(7) PERFORATIONS OR SCREEN:

Type of perforation or name of screen R-M Fulo-Flo

From ft.	To ft.	Perf. per row	Rows per ft.	Size in. x in.
200	480	10	12	3/32"X2 3/4"

(8) CONSTRUCTION:

Was a surface sanitary seal provided? Yes X No ☐ To what depth 60 ft.
Were any strata sealed against pollution? Yes ☐ No X If yes, note depth of strata
From ft. to ft.
From ft. to ft.
Method of sealing

(9) WATER LEVELS:

Depth at which water was first found, if known ft.
Standing level before perforating, if known ft.
Standing level after perforating and developing ft.

(10) WELL TESTS:

Was pump test made? Yes X No ☐ If yes, by whom? C&M
Yield: gal./min. with ft. drawdown after hrs.
Temperature of water Was a chemical analysis made? Yes ☐ No ☐
Was electric log made of well? Yes X No ☐ If yes, attach copy

(11) WELL LOG:

Total depth 500 ft. Depth of completed well 500 ft.
Formations: Describe by color, character, size of material, and structure

ft. to	ft.	
0	18	Boulders and sand
18	20	" " "
20	21	" " "
21	33	" " " " hard
33	42	Blue clay - few boulders
42	54	Hard blue sandy clay - few boulders
54	76	Gravel and boulders
76	86	Gravel and boulders
86	89	Blue sandy clay
89	100	Gravel and boulders
100	120	Cemented gravel and boulders
120	145	Shale and boulders
145	150	" " "
150	154	" " " " hard
154	160	Hard yellow sandy clay
160	210	Gravel and tight yellow clay
X 210	227	Hard shale - black
227	256	Hard shale and some gravel
256	290	Gravel and hard yellow clay
290	299	Gravel - tight and few boulders, Yellow clay
299	400	Blue hard shale
400	478	Hard blue shale - some yellow
478	500	Hard blue shale and some sand

Work started 7/3 19 73 Completed 9/8 19 73

WELL DRILLER'S STATEMENT:

This well was drilled under my jurisdiction and this report is true to the best of my knowledge and belief.

NAME C & M Pump and Well Co. 000 14
(Person, firm, or corporation) (Typed or printed)
Address 1794 Walsh Ave.
Santa Clara, Ca. 95050
(Well Driller)
License No. 68648 Dated 10-31-73

SKETCH LOCATION OF WELL ON REVERSE SIDE

DWR 188 (REV. 9-63)

Figure E-4. CWS 49

IS THIS A CWS WELL ?

22N/2E-17

ORIGINAL
File with DWR

WATER WELL DRILLERS REPORT

THE RESOURCES AGENCY OF CALIFORNIA

DEPARTMENT OF WATER RESOURCES

22N/2E-17N80

11-29-73

Do Not Fill In

№ 41106

State Well No.

Other Well No.

CONFIDENTIAL LOG Water Code Sec. 13752

(1) OWNER:

Name: Jack Graham

Address: 16661 Ventura Blvd

Enciano, California 91316

(2) LOCATION OF WELL:

County: Butte — Owner's number, if any: # 1

Township, Range, and Section: Sec 17 R2E T22N

Distance from cities, roads, railroads, etc.: 4 Mi East of city of Chico

(3) TYPE OF WORK (check):

New Well ☒ Deepening ☐ Reconditioning ☐ Destroying ☐

If destruction, describe material and procedure in Item 11.

(4) PROPOSED USE (check):

Domestic ☐ Industrial ☐ Municipal ☒

Irrigation ☐ Test Well ☐ Other ☐

(5) EQUIPMENT:

Rotary ☒

Cable ☐

Other ☐

(6) CASING INSTALLED:

STEEL: SINGLE ☒ DOUBLE ☐ OTHER:

From ft.	To ft.	Diam.	Gage or Wall
0	52	26	½
0	574	14"	5/16

If gravel packed

Diameter of Bore	From ft.	To ft.
26"	52	574
32	0	52

Size of shoe or well ring:

Size of gravel: ½x3/8

Describe joint

(7) PERFORATIONS OR SCREEN:

Type of perforation or name of screen

From ft.	To ft.	Perf. per row	Rows per ft.	Size in. x in.
164	324	14	2	3/32x2½
434	454	Full flow	loover	1/8
520	540	full flow	loover	1/8
554	568	full flow	loover	1/8

(8) CONSTRUCTION:

Was a surface sanitary seal provided? Yes ☒ No ☐ To what depth 52 ft.

Were any strata sealed against pollution? Yes ☒ No ☐ If yes, note depth of strata

From 3 ft. to 40 ft.

From ft. to ft.

Method of sealing: pump pure cement from bottom up

(9) WATER LEVELS:

Depth at which water was first found, if known: 13 ft.

Standing level before perforating, if known: ft.

Standing level after perforating and developing: 115 ft.

(10) WELL TESTS:

Was pump test made? Yes ☒ No ☐ If yes, by whom? Lassen Pump

Yield: 2500 gal./min. with 167 ft. drawdown after 22 hrs.

Temperature of water — Was a chemical analysis made? Yes ☒ No ☐

Was electric log made of well? Yes ☒ No ☐ If yes, attach copy

(11) WELL LOG:

Total depth 600' ft. Depth of completed well 574

Formation: Describe by color, character, size of material, and structure

ft.	to ft.	
0	3	top soil
3	38	lava boulders
38	110	lava
110	122	lava sd & gravel
122	146	lava sd fine to med
146	215	lava sd chips
215	250	sdy clay
250	300	lava chips
300	315	fine sd.
315	395	clay & sd.
395	420	clay w/ streeks sd.
420	430	snd.
430	440	clay
440	454	med sd
454	500	clay w/ fine sd.
500	520	clay
520	540	sd.
540	554	clay
554	568	sand
568	578	clay
578	590	volcanic ash
590	600	clay

CONFIDENTIAL LOG
Water Code Sec. 13752

Work started 11/4/71, Completed 2/12 19 72

WELL DRILLER'S STATEMENT:

This well was drilled under my jurisdiction and this report is true to the best of my knowledge and belief.

NAME: Lassen Pump & Motor Wks
(Person, firm, or corporation) (Typed or printed)

Address: P.O. Box 3376 Chico, Calif

[Signed] (Well Driller)

License No. 59221- C-57 Dated 3/15/72

SKETCH LOCATION OF WELL ON REVERSE SIDE

52' of drawdown ...

DWR 188 (REV. 8-65)

Figure E-5. CWS 41106

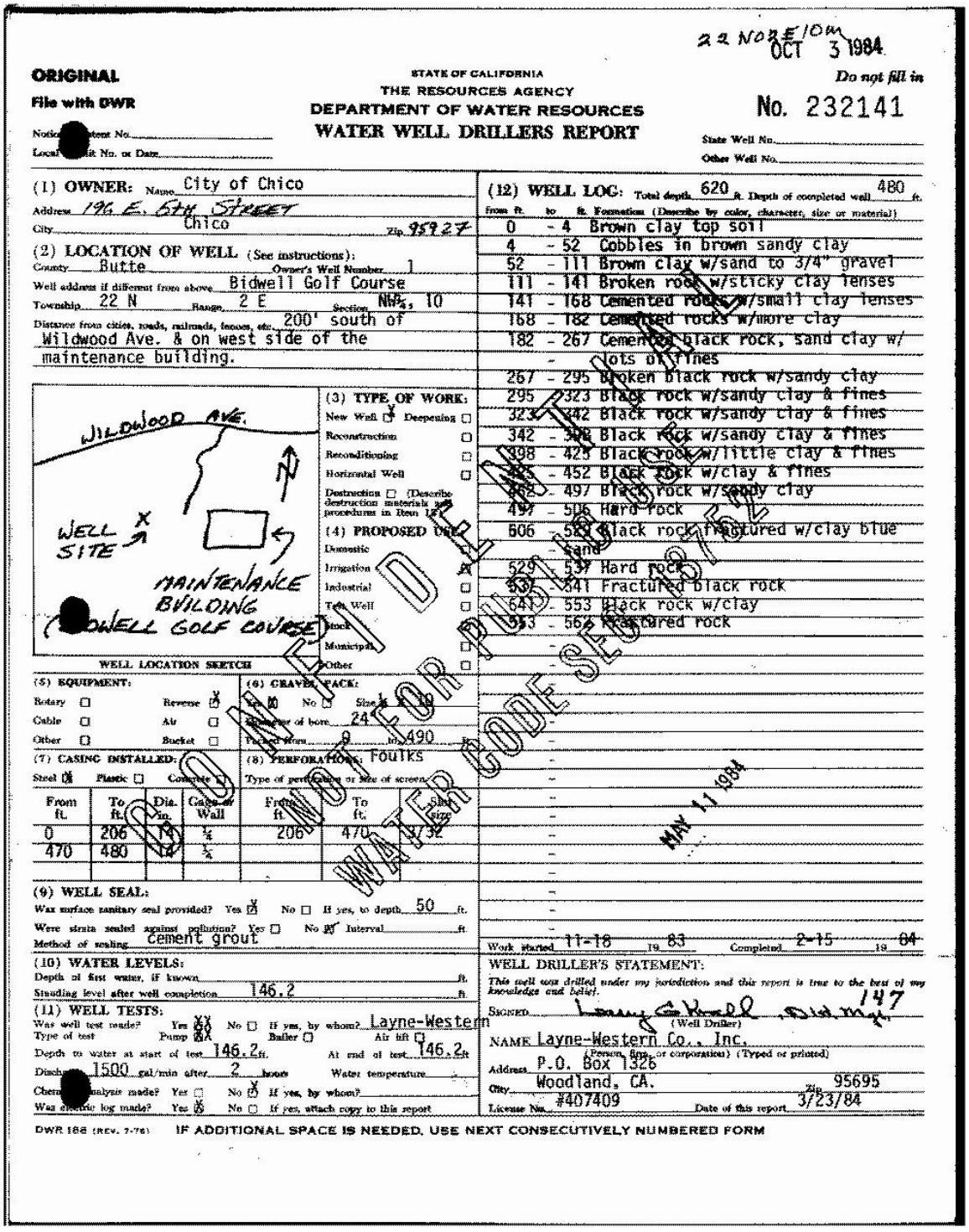

22 N02E/10M
OCT 3 1984

ORIGINAL
File with DWR

STATE OF CALIFORNIA
THE RESOURCES AGENCY
DEPARTMENT OF WATER RESOURCES
WATER WELL DRILLERS REPORT

Do not fill in
No. 232141

Notice of Intent No.
Local Permit No. or Date
State Well No.
Other Well No.

(1) OWNER: Name City of Chico
Address 196 E. 6th Street
City Chico Zip 95927

(2) LOCATION OF WELL (See instructions):
County Butte Owner's Well Number 1
Well address if different from above Bidwell Golf Course
Township 22 N Range 2 E Section NW¼, 10
Distance from cities, roads, railroads, fences, etc. 200' south of Wildwood Ave. & on west side of the maintenance building.

WELL LOCATION SKETCH

(3) TYPE OF WORK:
New Well X Deepening
Reconstruction
Reconditioning
Horizontal Well
Destruction (Describe destruction materials and procedures in Item 12)

(4) PROPOSED USE:
Domestic
Irrigation X
Industrial
Test Well
Stock
Municipal
Other

(5) EQUIPMENT:
Rotary Reverse X
Cable Air
Other Bucket

(6) GRAVEL PACK:
Yes X No Size 1/4 x 1/2
Diameter of bore 24
Packed from 0 to 490 ft.

(7) CASING INSTALLED:
Steel X Plastic Concrete

(8) PERFORATIONS: Louvks
Type of perforation or size of screen

From ft.	To ft.	Dia. in.	Gage or Wall	From ft.	To ft.	Slot size
0	206	14	¼	206	470	3/32
470	480	14	¼			

(9) WELL SEAL:
Was surface sanitary seal provided? Yes X No If yes, to depth 50 ft.
Were strata sealed against pollution? Yes No X Interval ft.
Method of sealing cement grout

(10) WATER LEVELS:
Depth of first water, if known ft.
Standing level after well completion 146.2 ft.

(11) WELL TESTS:
Was well test made? Yes X No If yes, by whom? Layne-Western
Type of test Pump X Bailer Air lift
Depth to water at start of test 146.2 ft. At end of test 146.2 ft.
Discharge 1500 gal/min after 2 hours Water temperature
Chemical analysis made? Yes No X If yes, by whom?
Was electric log made? Yes X No If yes, attach copy to this report

(12) WELL LOG: Total depth 620 ft. Depth of completed well 480 ft.

From ft.	to ft.	Formation (Describe by color, character, size or material)
0	4	Brown clay top soil
4	52	Cobbles in brown sandy clay
52	111	Brown clay w/sand to 3/4" gravel
111	141	Broken rock w/sticky clay lenses
141	168	Cemented rocks w/small clay lenses
168	182	Cemented rocks w/more clay
182	267	Cemented black rock, sand clay w/ lots of fines
267	295	Broken black rock w/sandy clay
295	323	Black rock w/sandy clay & fines
323	342	Black rock w/sandy clay & fines
342	398	Black rock w/sandy clay & fines
398	428	Black rock w/little clay & fines
428	452	Black rock w/clay & fines
452	497	Black rock w/sandy clay
497	506	Hard rock
506	529	Black rock fractured w/clay blue sand
529	537	Hard rock
537	641	Fractured black rock
641	553	Black rock w/clay
553	566	Fractured rock

Work started 11-18 19 83 Completed 2-15 19 84

WELL DRILLER'S STATEMENT:
This well was drilled under my jurisdiction and this report is true to the best of my knowledge and belief.
NAME Layne-Western Co., Inc. (Person, firm, or corporation) (Typed or printed)
Address P.O. Box 1326
City Woodland, CA. Zip 95695
License No. #407409 Date of this report 3/23/84

DWR 188 (REV. 7-76) IF ADDITIONAL SPACE IS NEEDED, USE NEXT CONSECUTIVELY NUMBERED FORM

Figure E-6. CWS 41106